Departamento de Ingeniería

Escuela Superior de Ingeniería

TESIS DOCTORAL

Hardware y Software Avanzado en la Construcción de Analizadores Inteligentes para Consumo y Calidad Eléctrica e Internet de las Cosas

Advanced Hardware and Software to Create Smart Analysers for Power Consumption and Power Quality and Internet of Things

AUTOR

Eduardo José Viciana Gámez

Tesis Doctoral presentada para optar al Grado de Doctor por la Universidad de Almería

Programa de Doctorado en Tecnología de Invernaderos e Ingeniería Industrial y Ambiental (RD99/11)

DIRECTORES

Dr. Francisco Gil Montoya

Dr. Raúl Baños Navarro

Universidad de Almería, diciembre 2021

Agradecimientos

Han sido tres años de trabajo para la elaboración de esta tesis y cada día he podido aprender cosas nuevas de mis compañeros y personas que me han apoyado. Sin ellos todo esto no hubiera sido posible. Quiero trasladarle mi más profundo agradecimiento.

Quiero agradecer a mis directores Francisco Gil y Raúl Baños la oportunidad que me han dado de seguir formándome junto a enormes profesionales. Han sido unas excelentes personas, compañeros y amigos, siempre dispuestos a ayudar y a ofrecer todo su conocimiento, no solo del mundo académico.

No me olvido del resto de personas que han hecho posible esta tesis como Alfredo Alcaide, Antonio Zapata, Francisco Arrabal, Francisco Manzano y Juan Martínez que han sido coautores de los artículos que se presentan.

Después de tantos años, no me puedo olvidar de la institución que me ha acogido y formado, la Universidad de Almería, ha sido una segunda casa para mí, donde he pasado muchos momentos que siempre recordare, unos buenos y otros malos, pero siempre rodeado de buena gente, en ella he conocido a gran cantidad de amigos y a mi mujer, a la que también quiero darle mi agradecimiento por ayudarme en todo lo que está en su mano.

¡Mil gracias a todos!

ÍNDICE GENERAL

FIGURAS

TABLAS

PREÁMBULO

La investigación llevada a cabo en la presente tesis doctoral queda reflejada en cuatro publicaciones científicas internacionales. Tres de ellas corresponden a artículos publicados en revistas incluidas en el Journal Citation Reports (JCR) de la Web of Science (WOS), mientras que la cuarta aportación corresponde a un artículo que se encuentra en revisión en una revista internacional indexada en JCR en el momento de depósito de esta tesis doctoral. Todas estas publicaciones constituyen la descripción científica de un completo sistema abierto de analizadores de consumo y calidad eléctrica en cualquier tipo de red o instalación eléctrica con capacidades de Internet de las Cosas.

A continuación, se resumen todas estas publicaciones, así como sus correspondientes referencias bibliográficas.

PUBLICACIÓN CIENTÍFICA 1

En el Capítulo 2 se describe el artículo titulado "*OpenZmeter: An Efficient Low-Cost Energy Smart Meter and Power Quality Analyzer*", publicado en la revista Sustainability, indexada en Journal Citation Reports.

Dicha aportación describe en detalle la problemática existente en las redes eléctricas comerciales, industriales y residenciales, originada por el aumento significativo de dispositivos conectados de distinta naturaleza, la mayoría de los cuales son cargas no lineales, y como la medida de parámetros de calidad eléctrica toma mayor relevancia al facilitar al usuario final información en tiempo real sobre multitud de parámetros de la red. Al objeto de dar respuesta a la necesidad de disponer de analizadores de alta precisión y coste reducido, este artículo presenta el dispositivo openZmeter, basado en tecnologías libres y cuyas capacidades aplicadas demuestran cumplir los objetivos planteados en el diseño.

PUBLICACIÓN CIENTÍFICA 2

En el Capítulo 3 se presenta el artículo "*An Open Hardware Design for Internet of Things Power Quality and Energy Saving Solutions*", publicado en la revista Sensors, indexada en Journal Citation Reports.

Esta aportación describe exhaustivamente el diseño hardware autónomo para la monitorización de parámetros de calidad eléctrica y consumo energético en redes monofásicas, con capacidades de comunicación e integración basadas en "Internet de las cosas" (Internet of Things, IoT). Se ha conseguido un diseño abierto, de reducido tamaño y bajo coste, que integra amplias funcionalidades, entre las que podemos destacar la adquisición de datos de la red, análisis de estos para la extracción de multitud de parámetros eléctricos, el almacenamiento de los resultados obtenidos y la presentación de dichos datos al usuario mediante una interfaz WEB empotrada, además de las capacidades para la comunicación entre dispositivos y el envío de todos los datos de forma telemática. A todo esto, se suma la capacidad de servir de herramienta a la comunidad científica y como base para siguientes investigaciones y desarrollos, al ser toda la información fácilmente accesible.

PUBLICACION CIENTIFICA 3

En el Capítulo 4 se expone el artículo "*All-in-one three-phase smart meter and power quality analyzer with extended IoT capabilities*", actualmente en revisión en una revista internacional indexada en el Journal Citation Reports.

Este trabajo describe de forma completa la ampliación tanto a nivel hardware como del software de análisis del concepto de "openZmeter" a redes trifásicas, ofreciendo un dispositivo IoT de fácil uso para el análisis y monitorización de distintas configuraciones de red, con multitud de parámetros y configuraciones disponibles. Como validación de los resultados obtenidos el equipo diseñado es comparado en prestaciones y precisión con equipos comerciales utilizando distintos dispositivos de calibración, mostrando unos resultados que lo convierten en una herramienta sumamente útil en aplicaciones industriales del mundo real, incluyendo las plantas de generación de energías renovables, como es el caso de una planta fotovoltaica, que es utilizada como caso de estudio para demostrar las capacidades del dispositivo trifásico. Además, este dispositivo trifásico es de gran utilidad para el desarrollo de futuras investigaciones de laboratorio relacionadas con ingeniería eléctrica.

PUBLICACION CIENTIFICA 4

En el Capítulo 5 se presenta el artículo "*Analysis of non-active power in non-sinusoidal circuits using geometric algebra*", publicado en la revista International Journal of Electrical Power & Energy Systems, indexada en Journal Citation Reports.

Presenta una actualización al sistema de análisis de potencia implementado en "openZmeter", en que se reemplazan los cálculos clásicos para el análisis de la potencia, por una nueva teoría que permite, mediante la aplicación del algebra geométrica, solventar distintas singularidades. En este nuevo enfoque se consideran las interacciones entre tensiones y corrientes, en sus respectivos armónicos, para redes monofásicas. Los resultados obtenidos confirman que la flexibilidad de esta técnica permite un análisis con un balance de potencia que mantiene el principio de conservación de la energía al aplicarse sobre distintas cargas y fuentes, tanto lineales como no lineales, lo cual supone en efecto un nuevo enfoque en el análisis de potencia de circuitos eléctricos, solventando las limitaciones de las teorías clásicas y permitiendo, entre otros, realizar distintas optimizaciones enfocadas a reducir el total de corriente circulante por las instalaciones.

REFERENCIAS DE LAS PUBLICACIONES

PUBLICACION CIENTIFICA 1

Título: "*OpenZmeter: An efficient low-cost energy smart meter and power quality analyzer*"

Autores: Eduardo Viciana, Alfredo Alcayde, Francisco G. Montoya, Raúl Baños, Francisco M. Arrabal-Campos, Antonio Zapata-Sierra, Francisco Manzano-Agugliaro

Revista científica: Sustainability

Volumen: 10(11) - Año 2018

Doi: 10.3390/su10114038

Datos JCR (Journal Citation Reports):

Factor de impacto (2018): 2,075

Categorías:

ENVIRONMENTAL STUDIES -SCIE (Ranking 105/251, Cuartil Q2)

GREEN & SUSTAINABLE SCIENCE & TECHNOLOGY – SCIE (Ranking 20/35, Cuartil Q3)

Editor: MDPI AG. **-** Suiza

PUBLICACION CIENTIFICA 2

Título: "*An open hardware design for internet of things power quality and energy saving solutions*"

Autores: Eduardo Viciana, Alfredo Alcayde, Francisco G. Montoya, Raúl Baños, Francisco M. Arrabal-Campos, Francisco Manzano-Agugliaro

Revista científica: Sensors

Volumen: 19(3) - Año 2019

Doi: 10.3390/s19030627

Datos JCR (Journal Citation Reports):

Factor de impacto (2017): 3,275

Categorías:

INSTRUMENTS & INSTRUMENTATION – SCIE (Ranking 15/64, Cuartil Q1)

ENGINEERING, ELECTRICAL & ELECTRONIC – SCIE (Ranking 77/266, Cuartil Q2)

CHEMISTRY, ANALYTICAL – SCIE (Ranking 22/86, Cuartil Q2)

Editor: MDPI AG. **-** Suiza

PUBLICACION CIENTIFICA 3

Título: "*All-in-one three-phase smart meter and power quality analyzer with extended IoT capabilities*"

Autores: Eduardo Viciana, Francisco M. Arrabal-Campos, Alfredo Alcayde, Raul Baños, Juan A. Martínez-Lao, Francisco G. Montoya

Revista: IEEE Transactions on Instrumentation and Measurement (En revision)

PUBLICACION CIENTIFICA 4

Título: "Analysis of non-active power in non-sinusoidal circuits using geometric algebra"

Autores: Francisco G. Montoya, Raúl Baños, Alfredo Alcayde, Francisco M. Arrabal-Campos, Eduardo Viciana

Revista científica: International Journal of Electrical Power & Energy Systems

Volumen: 116 - Año 2020

Doi: 10.1016/j.ijepes.2019.105541

Datos JCR (Journal Citation Reports):

Factor de impacto (2020): 4,630

Categorías:

ENGINEERING, ELECTRICAL & ELECTRONIC – SCIE (Ranking 45/273, Cuartil Q1)

Editor: ELSEVIER SCI LTD – Reino Unido

RESUMEN

Las medidas de calidad eléctrica y de consumo de energía permiten a proveedores y usuarios conocer la información necesaria sobre su suministro en el ámbito residencial, comercial e industrial. Esta información es obtenida por medio de distintos elementos de medida que analizan las señales eléctricas que viajan por la red. Aunque en las últimas décadas se han desarrollado dispositivos avanzados para llevar a cabo estas medidas, el interés por el desarrollo de nuevos dispositivos inteligentes ha crecido de forma especial en los últimos años, debido a las nuevas necesidades requeridas por los objetivos energéticos planteados para la sociedad por diferentes organismos internacionales.

En la actualidad, el cambio climático, las tendencias del mercado eléctrico, la eficiencia, la promoción de las energías renovables, entre otros factores, han originado un cambio drástico en el modelo energético, pasando de ser un sistema con control centralizado a una red distribuida con multitud de participantes en todo el proceso, que incluye la generación eléctrica, el transporte de la energía y el consumo final. Dadas las nuevas necesidades de coordinación existentes, resulta necesario procesar un importante número de variables eléctricas en diferentes puntos del sistema eléctrico. Es por ello que en los últimos años ha surgido la necesidad de desarrollar medidores inteligentes que sean capaces de proporcionar información adicional a la de un medidor convencional, permitiendo además una comunicación entre dispositivos o con puestos de monitorización/control donde se pueda supervisar el sistema, tanto a gran escala (por ejemplo, el sistema eléctrico nacional o regional) como a pequeña escala (por ejemplo, una instalación eléctrica doméstica o industrial).

La estabilidad de la red depende en gran medida de la coordinación entre las diversas fuentes de generación y consumo, y ésta solo puede llevarse a cabo conociendo el estado real de la red. Así, a corto plazo, el sistema debe adaptarse a la generación disponible y a la propia situación de la red, determinando las estrategias a seguir en caso de que surja cualquier tipo de contingencia en base a las mediciones tomadas en diferentes puntos del sistema. A largo plazo, estas mediciones pueden ser utilizadas para establecer políticas de mantenimiento y mejora del sistema, así como establecer procedimientos de mejora en cuanto a la adaptación de la generación a la demanda, de forma que se pueda incluso

almacenar la energía generada y no consumida en un momento, para ser utilizada en momentos posteriores, especialmente aquellos en los que los picos de demanda sean superiores a la generación disponible.

Además de ser necesario medir datos de potencia generada y consumida en una red eléctrica de cualquier escala, desde el sistema eléctrico nacional hasta cualquier instalación eléctrica industrial o doméstica, es necesario considerar otras variables eléctricas de gran relevancia. En particular, existen diferentes parámetros que determinan la calidad eléctrica del sistema que son de gran interés para el correcto funcionamiento de la red, así como de los dispositivos (cargas) conectadas a la misma. Cabe hacer mención especial al hecho de que el aumento de cargas no lineales en los últimos años ha dado lugar a que la distorsión armónica se convierta también en un nuevo reto para las redes de distribución, al aparecer transitorios, sobrecalentando transformadores o provocando subidas, bajadas o incluso interrupciones de suministro en puntos concretos de la red, además de los propios daños que se pueden producir en las cargas conectadas al sistema.

Pese a la gran complejidad y reto que supone este nuevo paradigma descentralizado, son múltiples los estudios que resaltan sus ventajas desde el punto de vista de gestión del sistema. Así, por ejemplo, es posible diseñar microrredes en viviendas e instalaciones industriales que, ante eventuales caídas en el suministro eléctrico por parte de la compañía distribuidora, permitan su funcionamiento autónomo mediante almacenamiento de energía generada con fuentes renovables (eólica, fotovoltaica principalmente). Este tipo de instalaciones constituyen otra aplicación importante de los analizadores de red inteligentes con capacidades IoT, puesto que incluso las instalaciones de pequeña y mediana escala requieren tomar medidas en diferentes partes de la instalación eléctrica para llevar a cabo una correcta gestión del sistema.

Por otro lado, el aumento de complejidad en la red eléctrica afecta de manera muy directa al consumidor final ya que, a pesar de todos los cambios citados anteriormente para la red de generación y distribución, en la mayoría de casos este solo tiene acceso valor de consumo de energía. Y es precisamente en este punto en el que los analizadores de red inteligentes muestran otra de sus grandes potencialidades como es el impacto económico que puede suponer su implantación en sistemas e instalaciones eléctricas. En el caso de las instalaciones domésticas, estos dispositivos pueden permitir a los gestores de las mismas controlar los niveles de consumo eléctrico y establecer políticas de ahorro energético. Esta

situación es aun más importante en las instalaciones industriales, ya que en estos casos las compañías suministradoras pueden incluso penalizar al cliente por conceptos que, como es el caso de la energía reactiva consumida, no pueden ser gestionados correctamente al no disponer de herramientas y procedimientos para para medir y corregir. También, la presencia de dispositivos domésticos e industriales de componentes electrónicos de conmutación hace a estos dispositivos más sensibles a eventos, como subidas o bajadas de tensión, de las que el cliente no dispone de información y pueden originar averías o el acortamiento importante en la vida útil de los equipos. Por estos motivos, los usuarios necesitan herramientas que les faciliten el acceso a distintos parámetros de la red, incluyendo valores de calidad eléctrica, más allá del total de consumo energético que facilite la compañía suministradora. Aunque en el mercado existen multitud de equipos de medida, su elevado coste y su dificultad de uso restringe su acceso al consumidor final, que no dispone de herramientas para evaluar el suministro que recibe.

Como herramienta para este propósito se ha diseñado “openZmeter”, tanto en su versión monofásica (oZm) como trifásica (3Ph-oZm) que, bajo la supervisión del grupo de investigación TIC221 de la Universidad de Almería, se ha convertido en una completa plataforma accesible para el análisis de redes eléctricas de cualquier escala. Además de presentar un diseño software avanzado, pero a su vez compacto, el software realiza las funciones de análisis de señal, almacenamiento de datos, presentación al usuario y comunicación con otros dispositivos, y de dos dispositivos de captura diseñados hasta el momento, que son los responsables de tomar información de las ondas de tensión y corriente, para que el software pueda procesarlas y obtener todos los parámetros de utilidad.

Un punto clave de esta plataforma ha sido elaborar un dispositivo de bajo coste, con gran funcionalidad y adaptable a multitud de rangos de medida, que permita una fácil instalación y sea usable tanto para cualquier tipo de consumidor, tanto usuarios domésticos como para profesionales del ámbito de la ingeniería eléctrica. Cuenta con una interface WEB, que hace uso de las últimas tecnologías para mostrar la información de una manera clara e intuitiva, tanto en un dispositivo móvil como en un ordenador y todo esto en tiempo real. Otra importante funcionalidad incluida en los analizadores diseñados es que permite la comunicación entre diferentes equipos de medida de cara a procesar, analizar y visualizar los datos de medida de forma centralizada.

Al ser un dispositivo enfocado a incorporar las últimas técnicas de análisis disponibles, pensando en la investigación, ha sido desarrollado completamente usando hardware y software libre, con una interface de aplicación (API) abierta y documentada, donde toda la información es accesible y exportable. El buen rendimiento de los dispositivos de captura desarrollados, y la continua mejora del software de análisis y visualización, ha llevado al desarrollo de un tercer modelo, con diversas funciones enfocadas a un usuario más avanzado y al plano de la investigación.

Los cambios descritos en la red eléctrica en los últimos años han sido tan profundos que no solo han afectado a productoras, redes de distribución y usuarios, desde un punto de vista meramente económico o de calidad eléctrica, si no que han hecho que las propias teorías matemáticas que se aplican tradicionalmente para la determinación de los flujos de energía y potencia deban ser revisadas. Los estándares comúnmente aceptados para el cálculo de la potencia en sistemas de corriente alterna parten del supuesto de que las señales siguen una forma de onda puramente senoidal. Aunque en la realidad esto no es cierto, normalmente se han aceptado por suponer una aproximación bastante precisa, sin embargo la proliferación de microgrids, la incorporación de fuentes renovables y el aumento de cargas con electrónica de potencia han supuesto un aumentado considerablemente de los armónicos presente en la red haciendo que las teorías clásicas no permitan un análisis correcto, hasta el punto de que el uso de estas técnicas para el diseño de filtros y optimización de flujos de energía pueda desencadenar el efecto contrario por la cantidad de información no contemplada. Como respuesta a esta limitación, se ha desarrollado una nueva teoría de cálculo de energía en circuitos no senoidales, que con la aplicación del algebra geométrica permite obtener de forma precisa la potencia en un circuito, incorporando al cómputo la información contenida en los distintos armónicos de tensión y corriente, además aporta un significado físico al método de cálculo que no está presente en las teorías habituales.

ABSTRACT

Power quality and energy consumption measurements allow suppliers and users to know the necessary information about their residential, commercial and industrial supply. This information is obtained by means of different measuring elements that analyze the electrical signals that travel through the network. Although in the last decades advanced devices have been developed to carry out these measurements, the interest in the development of new intelligent devices has grown especially in recent years, due to the new needs required by the energy objectives set for society by different international organizations.

At present, climate change, electricity market trends, efficiency, promotion of renewable energies, among other factors, have caused a drastic change in the energy model, from a system with centralized control to a distributed network with a multitude of participants in the whole process, including electricity generation, energy transport and final consumption. Given the new coordination needs, it is necessary to process a large number of electrical variables at different points of the power system. This is why in recent years the need has arisen to develop smart meters that are capable of providing additional information to that of a conventional meter, also allowing communication between devices or with monitoring/control stations where the system can be supervised, both on a large scale (e.g. the national or regional electricity system) and on a small scale (e.g. a domestic or industrial electrical installation).

The stability of the grid depends to a large extent on the coordination between the various sources of generation and consumption, and this can only be achieved by knowing the real state of the grid. Thus, in the short term, the system must adapt to the available generation and the grid situation itself, determining the strategies to be followed in the event of any type of contingency based on measurements taken at different points in the system. In the long term, these measurements can be used to establish system maintenance and improvement policies, as well as to establish procedures to improve the adaptation of generation to demand, so that energy generated and not consumed at a given moment can be stored for use at later times, especially those in which demand peaks are higher than the available generation.

In addition to the need to measure data on power generated and consumed in an electrical network of any scale, from the national electrical system to any industrial or domestic electrical installation, it is necessary to consider other electrical variables of great relevance. In particular, there are different parameters that determine the electrical quality of the system that are of great interest for the correct operation of the network, as well as of the devices (loads) connected to it. Special mention should be made of the fact that the increase in non-linear loads in recent years has meant that harmonic distortion has also become a new challenge for distribution networks, as transients appear, overheating transformers or causing surges, dips or even supply interruptions at specific points in the network, in addition to the damage that can be caused to the loads connected to the system.

Despite the great complexity and challenge posed by this new decentralized paradigm, there are many studies that highlight its advantages from the point of view of system management. Thus, for example, it is possible to design microgrids in homes and industrial facilities that, in the event of power supply failures by the distribution company, allow them to operate autonomously by storing energy generated from renewable sources (mainly wind and photovoltaic). This type of installation is another important application for smart grid analyzers with IoT capabilities, since even small and medium-scale installations require measurements to be taken in different parts of the electrical installation for proper system management.

On the other hand, the increased complexity of the power grid affects the end consumer in a very direct way since, despite all the changes mentioned above for the generation and distribution network, in most cases this only has access to the energy consumption value. And it is precisely at this point that smart grid analyzers show another of their great potentialities, such as the economic impact that their implementation can have on electrical systems and installations. In the case of domestic installations, these devices can enable their managers to control electricity consumption levels and establish energy saving policies. This situation is even more important in industrial installations, since in these cases the supply companies can even penalize the customer for items that, as in the case of reactive energy consumed, cannot be managed correctly because they do not have the tools and procedures to measure and correct. Also, the presence of domestic and industrial devices with electronic switching components makes these devices more sensitive to events, such as voltage surges or dips, of which the customer has no information and which can cause breakdowns or a significant

shortening of the useful life of the equipment. For these reasons, users need tools that provide them with access to different network parameters, including power quality values, beyond the total energy consumption provided by the utility company. Although there is a multitude of metering equipment on the market, its high cost and difficulty of use restricts its access to the end consumer, who does not have the tools to evaluate the supply he receives.

As a tool for this purpose, "openZmeter" has been designed, both in its single-phase (oZm) and three-phase (3Ph-oZm) versions, which, under the supervision of the TIC221 research group of the University of Almeria, has become a complete accessible platform for the analysis of electrical networks of any scale. In addition to presenting an advanced software design, but at the same time compact, the software performs the functions of signal analysis, data storage, presentation to the user and communication with other devices, and two capture devices designed so far, which are responsible for taking information from the voltage and current waves, so that the software can process them and obtain all the useful parameters.

A key point of this platform has been to develop a low cost device, with great functionality and adaptable to a multitude of measurement ranges, allowing easy installation and usable for any type of consumer, both home users and professionals in the field of electrical engineering. It has a WEB interface, which makes use of the latest technologies to display the information in a clear and intuitive way, both on a mobile device and on a computer, and all this in real time. Another important functionality included in the designed analyzers is that it allows communication between different measurement equipment in order to process, analyze and visualize the measurement data in a centralized way.

Being a device focused on incorporating the latest analysis techniques available, with research in mind, it has been developed entirely using free hardware and software, with an open and documented application interface API), where all information is accessible and exportable. The good performance of the developed capture devices, and the continuous improvement of the analysis and visualization software, has led to the development of a third model, with several functions focused on a more advanced user and research level.

The changes described in the power grid in recent years have been so profound that they have not only affected producers, distribution networks and users, from a purely economic or power quality point of view, but have also meant that the mathematical theories

traditionally applied for the determination of energy and power flows have had to be revised. The commonly accepted standards for calculating power in alternating current systems assume that signals follow a purely sinusoidal waveform. However, the proliferation of microgrids, the incorporation of renewable sources and the increase of loads with power electronics have led to a considerable increase in the harmonics present in the grid, making the classical theories not allow a correct analysis, to the point that the use of these techniques for the design of filters and optimization of power flows can trigger the opposite effect due to the amount of information not contemplated. In response to this limitation, a new theory of energy calculation in non-sinusoidal circuits has been developed, which with the application of geometric algebra allows to obtain precisely the power in a circuit, incorporating to the computation the information contained in the different voltage and current harmonics, in addition it provides a physical meaning to the calculation method that is not present in the usual theories.

CAPÍTULO 1 - INTRODUCCIÓN

1.1. ANTECEDENTES

Durante décadas el crecimiento de las redes eléctricas no ha ido acompañado por la incorporación de nuevos dispositivos de medida remotos. Desde que en 1977 Paraskevakos [32] patentó el primer dispositivo de telemedida, se han propuesto diferentes equipos de medida orientados a obtener información en redes eléctricas [1].

En los últimos años han surgido nuevas líneas de actuación derivadas de la necesidad de mejorar la eficiencia energética para combatir las tendencias negativas observadas en diferentes variables asociadas al cambio climático. En concreto, la eficiencia energética y el uso de las energías renovables constituyen actualmente una tendencia que rige el desarrollo de los sistemas de energía a nivel mundial, como una parte importante de la orientación circular en la explotación de los recursos. Estos cambios han dado lugar a una nueva estructura de generación distribuida donde la red eléctrica ha evolucionado a una serie de redes interconectadas, de forma que hoy día es habitual hablar de conceptos como generación distribuida, microrredes y redes inteligentes. Estos nuevos conceptos requieren establecer procedimientos que determinen el estado de la red para garantizar una generación y distribución fiables [2]. Una red inteligente podría definirse como una red eléctrica que une los puntos de generación con los de consumo en un entorno controlado, incorporando distintas fuentes de generación de una manera eficiente y descentralizada [39], [40], reconociendo el estado real de la red. Dado que una red inteligente está concebida para suministrar electricidad, son necesarias nuevas tecnologías y el desarrollo en los campos de generación, transmisión y distribución energética para afrontar los nuevos retos. Este tipo de estructura ha sido impulsada por los recientes avances en las fuentes de energía renovables y las modernas tecnologías de comunicación y computación [36].

No obstante, la red eléctrica es más que una infraestructura de generación y transmisión. Es un ecosistema con activos de gobiernos, proveedores, fabricantes y propietarios. Su correcto aprovechamiento se fundamenta en complejos modelos de potencia que combinan las fuentes de energía renovables avanzadas con sistemas de control y procesamiento informático [37]. La gestión de estas tecnologías avanzadas requiere de sensores avanzados, conocidos como analizadores de red o contadores inteligentes [38], que permiten a los

operadores evaluar la estabilidad de la red y proporcionar a los consumidores una información completa y de calidad sobre las variables eléctricas, incluyendo la notificación automática de interrupciones en el suministro. Los sistemas incluyen seccionadores que detectan y se recuperan de los fallos en una subestación de forma automática, interruptores de alimentación automatizados y baterías que almacenan excedentes de energía en determinados momentos, y que pueden ser utilizados posteriormente para satisfacer la demanda de los clientes.

La capacidad de una red inteligente para realizar el mejor aprovechamiento de los recursos disponibles parte del conocimiento preciso de la demanda y situación actual de la red que proporcionan distintos elementos de medida presentes en la red. Siguiendo la evolución de la tecnología involucrada en las redes eléctricas se precisa de medidores inteligentes, que se definen como "un sistema electrónico que puede medir el consumo de energía, proporcionando más información que un contador convencional, y puede transmitir y recibir datos utilizando una forma de comunicación electrónica". Esta definición fue establecida por el Parlamento Europeo en su directiva 2012/27/CE [34].

Muchos estudios han destacado las ventajas derivadas del desarrollo progresivo de los sistemas de generación distribuida, las redes inteligentes y las micro redes [39] [40]. Bajo este nuevo paradigma, algunos autores han llamado la atención sobre la importancia de desarrollar nuevos sensores y herramientas para la monitorización y el control en tiempo real del flujo de energía entre diferentes partes de un sistema eléctrico, así como la calidad del suministro. Estos sistemas de medición inteligente suelen integrarse con tecnologías informáticas y de comunicación para mejorar la eficiencia y la fiabilidad de los futuros sistemas eléctricos con recursos energéticos renovables [43]. Además, los contadores inteligentes incluyen algoritmos eficientes de control y procesamiento [44].

No solo las redes eléctricas han sufrido un cambio progresivo en su estructura, también las cargas conectadas han evolucionado. Actualmente, millones y millones de dispositivos electrónicos se conectan a la red, introduciendo perturbaciones en esta. Con el aumento de las cargas electrónicas no lineales como cargadores de coches eléctricos, rectificadores, iluminación LED, ordenadores personales, lámparas fluorescentes con balasto electrónico, fuentes de alimentación conmutadas y otros dispositivos electrónicos de potencia [51], las perturbaciones como las subidas de tensión, bajadas, interrupciones del suministro, los transitorios oscilatorios, el parpadeo o la distorsión armónica, se están convirtiendo en un

reto para los sistemas eléctricos. Estas perturbaciones pueden repercutir en los consumidores añadiendo potencia reactiva, costes de redistribución, costes de reducción de carga [115] y dañar los dispositivos conectados en su instalación [113], [114]. Además, estos problemas de calidad eléctrica pueden sobrecalentar los transformadores, dañar las baterías de condensadores y afectar a equipos electrónicos sensibles [52]. Debido al aumento de estos problemas, los científicos e ingenieros han comenzado a estudiarlos a través de un número significativo de estudios de calidad eléctrica (*Power Quality,* o *PQ,* por sus siglas en inglés) [53] [54] [55] [56]. La monitorización de la calidad de la energía eléctrica se ha convertido en una parte esencial de estos estudios [57].

Deben tomarse medidas que permitan mitigar las perturbaciones de red, y también deben identificarse con precisión sus fuentes y causas. Las perturbaciones que afecten a la calidad eléctrica deben ser detectadas, reconocidas y clasificadas [58] [59]. Los ingenieros tienen que seleccionar las técnicas adecuadas para extraer cualquier perturbación de la red con el fin de reconocerlas y clasificarlas. En los últimos años, se han implementado muchas técnicas, entre las cuales la Transformada de Fourier (FT) es la más utilizada hasta la fecha. Otros métodos que se han popularizado en los últimos años son la transformada de Fourier de tiempo corto (STFT) [117], la transformada de Hilbert-Huang (HHT), la transformada de Stockwell (ST) y la transformada Wavelet (WT) [118].

No solo se viene trabajando en el desarrollo de técnicas para detectar y evaluar eventos. La presencia de perturbaciones, como los armónicos, hacen necesario el desarrollo de nuevas técnicas que permitan la medida precisa de distintos parámetros de la red en estas nuevas condiciones. En este sentido son de mencionar las teorías que describen los flujos de potencia dentro de un sistema que son objeto de debate y controversia desde hace más de cien años [3] [4] [5]. Tradicionalmente, dos proposiciones han dominado la mayoría de estudios durante este periodo: las técnicas basadas en el dominio del tiempo [6], las basadas en el dominio de la frecuencia [4]. Existen otras teorías alternativas que se sitúan a medio camino de las anteriores [3] y que también han tenido un impacto significativo. Estas teorías no tienen un claro significado físico y bajo las condiciones de trabajo de las redes actuales se dan situaciones en las que el principio de conservación de la energía no se cumple. El nuevo modelo energético supone también un importante reto para el consumidor, los medidores de energía tradicionales instalados en empresas o viviendas tienen el propósito fundamental de facturar el consumo eléctrico, pero está ya no es la única preocupación para el cliente final

y los conceptos como la calidad eléctrica son factores de consideración por parte de los consumidores que requiere de una nueva generación de dispositivos que permitan evaluar, además de la cantidad de energía consumida, también su calidad.

Algunos investigadores académicos han presentado contadores de energía y analizadores de calidad de la energía, pero hasta ahora la mayoría de las instalaciones se controlan utilizando dispositivos comerciales. Sin embargo, estos dispositivos suelen ser caros y difíciles de manejar por usuarios no expertos. Por ello, es un reto desarrollar dispositivos de bajo coste y alta precisión para su uso general en cualquier tipo de instalación eléctrica. Esta es precisamente la principal aportación de esta tesis doctoral, el desarrollo de un medidor de potencia y energía eléctrica de pequeño tamaño, de código abierto, preciso y fiable, cuyo objetivo es ayudar a las personas a analizar y visualizar las medidas de consumo de energía cumpliendo con las normas internacionales como la IEC 61000-4-30 y la EN-50160. Este dispositivo, *openZmeter*, constituye una parte clave de una infraestructura de medición inteligente. Este dispositivo electrónico es un importante rediseño del prototipo básico de [74]. En concreto, se basa en una política de hardware abierto, de bajo coste, y con capacidades bidireccionales avanzadas aplicadas a la monitorización de las características eléctricas y a la recopilación de datos basada en la nube. Este contador inteligente presenta una amplia gama de características, que cumplen los requisitos mínimos deseables para un contador inteligente de electricidad, tal y como se publicó en la recomendación 2012/148/UE [75]. El contador inteligente aquí presentado es útil para monitorizar y prevenir problemas en la red de distribución. Gracias a las características de oZm, es posible recibir información sobre eventos significativos detectados en las instalaciones eléctricas. Mediante la monitorización de estas situaciones anómalas, por ejemplo, altos consumos de energía o perturbaciones significativas en la calidad de la misma es posible aplicar diferentes estrategias preventivas.

El diseño abierto de *openZmeter* está pensado para convertirse en una herramienta para el investigador que desee profundizar en las distintas técnicas de análisis de calidad o consumo eléctrico y como parte de esta propuesta se expone el desarrollo de una teoría novedosa que aplica herramientas matemáticas como el algebra geométrica para dar respuesta a las limitaciones que presentan las teorías más habituales para el cálculo de potencia en redes con señales no senoidales. Esta teoría parte de la descomposición de corrientes propuesta por Castro-Nuñez, unida a los trabajos propuestos por Fryze y Czarnecki,

cuyos desarrollos han sido ampliados, tal y como se muestra en la tesis doctoral. Este desarrollo es de especial importancia al aplicarse en técnicas de ahorro energético, ya que permite la optimización de sistemas, en los que con las técnicas tradicionales no era posible determinar los parámetros óptimos de operación.

1.2. MOTIVACIÓN Y JUSTIFICACIÓN

La principal justificación que ha motivado el desarrollo de esta tesis ha sido la necesidad de proveer a la comunidad científica de nuevas técnicas y herramientas, que permitan un mejor análisis y acceso a los parámetros requeridos para el estudio de las redes eléctricas, enfocándose en varios campos, como previsión de fallas de red o calidad eléctrica. Además, el incremento de la complejidad de los sistemas, en parte originada por la incorporación de las energías renovables y al aumento de la demanda, han surgido nuevas necesidades de información y han abierto nuevas vías de investigación.

A pesar de que existen dispositivos que permiten realizar un gran número de medias eléctricas en diferentes redes eléctricas, se han detectado ciertas limitaciones en los mismos que los hacen poco adecuados para la investigación y limitan su uso en los estudios sobre la materia. Las limitaciones encontradas han sido:

- Los equipos que ofrecen un análisis avanzado de la red tienen un precio muy elevado, gran tamaño, dificultad de instalación y, a menudo, su uso es complejo. Esto hace que sea inviable la obtención simultánea de parámetros de red a gran escala, es decir, en una gran cantidad de puntos físicos distantes físicamente.
- Los equipos de medida no ofrecen información sobre las técnicas que usan para el cálculo de distintos parámetros. Al tratarse de desarrollos comerciales, no resulta fácil acceder y procesar los datos obtenidos de las medidas. En muchas ocasiones el mero acceso a los datos para la transmisión a otro sistema requiere de la adquisición de licencias adicionales.
- La gestión de los datos suele ser compleja. El uso de interfaces cerradas por parte de los distintos fabricantes hace necesario que la recolección de distinta información, desde distintas ubicaciones pueda ser compleja.
- El uso de dispositivos cerrados imposibilita la implementación y prueba de nuevas técnicas sobre los propios dispositivos de medida, obligando a que el

análisis no pueda realizarse en tiempo real, sino que requiera previamente descargar los datos del dispositivo.

- La mayoría de los equipos comerciales están orientados a funciones específicas (medida de potencia consumida, facturación, calidad eléctrica, automatización, etc.), no siendo habitual encontrar dispositivos que puedan desempeñar todas estas funciones de forma simultánea.

1.3. HIPÓTESIS

La hipótesis que se plantea en esta tesis, teniendo en cuenta las limitaciones indicadas en el punto anterior, consiste en intentar diseñar nuevas herramientas de medida que ayuden a superar las limitaciones de las soluciones comerciales. La solución deberá corresponder a una política de software libre, permitiendo el acceso a la información que se obtenga, a los métodos usados para su obtención e incluso al hardware necesario para la captura de esta información. Deberá de ser una herramienta de utilidad para distintos perfiles, incluyendo el de usuarios domésticos que demanden información básica sobre su consumo, usuarios más avanzado que desee conocer el estado de su instalación, usuarios industriales que necesiten automatizar diferentes procesos en función de determinados parámetros eléctricos, investigadores que implementen nuevas técnicas de análisis de variables eléctricas, e incluso estudiantes que intenten evaluar, por ejemplo, el impacto de distintas sobre los parámetros eléctricos de la red.

Para lograr este cometido, primero será necesario realizar una investigación del estado del arte de los dispositivos, algoritmos y técnicas existentes en el ámbito de los analizadores de red y medidores de calidad eléctrica. Una vez realizada, se diseñarán e implementarán los elementos hardware y software capaces de cumplir con los objetivos planteados. Sobre los elementos diseñados se desarrollarán estrategias de análisis para demostrar la flexibilidad del equipo. Una vez se disponga de este conjunto de elementos, estos deberán ser sometidos a examen en un entorno real y de laboratorio, donde se comprobará su funcionalidad y validez para su uso en distintas aplicaciones.

1.4. OBJETIVOS

El objetivo general que se persigue en esta tesis doctoral es analizar, diseñar, implementar y validar nuevas herramientas de análisis de redes eléctricas que permitan la obtención de

parámetros avanzados haciendo esta información accesible a todo tipo de usuario y solventando las distintas limitaciones existentes en los dispositivos comerciales. Para esto se establece una serie de hitos a alcanzar:

- *Fácil uso*: Los analizadores de red y medidores de calidad eléctrica, a menudo, son complejos de utilizar y su complejidad aumenta conforme se incrementa la información que facilitan. Por esto se busca que los dispositivos y software creados sean de uso sencillo, tanto en su instalación como manejo. Teniendo en consideración el amplio rango de perfiles al que se pretende servir será necesario proveer a los analizadores a desarrollar de la mayor simplicidad posible en cuanto a instalación se refiere, para lo cual se plantea un diseño versátil y de dimensiones reducidas. Además, se debe proporcionar una interface clara y concisa que permita un acceso estructurado y atractivo a la distinta información obtenida. En este sentido se considera que el dispositivo sea accesible desde cualquier navegador WEB, incluido el de dispositivos móviles.
- *Libre*: Entre los principales problemas de los dispositivos comerciales es la falta de transparencia, al ser imposible determinar los algoritmos usados internamente para los cálculos de variables de consumo o de calidad eléctrica. Por tanto, uno de los aspectos centrales que se plantean es que se trate de un diseño abierto, en todos los sentidos. Es decir, las herramientas utilizadas deben basarse en software libre, de forma que permitan al usuario reproducir todo el trabajo realizado. Además, los desarrollos también estarán abierto a la comunidad permitiendo a cualquier usuario tener acceso a los métodos de análisis implementados, al diseño completo del hardware, así como a su modificación y mejora, al objeto de adaptarse a las necesidades específicas que se puedan plantear en cada aplicación real.
- *Cumplimiento de estándares*: No todos los analizadores de red y medidores de calidad eléctrica están diseñados para el cumplimiento de los estándares, sino que se suelen limitar a aquellos de alta gama. No obstante, se plantea el cumplimiento de diferentes normas y estándares existentes, de forma que la precisión de las mediciones se pueda asimilar a los equipos de referencia. Como punto de partida se considera implementar las normas IEC 61000-4-30 en lo

referente a medida de parámetros de la red y la norma EN 50160 en cuanto a detección y clasificación de eventos.

- *Bajo coste*: El coste de los dispositivos de medida está directamente determinado por el número y características de las funcionalidades incorporadas. Así, no es extraño encontrar distintas versiones de una misma familia de analizador eléctrico cuyo coste varía sensiblemente dependiendo de las funciones programadas que incluyen. Por norma general es imposible para determinados usuarios obtener los parámetros de red requeridos por situarse los equipos de medida fuera de sus posibilidades. En otros casos, aunque los equipos no tengan un coste elevado, este sigue siendo alto para realizar el despliegue de gran cantidad de unidades en una red eléctrica y poder obtener datos simultáneos de distintos puntos de medida. Para solventar esta limitación el dispositivo debe de tener un coste muy reducido, que permita a un usuario doméstico su adquisición, o a una empresa o institución poder desplegar una red de distintos sensores de medida. El coste vendrá impuesto por un hardware de captura de señal y un SOM (*System On Module*) que realizará el análisis, esta arquitectura asegura que con un mínimo coste se pueda implementar el cálculo de todos los parámetros.
- *Accesibilidad a la información*: Un punto débil de los equipos de medida suele ser el acceso a la información obtenida. En muchos casos esta información es solo visualizable desde el propio software del equipo, en los casos que puede exportarse se utilizan formatos propietarios o la información está limitada. Aunque para un usuario doméstico esto puede no suponer un problema, el desarrollo de nuevas técnicas de análisis por parte de los investigadores requiere de un fácil acceso a los datos por parte de aplicaciones matemáticas u otro tipo. En otros sectores esta información puede ser necesaria para realizar informes, sobre facturación, estadísticas de consumo u otras variables. Una característica requerida, en línea con el carácter libre del desarrollo, es la disponibilidad de la información obtenida por distintos medios, de forma que según el nivel de usuario pueda elegirse el método más adecuado.
- *Capacidades de comunicación e integración en la nube*: Una característica necesaria, sobre todo cuando se trabaja con múltiples dispositivos que pueden estar desplegados en distintas ubicaciones, es la capacidad de acceso a la información generada de forma remota, independientemente de la ubicación del

dispositivo, del método de conexión utilizado o incluso de si este tiene conexión permanente o de forma intermitente. La disponibilidad de los datos en la nube es una característica habitual en algunos dispositivos domésticos, aunque es una función poco común en analizadores de red. Estas capacidades de comunicación para el envío a distancia de los datos permitirán dotar al dispositivo diseñado de las funcionalidades necesarias para ser utilizado en entornos en los que Internet de las Cosas puedan mejorar la operatividad.

- *Flexibilidad*: Sin duda uno de los objetivos de este trabajo es que los métodos y herramientas expuestos sean de ayuda al usuario, pero al mismo tiempo se permita la creación de nuevas funciones, módulos o incluso hardware de captura con más precisión o adaptado a otros rangos de medida. Esta funcionalidad se pretende demostrar con la incorporación de una técnica de análisis de potencia alternativa, que permita contrastar la información obtenida con las técnicas tradicionales.

1.5. METODOLOGÍA

El proceso de desarrollo de esta tesis se ha dividido en cuatro etapas claramente diferenciadas entre sí. En un primer lugar, se ha realizado el estudio de las diferentes disciplinas involucradas. Posteriormente se ha realizado el diseño e implementación de un dispositivo que integrara el hardware y software capaz de cumplir los objetivos propuestos. En una tercera etapa se ha evaluado el diseño realizado, aplicándose tanto en situaciones reales como en test de laboratorio. Como última etapa de este trabajo se ha ampliado el dispositivo diseñado, incorporando una teórica que permita reemplazar las técnicas clásicas de análisis de potencia en circuitos de corriente alterna, proponiendo una alternativa basada en herramientas matemáticas avanzadas.

Estas cuatro etapas pueden ser desglosadas en múltiples tareas que pretenden cumplir la hipótesis y los objetivos propuestos:

- La primera etapa ha incluido tareas como la formación e investigación previa para conocer tanto el estado del arte, como las técnicas y tecnologías que se consideran necesarias para el desarrollo de esta tesis, por tratarse del diseño e implementación de un dispositivo completo, se ha profundizado en los algoritmos de análisis de redes eléctricas, evaluación de calidad eléctrica y teoría de circuitos, pero también se han utilizado recursos

en el campo de la electrónica digital y analógica, programación de microcontroladores y sistemas operativos Linux.

- Durante una segunda etapa se ha elaborado un hardware de captura, que permita la adquisición de las distintas ondas de tensión y corriente desde la red eléctrica para alimentar el software del dispositivo en donde se ejecutará una serie de algoritmos de análisis, estadística, almacenamiento de datos, e interface de presentación al usuario. Esta etapa a su vez puede desglosarse en:
    - Selección de la plataforma más adecuada para la implementación, evaluando los módulos existentes en el mercado con la capacidad de ejecutar Linux u otros sistemas operativos abiertos, donde puedan ejecutarse aplicaciones como sistemas de gestión de bases de datos y servidores WEB que dispongan de potencia de cómputo suficiente para la implementación de distintos algoritmos de análisis, habilidades para comunicación inalámbrica, coste total, facilidad de uso dimensiones del módulo y consumo energético.
    - Evaluación de los microcontroladores existentes, valorando sus capacidades analógicas y opciones de comunicación con el módulo de control principal. Sera necesario evaluar los requisitos mínimos de memoria para la implementación del sistema de control y captura de las señales de tensión y corriente. Se optará por el microcontrolador más económico que cumpla con los objetivos.
    - Diseño del equipo que integre todos los elementos hardware, proporcionando la alimentación al sistema y adapte las señales de tensión y corriente para poder ser adquiridos por el microcontrolador. Una vez finalizado el diseño será fabricado un prototipo y será necesaria su validación para comprobar que cumple los objetivos de precisión de captura.
    - Selección de herramientas de programación, optando por aquellas que ofrezcan un alto rendimiento y permitan interactuar con el hardware a bajo nivel. Se optará por C++. Respecto a la interface de usuario se valorarán los frameworks disponibles para el desarrollo WEB. Se evitarán en todo lo posible la ejecución en lado del servidor de tareas innecesarias o en lenguajes interpretados que puedan tener un alto consumo de memoria.
    - Se diseñarán las estructuras de datos necesarias para almacenar la información requerida, y se evaluarán los métodos de almacenamiento persistente en bases

de datos. Se implementarán los algoritmos necesarios para la obtención de los parámetros de red que determinan los estándares a utilizar.

  - Se diseñará una interface de usuario, que permita un acceso completo a los datos obtenidos, se trabajará en la flexibilidad de esta interface, permitiendo el acceso desde distintos tipos de dispositivos. La información estará estructurada por categorías, siendo de fácil uso a distintos perfiles de usuario.
  - Se crearán métodos de comunicación y sincronización que permitan el acceso a la información obtenida, construyendo un servicio de cloud que centralice la información.

- La tercera etapa consistirá en la validación del dispositivo obtenido, realizando medidas en laboratorio, comparándose con otros dispositivos comerciales e instalándose en un entorno real para observar las lecturas y la utilidad del mismo para su uso en diferentes aplicaciones.
- En la última etapa se probará la capacidad de ampliación del sistema incorporando una teoría alternativa para el análisis de potencia que podrá ser evaluada contra las teorías clásicas.

CAPÍTULO 2 – OPENZMETER: AN EFFICIENT LOW-COST ENERGY SMART METER AND POWER QUALITY ANALYZER

Power quality and energy consumption measurements support providers and energy users with solutions for acquiring and reporting information about the energy supply for residential, commercial, and industrial sectors. In particular, since the average number of electronic devices in homes increases year by year and their sensitivity is very high, it is not only important to monitor the total energy consumption, but also the quality of the power supplied. However, in practice, end-users do not have information about the energy consumption in real-time nor about the quality of the power they receive, because electric energy meters are too expensive and complex to be handled. In order to overcome these inconveniences, an innovative, open source, low-cost, precise, and reliable power and electric energy meter is presented that can be easily installed and managed by any inexperienced user at their own home in urban or rural areas. The system was validated in a real house over a period of two weeks, showing interesting results and findings which validate our proposal.

2.1. INTRODUCTION

Electric energy meters are devices that are often installed in buildings and businesses in order to measure the amount of consumed electric energy [7] (i.e. these meters are installed for billing purposes [8]). However, the increasing awareness about energy consumption is not the only concern today [9]. The quality of the supplied energy is also an important feature, so it is necessary to introduce new technologies that provide end-users with up-to-date, online, real-time information about the quantity and quality of the power supply they receive from the utility [10].

There are several commercial and research devices [11] [12] that can be used to either measure the electric energy consumption or the power quality (PQ; power quality analyzers). Further, there are devices that integrate both functions, such that they include application software to download, analyze, and report energy consumption and power quality data. For example, some power quality analyzers are used by engineers, electricians, maintenance, and

facilities technicians to record power quality, carry out diagnostic work on electrical systems or devices, identify energy waste in facilities (in kilowatt hours, kWh), and detect and prevent power issues before they happen. Unfortunately, they are expensive and difficult to use for unskilled users, being utilized to carry out advanced energy saving audits. We firmly believe that the introduction of new technologies based on the open source paradigm can help users to better understand how to interact with electrical devices. In this sense, the information traditionally provided by utilities has made it difficult to consider efficient energy saving scenarios.

In this paper, openZmeter (oZm), an efficient low-cost single-phase smart electric energy meter and power quality analyzer is presented. oZm is the result of six years of research under the supervision of the research group TIC221 of the University of Almeria. Thanks to a multidisciplinary group of computer and electrical engineers, it has been possible to design and build an advanced device that combines and improves many features of much more expensive commercial devices under the aegis of open source software. This is a low-cost device because it can be assembled for less than 50 USD. It can also be easily installed in buildings to retrieve and process a large amount of information regarding the power supply and energy consumption. The consumption pattern and power quality events are visualized through a user-friendly supervisory control and data acquisition (SCADA) system thanks to the implementation of a simple and intuitive interface that people without technical knowledge can easily understand.

It provides advanced usage statistics that other devices cannot provide in an affordable and structured way. It can help to find energy consumption patterns thanks to its multiple visualizations. The power required and the energy consumed can be analyzed together in such a way that the user can determine, for example, whether they are demanding less power than that which is actually contracted.

The rest of the paper is organized as follows: Section 2 presents a brief overview of electric energy metering. Section 3 presents the designed single-phase smart electric energy meter and power quality analyzer, including the technical specifications and the installation procedure in buildings. Section 4 presents an analysis of its usage in a real environment, while the main conclusions are summarized in Section 5.

2.2. AN OVERVIEW OF ELECTRIC ENERGY METERING

Since energy consumption is becoming more prevalent in residential, commercial, and industrial installations, the research in this topic has become significant in recent years. In particular, the rising energy prices are promoting higher levels of energy efficiency, which requires an accurate quantification and management of energy consumption. The energy management requirements at both service supplier and consumer sides promoted the evolution of smart grids [13], with the aim of reducing the generation and operation costs in power systems and the hydrocarbon emissions [14]. The smart grid is the evolution of the electrical grid thanks to using new technologies that increase the efficiency of the system and minimize outages. A smart grid is an electrical grid which includes a variety of operational and energy measures including smart meters and efficient energy resources, including renewable energy. These devices allow the electricity supplied to consumers to be controlled via two-way digital communication. Smart cities, smart buildings, and smart homes also play a key role in the new era of smart connected devices.

Smart metering favors the efficient use of energy resources by providing high-resolution data [15], such that this equipment is essential to study electrical installations and energy consumption in industrial [16], commercial [17], and residential [18] environments. In particular, real-time activity recognition for energy efficiency in buildings is a critical issue to design better buildings and automation systems [19]. In addition to the use of electric energy meters to retrieve information about the energy consumption, power quality monitoring is another important issue to be addressed [20]. Power quality analyzers allow the measurement of a wide variety of power quality parameters and events, including harmonic distortion and short-term disturbances such as transients, voltage sag, and swell or power-line flicker.

Many papers have analyzed the use of electric energy meters [21] and power quality analyzers [16] in different environments. Although there are many commercial electric energy meters and power quality analyzers, they are often expensive and difficult to use for the average consumer, being mainly used by engineers and technicians to perform maintenance activities or energy audits [22]. Only a few authors have proposed the use of low-cost devices to perform these tasks. For example, authors in [23] presented a portable battery-powered energy-logger circuit to monitor the energy harvested by different piezoelectric converters. Other researchers have designed devices that include the functionalities of a power quality

analyzer, an event logger, a synchronized phasor measurement unit, and an inter-area oscillation identifier [24]. Recently, a metering system that measures the reactive energy component through the Hilbert transform in low-cost measuring devices was presented [25]. A low-cost power quality analyzer based on frequency analysis was described in [26] for monitoring the power supply waveform and to detect some power quality events. The OpenEnergyMonitor is another open source home energy monitoring system for analyzing real-time power use and daily energy consumption [27]. The key role of open source systems is also revealed in [28], where smart meters and an energy management system are integrated in the smart grid context. The increasing trend that open source resources constitute nowadays is evidenced not only for energy measurement, but for a number of scopes as shown in [29] [30] [31] [32].

Being an open source system, you can add interesting features such as non-intrusive load monitoring (NILM), new statistics, etc., which cannot be done in closed and commercial systems. Although there are some other devices on the market, they generally have much lower functionalities. The energy monitors present on the market perform very basic functions and estimate energy with great error. oZm meets several international standards (e.g., IEC 62052 regarding energy metering) and guarantees a very small error in measurement. It is also very versatile and can display information from different sources and scopes. As shown in Table 1, oZm outperforms some very well know smart devices on the market, being the only one to simultaneously measure power, energy, frequency, voltage, current, harmonics, phase, power factor, THD, phasors, and many more. It is also the only open source system with an application programming interface (API) that allows real-time prices to be obtained from national utilities (e.g., REE in Spain) or wide set options for network communication based on Linux reliability.

Table 1 Feature comparison between commercial and open source meters.

	oZm (openZmeter)	Flukso	OpenEnergyMonitor	OpenPowerQuality	Geo Minim	Current Cost	Efergy	Alertme	Wibeee	Sense Energy Monitor	CURB	PQUBE3	Smapee	Neurio
Active Energy	Yes	Yes	Yes	No	Yes	Yes	Yes	Yes	Yes	Yes	Yes	Yes	Yes	Yes
Reactive Energy	Yes	No	No	No	No	No	No	No	No	No	No	Yes	No	No
Active Power	Yes	Yes	Yes	No	Yes	No	Yes	Yes	Yes	Yes	Yes	Yes	Yes	Yes
Reactive Power	Yes	No	No	No	No	No	No	No	No	No	No	Yes	No	No
Apparent Power	Yes	No	Yes	No	No	No	No	No	No	No	No	Yes	No	No
Frequency	Yes	No	No	Yes	No	No	No	No	No	No	No	Yes	No	No
RMS Voltage	Yes	No	Yes	Yes	No	No	No	No	Yes	No	No	Yes	Yes	Yes
RMS Current	Yes	No	Yes	No	No	No	No	No	Yes	Yes	No	Yes	Yes	Yes
Power Factor	Yes	No	No	No	No	No	No	No	No	No	No	Yes	No	No
Angle	Yes	No	No	No	No	No	No	No	No	No	No	Yes	No	No
Voltage Events	Yes	No	No	Yes	No	No	No	No	No	No	No	Yes	No	No
4 Quadrant	Yes	No	No	No	No	No	No	No	No	Yes	Yes	Yes	No	Yes
EN50160	Yes	No	No	No	No	No	No	No	No	No	No	Yes	No	No
IEC61000-4-30	Yes	No	No	Yes	No	No	No	No	No	No	No	Yes	No	No
High Samp. Rate	Yes	No	Yes	Yes	No	No	No	No	No	Yes	Yes	Yes	No	No
Aggr. Interv.	Yes	No	No	No	No	No	No	No	No	No	No	No	No	No
HTML5 Interface	Yes	Yes	Yes	Yes	No	No	No	Yes	Yes	Yes	Yes	No	Yes	Yes
Alert System	Yes	No	No	Yes	No	No	No	No	Yes	Yes	Yes	No	Yes	Yes
ITCI/CBEMA	Yes	No	No	Yes	No	No	No	No	No	No	No	No	No	No
Zero Crossing	Yes	No	Yes	Yes	No	No	No	No	No	No	No	Yes	No	No
FFT	Yes	No	No	Yes	No	No	No	No	No	Yes	No	Yes	No	No
Harmonics	Yes	No	No	Yes	No	No	No	No	No	No	No	Yes	No	No
THD	Yes	No	No	Yes	No	No	No	No	No	No	No	Yes	No	No
4G	Yes	Yes	No	No	No	No	No	No	No	No	No	No	No	No
Wi-Fi	Yes	Yes	Yes	No	Yes	No	No	No	Yes	Yes	Yes	No	Yes	Yes
Ethernet	Yes	Yes	Yes	Yes	No	No	No	Yes	No	No	No	Yes	No	No
API	Yes	Yes	Yes	No	No	No	No	No	No	No	No	No	No	No
Realtime Pricing	Yes	No	No	No	Yes	No	No	Yes	No	No	No	No	No	No
Phasor	Yes	No	No	No	No	No	No	No	No	No	No	No	No	No
Telegram	Yes	No	No	No	No	No	No	No	No	No	No	No	No	No
Open Source	Yes	Yes	Yes	Yes	No	No	No	No	No	No	No	No	No	No

2.3. THE OPENZMETER (OZM)

In this section, the physical layout is described and technical specifications of the open-source and open-hardware smart electric energy meter and power quality analyzer are presented, under the name of “openZmeter” (oZm, read as “open zeta meter”).

2.3.1. Physical layout

Figure 1 shows the general scheme of the single-phase oZm and a picture of the real device. oZm has an analog front end (AFE) that is responsible for capturing the voltage and current waveforms. The voltage is acquired using a simple resistive divider (0.1% and 100 ppm/ºC tolerances) that cut down the 120/230 voltage to a much smaller input value suited for the onboard analog-to-digital converter (ADC). The current is measured by an integrated Hall-effect (Infineon TLI4970) sensor up to 50 A of peak value and 1% precision (factory calibrated). Current clamp sensors or Rogowsky coils can also be used to measure hundreds or thousands of amperes in bigger buildings. Both Hall effect and current clamp/Rogowsky current channels are synchronized with the voltage resistor using software-corrected algorithms (maximum deviation is less than 0.5 µs) to avoid significant phase errors. The oZm device is powered directly by the grid using an isolated AC/DC source, which provides all the necessary energy for the circuitry. A lithium-ion battery is also used to power the board and keep the system running for hours in under-voltage or interruption conditions. When main power is restored, the system switches automatically (without restarting) and the battery is then recharged. The oZm has galvanic isolation for the voltage and current inputs and the ARM board through optocouplers.

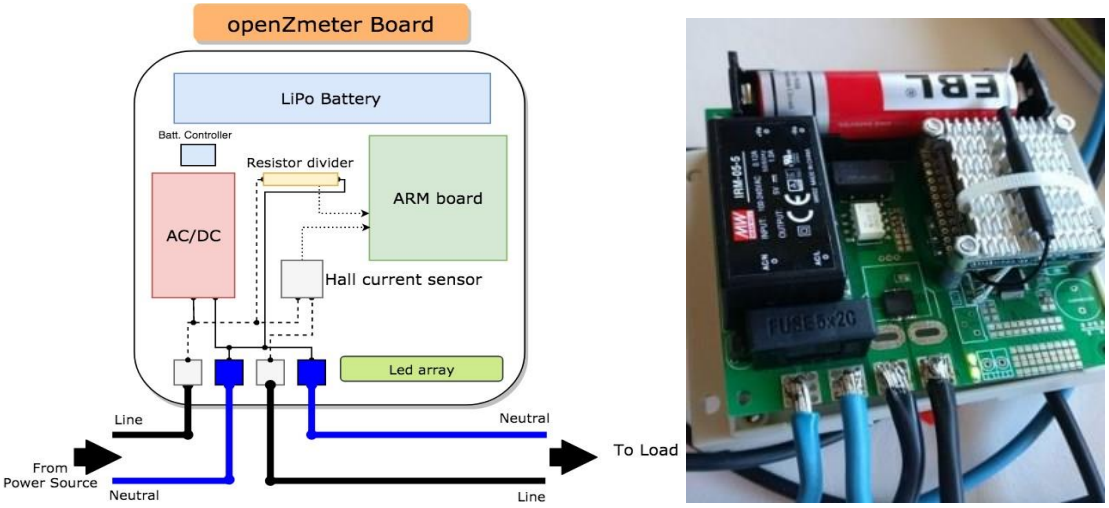

Figure 1 Schematic diagram of the oZm; Physical layout of the oZm.

Commonly used approaches for PQ monitoring and smart metering are widely based on the use of microprocessors, data acquisition cards, hybrids, and FPGA hardware. Each approach has its own advantages and drawbacks. In this case, the PQ monitoring and smart metering device is designed by coupling a Linux ARM board and an AFE managed by an STM32 microcontroller. The ARM Linux controller is easy to manage, and it is also low cost. The ARM Linux gives much more flexible software compared to any other device. We use the NanoPi Neo Air ARM board, which is a powerful system equipped with an H3 Allwinner Cortex-A7 quad-core at 1.2 GHz and 512 MB of DDR3 RAM.

Due to space limitations, it is difficult to conveniently detail all the components used as well as their structure and price (though it is worth mentioning that the ARM board is about 20 USD).

The interested reader can go to https://gitlab.com/zredalmeria/openZmeter/wikis/home (accessed on 8 May 2012), where there is a detailed list of components and the functionality of each element of the AFE and ARM.

2.3.2. Technical specifications

The accuracy of the measurement results depends on the correctness of the measurement algorithms implemented in the meter and the quality of its calibration [33], along with the quality and accuracy of the external probes used. The oZm fulfills these requirements by implementing a voltage divider for the voltage stage and a Hall-effect sensor with less than 1% error (calibrated from factory). The algorithm was implemented from scratch, combining our code with open source libraries. The system runs a Debian Linux operating system where some well-known open source libraries are used, such libmicrohttpd, postgresql, etc. (we refer the reader to our wiki mentioned above). All the data are stored locally thanks to the onboard EMC memory with up to 16 GB capacity. An SD card can also be added to extend the storage. This implies that oZm is completely autonomous and there is no need to use any external cloud. In any case, an API is provided to send data to the cloud. Remote monitoring can also be accomplished in two ways, that is, using a telegram bot specially designed to access the data in a simple and easy way or using a simple web browser (in this case the local router should be configured properly or a VPN should be used) to connect to the local web server which runs on top of the libmicrohttpd library. oZm implements a security feature to

access both the web interface (user and password by default), https protocol, and encrypted data for API communication. The main characteristics of oZm are:

- Free and open system: open source software and hardware.
- Electrical measurements: effective voltage and current values, active, reactive, apparent and distortion power, power factor, harmonics (up to order 50), active and reactive energy, frequency, voltage events (gaps, over-voltages, interruptions) in real-time and stored in database.
- Measurement in four quadrants to measure consumption and generation of energy. Valid for renewable energy systems (e.g., photovoltaic, wind, etc.).
- Testing according to the international standards IEC 61000-4-30 and EN 50160.
- Voltage measurement with precision of 0.1% for raw values. Frequency measurement with precision of 10 mHz (in the range 42.5–57.5 Hz). Current measurement up to 50 A (integrated Hall-effect sensor). Current clamp or Rogowsky coil as an option.
- Sampling frequency of 15,625 Hz (64 μs between samples).
- Frequency measurement is performed using a digital input filter to minimize noise and interharmonic components. According to IEC61000-4-30, 10 s of signal are taken and the zero-crossing method is applied.
- Aggregation in the voltage channel of 10 cycles, 3 s, 10 min according to standard and one hour as extra aggregation for energy.
- Cutting-edge web based on HTML5, CSS3, and JavaScript for data analysis and SCADA.
- Alert system and event management (ITIC/CBEMA, frequency, over voltage and under-voltage, interruptions, etc.).
- FFT integration, zero crossing, and RVC from scratch (Rapid Voltage Changes according to IEC61000-4-30 with 5% threshold).
- Time synchronization based on NTP time service. Time error less than 20 ms using Chronyd daemon.
- User-friendly and powerful interface.
- Modular, with the possibility of adding new capture modules.
- Connectivity: USB ports (Wi-Fi dongle, 3G/LTE/4G, etc.), Ethernet port, and Wi-Fi. SPI, I2C, UART and PWM are also available.

- Connection to the grid operator's information system (ESIOS) to get daily energy prices and calculate the cost of energy in real-time.
- Integration with Telegram applications for the generation of periodic reports and alerts in real time. Remote access to relevant information.
- Specific API for third-party integration based on JSON.

Despite the long list of features implemented in oZm, it is also necessary to note that there are some limitations that must be taken into account, and that are often present in some open source projects, such as the lack of technical support in hardware certification or the adoption of measures for a centralized mass deployment.

2.3.3. Building configuration and setup

The configuration of oZm can be easily achieved using Ethernet or Wi-Fi. The setup is typically carried out into the low-voltage circuit breaker panel of the building. Its placement and wiring is similar to any traditional or modern electric energy meter, so that nominal voltage is applied to an internal resistive divider that provides a low-voltage output linear to the input voltage for the ADC. The board tracks were precisely calculated for the current flowing through them. The width was calculated to avoid heating caused by Joule effect losses. Figure 2 shows the oZm setup. It is easily installed in any home circuit breaker panel. Moreover, the single-phase oZm can also be used in large buildings, by placing several devices in different locations to optimally and robustly monitor the electrical parameters [34].

2.4. USAGE ANALYSIS IN A REAL ENVIRONMENT

2.4.1. Description of the environment

The data acquired from an oZm installation in a home were analyzed. Specifically, it was a family home with two adults and three children. The house has 150 square meters in 5 rooms and a list of home appliances including an oven, a dishwasher, a washing machine, television, electric water heater, in addition to other electronic devices, plus 10 energy-saving light bulbs and 20 points of light (plugs) where other electronic devices such as laptops, tablets, or irons are sporadically connected. In order to show the most interesting information obtained by oZm, measurements were taken during two weeks (January–February 2018) every 200 ms (10 cycles of 50 Hz) as described in the following subsection.

Figure 2 Installation of oZm in the electric panel of a building.

2.4.2. Data analysis

The data collected allows information to be obtained about both the energy consumption and the power quality. This information is first retrieved and analyzed using statistical tools [35], and the results are then displayed in a powerful graphical interface that was specifically designed for oZm.

Figure 3 shows the main view or dashboard of oZm. It includes the basic magnitudes, including the active energy consumption (kWh) in different periods that can be displayed with different time span aggregation. All the plots shown share a common template based on HTML5, CSS3, JavaScript, and JQuery, thus providing information about the RMS voltage, RMS current, frequency, and active power for a 3 s aggregation interval. The top subplot in Figure 3 shows the active energy consumption for a fixed time span, but these data can be aggregated based on nominal values: 3 s, 1 min, 10 min, and 1 h. The data are stored in an SQL-like database (PostgreSQL) and can be retrieved for a day, week, month, or year. These measures can be analyzed with more detail. For example, Figure 4 shows the average, maximum, and minimum magnitudes of voltage in a time-period using different aggregation scales, and the voltage waveform (oZm can serve as an oscilloscope for waveform diagnosis).

The frequency of the alternating current (AC) in a power grid is mainly defined at 50 (e.g., Europe) and 60 (e.g., North America) Hz. Although the frequency of a power system is strictly regulated, it is not always stable due to the continuous load changes on the power grid, the generator's response to these changes, and the short-term scheduling of power plants. In this regard, Figure 5 shows how oZm is able to capture these variations in the frequency of the power supply. This graphic shows small variations that are probably due to changes in the loads of the power grid, and large variations due to the hour-by-hour scheduling of the power plant's generation controlled by Red Eléctrica de España (REE), the system operator in Spain. The accuracy of oZm is much higher than 10 mHz, although only 10 mHz steps are shown on the *Y*-axis.

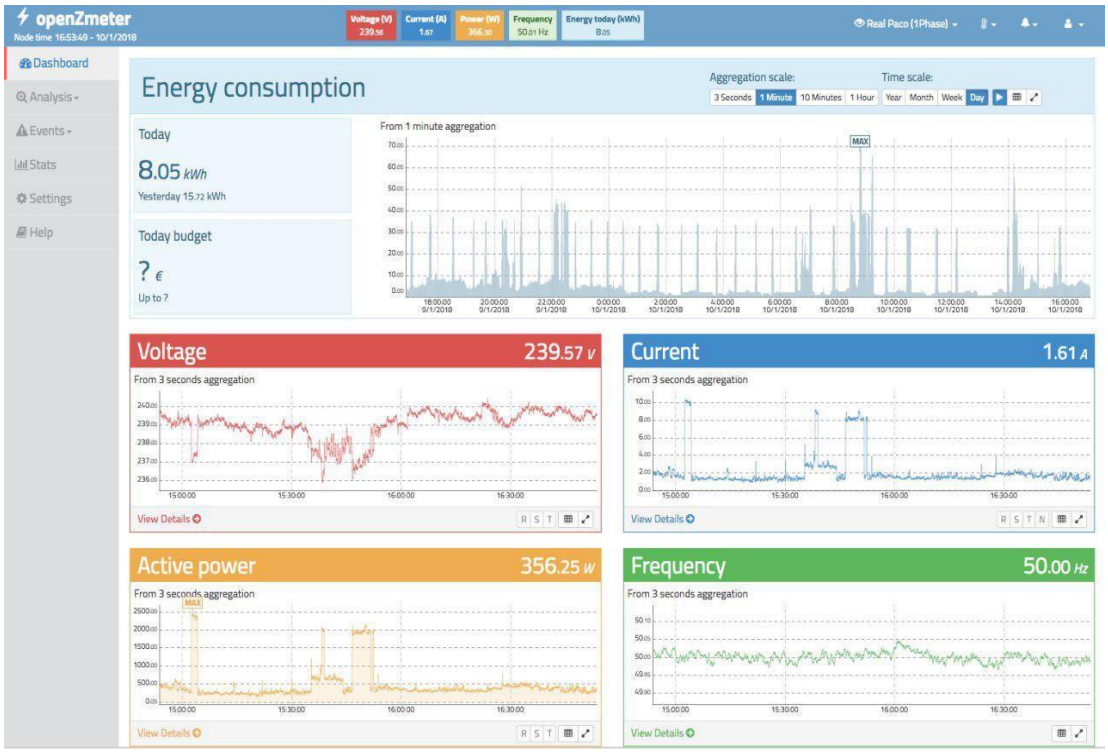

Figure 3 Dashboard of oZm. From top to bottom and left to right, active energy, RMS voltage, RMS current, active power, and frequency are shown.

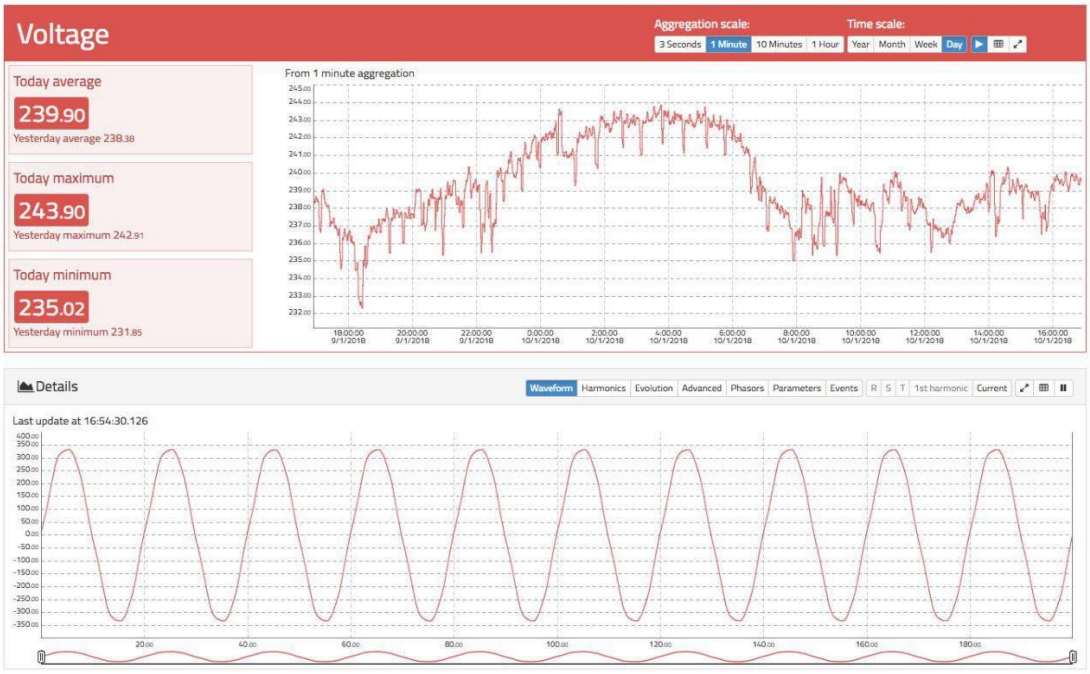

Figure 4 Detailed information about the voltage.

Figure 5 Frequency of the power supply.

oZm also provides detailed information about power quality measurements, and events captured during the normal and abnormal operation. For example, Figure 6 shows the ITIC (CBEMA) [36] tolerance curve, which is often used to visibly represent voltage events that can cause problems or undesired behavior in electronic devices. In particular, detecting harmonics in the electrical power distribution system is an important issue. Harmonics combine with the fundamental frequency (50 Hz in our case) supply to create distortion of the current and/or voltage waveforms. In Figure 7, an advanced time–frequency plot is shown for harmonics visualization. This visualization is suitable for plotting a high number of subgraphs using a reduced vertical space [37], such that every row represents a harmonic component for the last 24 h up to the 50th order. In particular, darker tones mean higher absolute values, while red color refers to values above 0 dB and blue refers to values below 0 dB.

Figure 6 The ITIC (CBEMA) curve in the oZm graphical interface.

Figure 7 Harmonic amplitude evolution for the first 16 harmonic components.

2.5. CONCLUSIONS

Electric energy meters and power quality analyzers are often used by power engineers and technicians to discover the health state of power systems. However, these professional devices are often expensive and difficult to handle for non-expert users. To overcome these

drawbacks, this paper presents openZmeter (oZm), an open source, low-cost, and efficient single-phase energy smart meter and power quality analyzer that can be easily installed and used by inexperienced users at their homes in urban or rural areas. This device is able to retrieve a large amount of information related to energy consumption and power quality, satisfying national and international power quality standards. This work demonstrates that the use of open source systems can help sustainability and, more specifically, sustainable energy use by providing valuable information to users so that they can make energy-saving decisions supported by reliable and open data obtained in real environments. The use of open devices that provide relevant information in real time within the framework of intelligent networks is therefore shown to be worthwhile. In order to show the novel features of this device, it was installed in the circuit breaker panel of a house for several weeks. Results obtained were satisfactory, since it was possible to verify how oZm retrieves an important amount of data that is processed and visualized using an advanced graphical interface. The graphs included in this paper (energy consumption, voltage and current waveforms, frequency, and power quality events) can be easily interpreted by expert and non-expert users. As a future work, it is planned to extend the analysis to large buildings by deploying a network of sensors in different locations. Furthermore, the three-phase version of oZm is in an advanced stage of development and should be available in the next months.

CAPÍTULO 3 - AN OPEN HARDWARE DESIGN FOR INTERNET OF THINGS POWER QUALITY AND ENERGY SAVING SOLUTIONS

An important challenge for our society is the transformation of traditional power systems to a decentralized model based on renewable energy sources. In this new scenario, advanced devices are needed for real-time monitoring and control of the energy flow and power quality (PQ). Ideally, the data collected by Internet of Thing (IoT) sensors should be shared to central cloud systems for online and off-line analysis. In this paper openZmeter (oZm) is presented as an advanced low-cost and open-source hardware device for high-precision energy and power quality measurement in low-voltage power systems. An analog front end (AFE) stage is designed and developed for the acquisition, conditioning, and processing of power signals. This AFE can be stacked on available quadcore embedded ARM boards. The proposed hardware is capable of adapting voltage signals up to 800 V AC/DC and currents up to thousands of amperes using different probes. The oZm device is described as a fully autonomous open-source system for the computation and visualization of PQ events and consumed/generated energy, along with full details of its hardware implementation. It also has the ability to send data to central cloud management systems. Given the small size of the hardware design and considering that it allows measurements under a wide range of operating conditions, oZm can be used both as bulk metering or as metering/submetering device for individual appliances. The design is released as open hardware and therefore is presented to the community as a powerful tool for general usage.

3.1. INTRODUCTION

As electricity distribution grids are being developed, the need for metering has increased. In 1977, Paraskevakos [38] presented the first automatic and commercialized remote meter. Nevertheless, the concept of remote and smart metering was not considered for many years. Many concerns in recent years have arisen, including climate change, trends in the electricity markets, efficiency, and the promotion of renewable energy resources. In addition, other

active agents in power systems are promoting distributed grids with distributed storage. This drastic change requires an evolution in the actual electricity model [2].

The core of the smart grid concept resides in an electricity grid model able to treat different energy sources in an efficient and decentralised manner. The capability for a new metering system or smart metering will manage this smart grid. Smart metering or an intelligent metering system is defined as “an electronic system that can measure energy consumption, providing more information than a conventional meter, and can transmit and receive data using a form of electronic communication.” This definition was established by the European Parliament in its 2012/27/EC directive [39]. The implementation of the energy efficiency directive can be found in [40].

This implementation of the energy efficiency directive is a consequence of the transition of power grids from centralised generation to distributed generation, motivated by global trends in environmentally friendly power generation systems. This is possible if the real state of the grids is known. This requires fine-grained knowledge of the state itself. The concept of the smart grid allows for the delivery of electricity in a controlled system.

A smart grid is an electric grid that joins points of generation to points of consumption, which recognize the real state of the net. Since a smart grid is conceived to deliver electricity, the consequence is the emergence of new and developing technologies in power generation, transmission, and distribution. This can be considered as a class of technology driven by recent advances in renewable energy sources and modern communications and computation technologies [41]. The electric grid is more than a generation and transmission infrastructure. It is an ecosystem with assets from government, providers, manufacturers, and owners. This technology set up three foundations: advanced renewable energy sources, control systems, and computer processing [42]. These advanced technologies must be composed with advanced sensors known as advanced measurement units or multipurpose network analysers and smart meters [43], allowing operators to assess grid stability and provide consumers with better information including automatically reported outages. The system includes relays that sense and recover from faults at a substation automatically, automated feeder switches that reroute power around problems, and batteries that store excess energy and make it available later to the grid to meet customer demand.

Many studies have highlighted the advantages derived from the progressive development of distributed generation systems, smart grids, and microgrids [44] [45]. Under this new paradigm, some authors have drawn attention to the importance of developing new sensors and tools for the real-time monitoring and control of the energy flow and power quality. For example, in [46] the residential power consumption is modelled using smart meters and data mining techniques. Other researchers have proposed systems for real-time detection and classification of power quality disturbances in smart grids [47]. These smart metering systems are often integrated with computing and communication technologies to enhance efficiency and reliability of future power systems with renewable energy resources [48]. Further, smart meters include efficient control and processing algorithms [49]. In [50] smart handheld devices were used to perform the real-time monitoring and fuzzy control strategies of an intelligent windowsill system in a smart home. In [51] neural network and swarm intelligence approaches were successfully applied to analyse the dynamic operation and control strategies for a microgrid hybrid power supply systems. Moreover, the system stability has also been considered in by some researchers. In [52] it was proposed a direct building algorithm for microgrid distribution ground fault analysis that consider the network topology changes. The topological characteristics of the microgrid are also considered in [53], where it was proposed an unsymmetrical faults analysis method with hybrid compensation for microgrid distribution systems. In [54] it was proposed an optimization algorithm to manage real-time congestions using all power system capabilities.

Complex networks and the advance of electronic devices have inspired the power quality (PQ) concept [55], that is, the measurement of the amount of disturbance in the electricity supply, which is later assessed. Millions and millions of electronic devices are plugged into the grid, affecting the global grid. Most PQ problems result from grid-connected distributed generations. In addition, nonlinear electronic loads introduce PQ disturbances into the grid because electric car chargers, rectifiers, lighting, switch-mode power supplies, and other power electronic devices are commonly used [56].

PQ disturbances such as swell, sag, interruption, oscillatory transients, flicker, and harmonic distortion are becoming challenging issues for power systems. Modulated power sinusoids have also been detected. Both can manifest as steady-state or transient states. These disturbances may impose penalties on consumers by adding reactive power, redispatch costs, and load curtailment costs. Moreover, these PQ problems can overheat the

transformers, damage capacitor banks, and affect sensitive electronic equipment [57]. Owing to the increase of these issues, scientists and engineers have started to study them through significant number of PQ studies [58] [59] [60] [61]. Electric power quality monitoring has become an essential part of these studies [62].

Mitigating actions against power quality disturbances must be taken, and their sources and causes must be identified accurately as well. Power quality disturbances must be detected, recognized, and classified [63] [64]. Engineers have to select the appropriate technique for extracting any power quality disturbance in order to recognise and classify them. In recent years, many techniques (apart from Fourier and Short Time Fourier Transform) have been implemented for extracting these features of power quality disturbances, including the S-transform [65] where a new detection and classification method of power quality disturbances based on S-transform, interpolating windowed fast Fourier transform (FFT), and probabilistic neural network (PNN) was proposed; wavelet transform [66] where wavelets and fuzzy support vector machines are used to automated detect and classify power quality (PQ) disturbances; Kalman filters [67] where a practical model describes the behaviour of electric arc furnaces in the simulation of power system for power quality issues; Gabor transform and Wigner distribution function [68] where improved Gabor-Wigner transform algorithm is studied and applied to power quality disturbance detection; empirical mode decomposition [69] where performance comparisons of Support Vector Machine (SVM) and different classification method for power quality disturbance classification is presented; compressive sensing (CS) [70] where a new approach for classifying multiple power quality disturbances (PQD) is presented; curvelet [71] where a new scheme based on curvelet transform and support vector machine is proposed; Hilbert transform [72] where a new classification method of transient disturbance based on Hilbert transform and classification trees is proposed; Hilbert-Huang transform [73] where the power quality in the distribution network is considered to characterize power signal disturbances; and hybrid transform-based methods [74] where a sparse method for PQ representation, starting from overcomplete dictionaries, is introduced. These techniques are used as input to a classifier such as support vector machine [75] where a new hybrid algorithm is presented for PQ disturbances detection in electrical power systems with SVM; fuzzy logic [76] where a fuzzy logic based online fault detection and classification of transmission line using Programmable Automation and Control technology based National Instrument Compact Reconfigurable i/o (CRIO) devices is

introduced; ensemble technique [69] where performance comparisons of SVM and different classification method like ensemble mode decomposition for power quality disturbance classification is analyzed; deep learning [77] where a deep learning-based method is introduced into the classification of power quality disturbances; artificial neural network [58] where a conjugate gradient back-propagation based artificial neural network for real time power quality assessment is proposed; and maximum likelihood classifier [78] where a newly developed CS, maximum likelihood (ML), and rule-based method for classification of power quality disturbances.

The technology for smart metering is a heterogenous infrastructure that includes many branches of engineering: communication networks, data processing, management, and installation. The minimum infrastructure for this system of smart metering is the electronic device for metering (smart meter), a cloud-based data gathering system, a communication system (normally based on the Internet), and a computational centralised center. A few academic researchers have presented energy meters and power quality analysers, but up to now, most of the installations are monitored by using commercial devices. However, these devices are often expensive and difficult to manage by non-expert users. Therefore, it is a challenge to develop low-cost and high-precision devices for general usage in any type of electrical installation. This is precisely the main contribution of oZm, a small-sized open source, low-cost, precise, and reliable power and electric energy meter aimed to help people to analyze and visualize energy consumption measures complying with international standards such as IEC 61000-4-30 and EN-50160. Herein, the openZmeter (oZm from now on) device is described as a key part of a smart metering infrastructure. This electronic device is a major redesign of the basic prototype in [79]. It is low-cost, single-phase open-hardware, with advanced bidirectional capabilities applied to monitoring electric features and cloud-based data gathering. This smart meter presents a wide range of features, which accomplish the minimum desirable requirements for an electricity smart meter as published in recommendation 2012/148/EU [80]. The smart meter here presented is useful to monitor and prevent distribution network problems. Thanks to the features of oZm, it is possible to receive information about significant events detected in the electrical installations. By monitoring these abnormal situations, e.g., high power consumption or significant power quality disturbances, it would be possible to implement preventive strategies.

The main contribution of this paper is to present a professional low-cost open-source hardware device for power quality and energy metering and submetering for the Internet of Things. The advanced design of oZm ensures reliable and accurate energy consumption and power quality measurements under a wide range of operating conditions in a single handy device. Given its small size and large variety of current probes, it can be easily installed at any electrical installation, i.e., it can be used both as bulk metering or as metering/submetering for individual units or appliances. Unlike other typical low-cost data loggers or meters like those analyzed in [81], oZm records all electrical parameters and events following international standards. Finally, other important contribution of the paper is to present and display a large number of measurements with an user-friendly interface that can be customized according the particular needs.

Table 2 Nomenclature

Nomenclature	
AC	Alternating Current
ADC	Analog Digital Converter
AFE	Analog Front End
ARM	Advanced RISC Machine
CBEMA	Computer & Business Equipment Manufacturer's Association
CRIO	Compact Reconfigurable i/o
CS	Comprensive Sensing
CSV	Comma-Separated Values
DC	Direct Current
DSP	Digital Signal Processing
FFT	Fast Fourier Transform
FPGA	Field Programmable Gate Array
HHT	Hilbert-Huang Transform
HTML	HyperText Markup Language
IC	Integrated Circuit
IEC	International Electrotechnical Commission
IoT	Internet of Things
ITIC	Information Technology Industry Council
JSON	JavaScript Object Notation
ML	Maximum Likelihood
MOSFET	Metal-Oxide-Semiconductor Field-Effect Transistor
NTP	Network Time Protocol
oZm	openZmeter
PCB	Printed Circuit Board
PNN	Probabilistic Neural Network
PQ	Power Quality
PQD	Power Quality Disturbances
RC	Resistor-Capacitor
RMS	Root Mean Square
RVC	Rapid Voltage Change
SVM	Support Vector Machine
THD	Total Harmonic Distortion

The rest of the paper is organized as follows: Section 2 presents a detailed overview of the hardware and software of the smart meter design. Section 3 presents an analysis of its usage in a real environment, while the main conclusions are summarized in Section 4. The acronyms used in the text are listed in Table 2 in alphabetic order together with their meaning in full words as found in literature.

3.2. IOT POWER QUALITY AND SMART METER DESIGN

Herein, an open-hardware platform for PQ monitoring and smart energy metering is designed, developed, and manufactured. This electronic device was designed for monitoring PQ events, voltage, and current waveforms (along with other advanced features) following the specifications given by international standards such as IEC 61000-4-30 and EN-50160. The system for PQ monitoring and smart metering can be considered an Internet-based power quality monitoring and smart metering system because of its accurate probes and embedded server that manage all PQ and energy information over the Internet or a local network. Raw and processed values can be accessed locally from an internal database through a web application or uploaded to a central server in the cloud for massive deployment.

Currently, single-phase hardware has been successfully built, and a three-phase version is already in the prototype stage. Because of its characteristics, this single-phase version is mainly used in domestic environments, but there is no limit to using it elsewhere if the current is below 35 A RMS because the Hall effect current sensor used is limited to a 50-A peak value. However, the system is able to accept any other current probe (split-core, Rogowski, etc.) if the voltage output is between ±1.25 V. All components are isolated from the main voltage in order to allow safe operation of the system. For industrial applications, the three-phase version is recommended. In this case, high-accuracy current clamps or Rogowski coils should be used to sense the current.

The core of the Analog Front End (AFE) is the STM32F373 from the STM32 microcontroller family, which combines high performance, real-time capabilities, digital signal processing, and low-power operation. The STM32F373 is the smallest micro in the family with onboard 16 bit Analog Digital Converter (ADC). In this case we looked for the highest precision without increasing too much the number of components, thus avoiding the use of external ADCs. Also, the manufacturer STMicroelectronics classifies this model as "High precision line" for metering purposes. The onboard ADC is used for signal sampling and conditioning. The

conditioned signal is filtered and limited. Then, a correction for gain and offset is applied. This ADC can sample values up to 16 kHz per channel.

The current and voltage signals converted are preprocessed by the digital signal processing (DSP) module of the STM32 using custom signal algorithms designed by the authors. Afterward, the output is sent to a powerful embedded ARM board for final processing. Complex calculations such as FFT, zero crossing, and RMS values are then executed by a Linux core (the host), where a daemon service is run in an endless loop in real time. This real-time strategy allows to implement priorities for threads and queues, so that critical processes are treated with a high priority and less critical processes have a low priority.

The software and hardware repository is publicly available and can be accesed at https://gitlab.com/zredalmeria/openZmeter.

3.2.1. Hardware structure of oZm

Advanced electronics such as microprocessors or field programmable gate array (FPGA) devices are commonly used for PQ monitoring and energy smart metering. Every choice has its own advantages and drawbacks. Recently, the use of highly efficient and low-cost ARM boards has been demonstrated to be a real option when coupled to other microcontrollers. In our case, smart metering and PQ monitoring are accomplished using a Linux ARM board and AFE managed by an STM32 microcontroller.

In terms of cost, this approach is the most efficient. Within the evolution of hardware, it is possible to find low-cost DSP devices that can work at high speeds with more integration and more features at a cheaper cost. Moreover, the ARM Linux controller is reliable, efficient, and low-cost. It has also been proven to be much more flexible than any other device thanks to its software repositories and packages. Figure 8 shows a block diagram for the oZm hardware, where four main blocks can be identified. The first one (coloured in green) is the signal acquisition stage for current and voltage. An accurate resistor divider is used to sense and reduce the main voltage to a low level around a few volts. Filtering and correction are applied using a low-pass filter in order to avoid aliasing effects. The current is sensed by means of a Hall effect integrated circuit (IC) from Infineon. The second block (coloured in orange) is composed of a power supply and management elements, including the Li-Po battery.

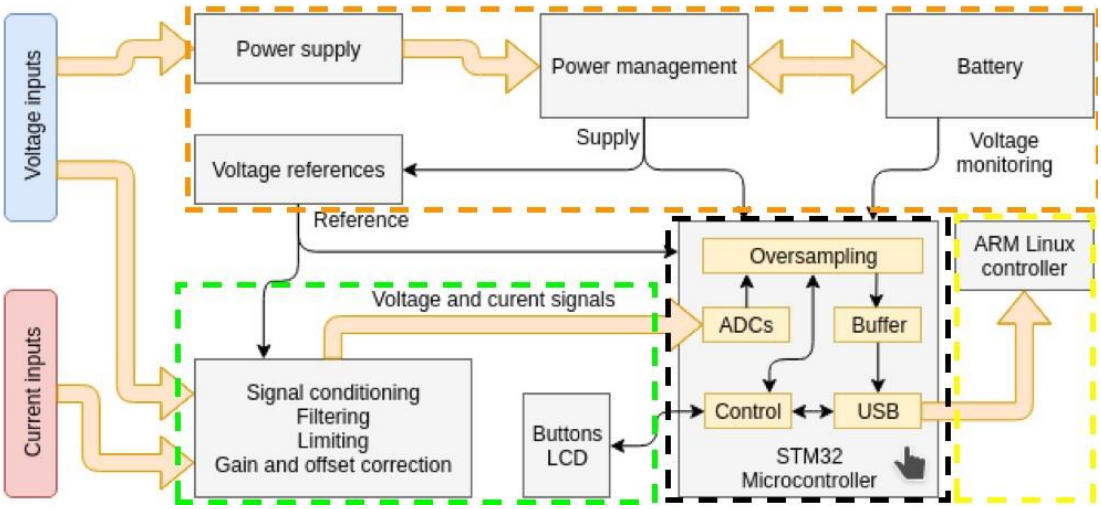

Figure 8 openZmeter (oZm) hardware block diagram. Block for signal acquisition coloured in green, power supply and management elements coloured in orange, STM32 microcontroller in black, and advanced RISC machine (ARM) Linux board controller in yellow.

The third block (coloured in black) is an STM32 microcontroller that handles all acquired signals, i.e., sampling, buffering, and USB communication with the fourth block (coloured in yellow), which is the ARM Linux board controller. Here, major processing tasks are executed along with database storage, web server functions, and web visualization.

Figure 9 presents some views of the hardware. A general view is on the left side, and a detailed component view is on the right. The ARM board, Li-Po battery, and AFE can be seen.

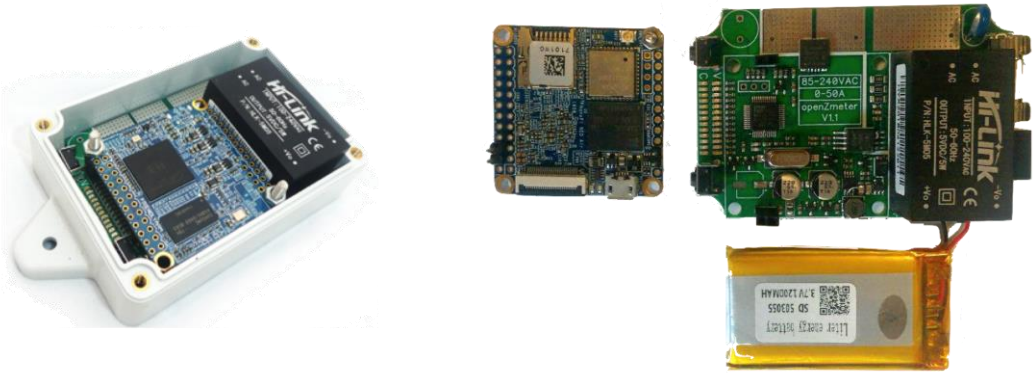

Figure 9 oZm hardware elements. (Left): full system including plastic enclosure. (Right): components side by side with ARM nanopi Air, analog front end (AFE), and Li-Po battery.

The voltage input is protected against overvoltage and transients. Protection is realized by means of a voltage limiter using a varistor. To protect against overcurrent, a fuse is also installed. Moreover, the resistance of the fuse limits the high current required during the connection because of the charging of capacitors from the main voltage. A jumper selects the operating mode, which must be provided with the appropriate connection. The oZm is single phase and has an integrated Hall-effect sensor.

In Figure 10, the proposed electronic scheme is presented along with a flowchart in Figure 11. It can be seen that the current flows in the oZm through a Hall-effect sensor integrated in the PCB (Infineon TLI4970). Figure 12 shows a detailed silkscreen of the PCB made with opensource software Kicad [82]. For safety reasons, the PCB tracks are sized for the maximum current of 50 A allowed by the sensor. No further processing is required on this channel thanks to the serial SPI connection to our STM32. The samples of the voltage channel are obtained through the isolation amplifier (U3) ACPL-C79 model from Broadcom. This device provides the necessary isolation from the mains voltage.

To obtain the input signal, a phase-to-neutral resistive divider is used. This reduces the voltage to ±200 mV for an input range of approx. ±300 V. This output is then redirected to a Broadcom ACPL-C79 isolation amplifier (input signal of ±200 mV), which converts to a differential output signal of ±2.5 V. The splitter incorporates an RC filter that attenuates frequencies above 16 kHz. The ACPL-C79 incorporates a ΣΔ modulator that converts the input voltage into a train of pulses that are transmitted optically to a ΣΔ converter that restores the signal to the output range set internally to ±2.5 V. The optical coupling provides the required insulation.

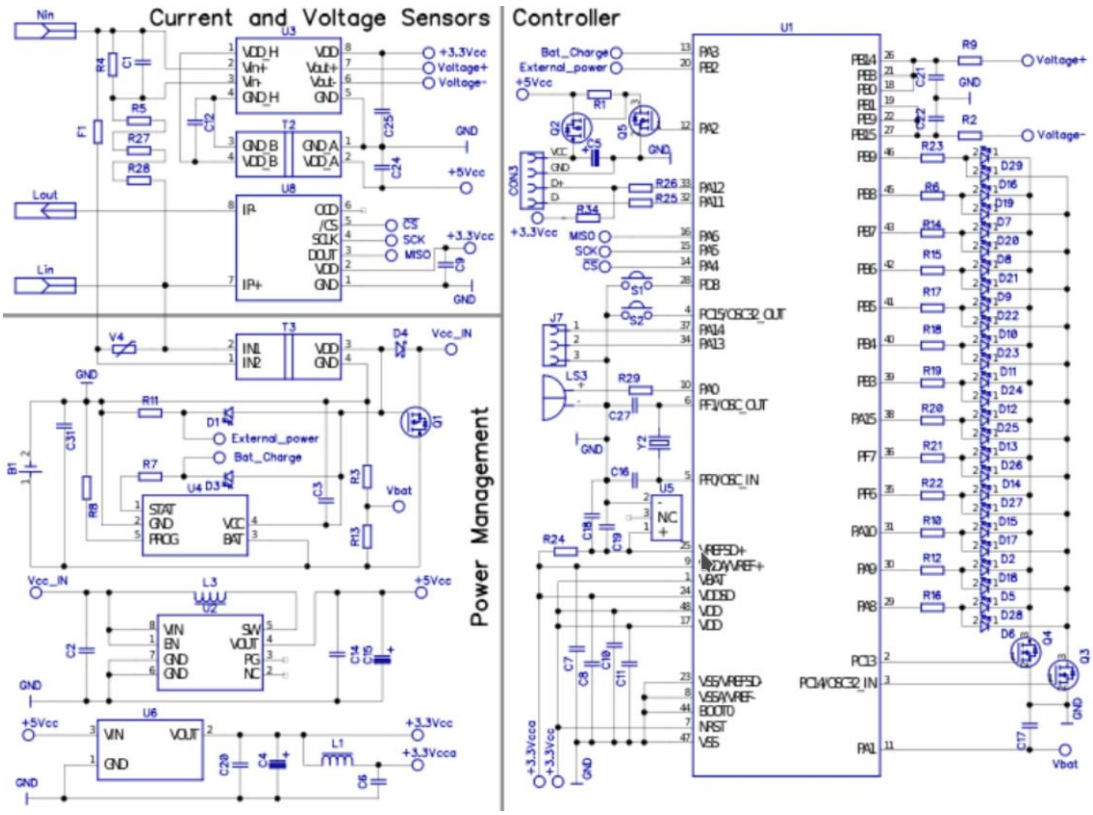

Figure 10 Electronic scheme of single-phase device. Controller, current/voltage sensor, and power management are shown.

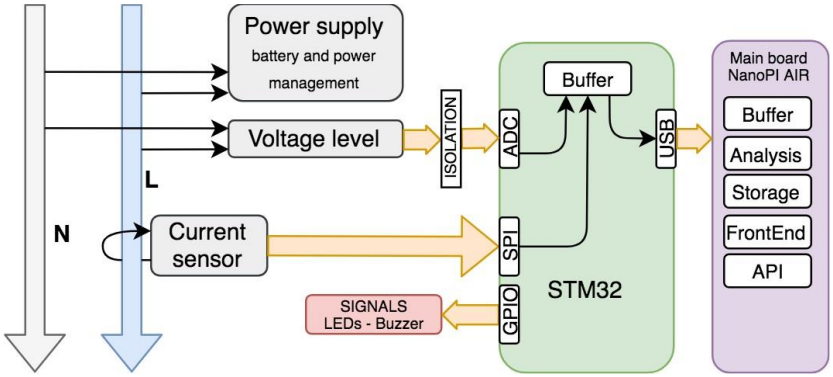

Figure 11 Flowchart for the electronic scheme.

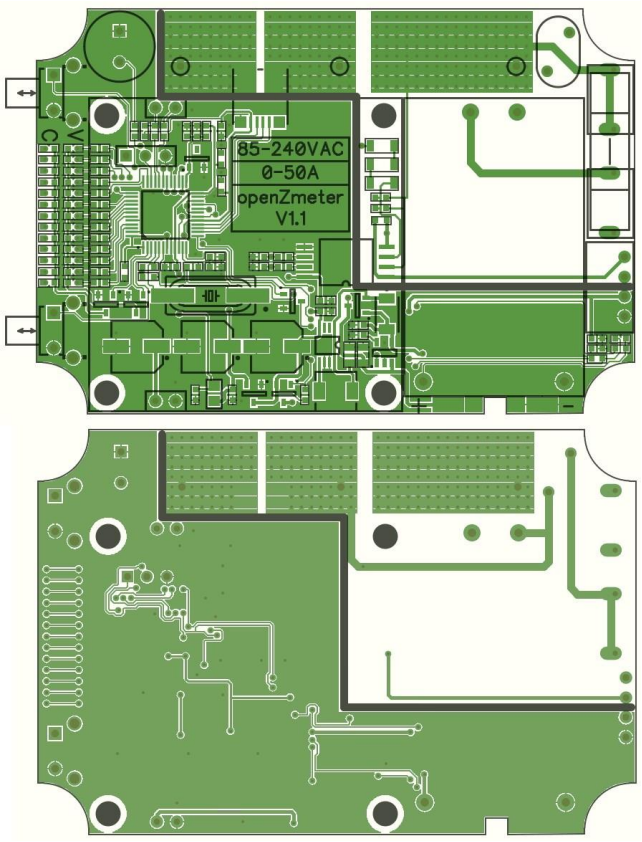

Figure 12 Printed circuit board (PCB) silkscreening of oZm board.

This topology requires a power supply for the part connected to the network that is isolated from the power supply of the module. This function is performed by a DC/DC converter (Recom RFM-0505S). The obtained signal from the isolation amplifier is injected into the three ADC channels of the STM32 after passing through an RC filter that attenuates out-of-range frequencies, from where the sample conversion can be coordinated. Conversion is performed with 16-bit accuracy and a maximum speed of 16 kHz per ADC channel. The STM32 has a great flexibility in the capture process, allowing for the use of only one connected channel and for 16-kHz sampling or sequencing of the three channels, thus increasing the

sampling frequency. These functions, as well as the synchronization of the voltage and current samples, are performed by the firmware running on the STM32.

The voltage is conditioned to the appropriate level. An AC/DC converter module gives a stable 5-V output in the range of 85 to 265 VAC for the single-phase version. The galvanic isolation is set between the network and the PCB components. Four blocks are implemented in the power supply:

- Input rectifier: Rectifier diodes convert AC to DC, which must withstand at least twice the mains voltage. The device can be used, in safety conditions, up to 1000 V.
- Input filter: To prevent noise sources from spreading to the mains, and to stabilize the rectified voltage.
- Buck converter: Reduces the voltage to 22 V in order to offer up to 4.5 W.
- Secondary buck converter: The IC used has some limitations. The voltage must be set at 5 V, and this voltage must be stable. A second buck converter is used with the MCP16312 to obtain a stable voltage at 5 V, with low ripple and up to 1 A of current.

A battery is also integrated in the power chain circuitry. oZm is manufactured to remain active even when there is no voltage in the inputs, or when the power supply is not in the operating range. A lithium-ion battery with built-in protection is included. The battery provides a voltage between 3.5 V and 4.2 V, incorporating the necessary electronics to avoid overloads and accelerated discharges. The PCB incorporates a charge controller to store energy while connected to the mains. The load manager is the MCP73832 module, which limits the maximum load current to about 100 mA.

The components of the oZm require 5 V to operate correctly. A DC/DC boost converter (MCP1642) is necessary to adjust the voltage from the battery (voltage between 3.5 V and 4.2 V) and some oscillations in the power supply. Therefore, a final conversion is performed to adjust the voltage to 5 V. The circuit designed uses a typical layout offered by the manufacturer. The selection of one input or another (battery or external power supply) is made by means of a MOSFET, which connects the battery to the input of the converter when there is no voltage in the input converter.

3.2.2. Real-time PQ monitoring and smart metering software

The oZm software consists of an embedded ARM unit, where a daemon service runs in an endless loop. The acquisition is performed in real time using an STM32 microprocessor and buffers the ARM unit running a real-time kernel (Linux RT). The daemon service is mainly coded in C++ to obtain a robust and reliable system. Being an Internet-based sensor, it incorporates a wireless module (Ampak AP6212) with WiFi: 802.11b/g/n and Bluetooth: 4.0 dual mode. This makes it possible to connect to the device and monitor the PQ parameters using a web browser with https secure encryption layer. The real-time electric measurement list is as follows:

- RMS values for voltage and current
- Active power, reactive power, and apparent power
- Phase between current and voltage
- Power factor
- Harmonics up to 50th for current and voltage
- Active energy and reactive energy
- Frequency
- Voltage events such swell, sags/dips, and interruptions

Based on the above list of measurements, the service can present clear visualizations based on the following features:

- Energy consumption and generation in four quadrants
- Operation in accordance with international standards IEC 61000-4-30 and EN-50160
- Aggregation for the voltage channel of 3 s, 1 min, 10 min, and 1 h as extra aggregation for energy metering purposes
- Alert system and event management (ITIC/CBEMA, frequency, etc.)
- Cutting-edge HTML, Javascript, and CSS3 technologies for a user-friendly dashboard interface
- API for third-party integration using JSON

Figure 13 Dashboard of real-time power quality (PQ) monitoring and smart-metering software.

Figure 13 shows a main view of the real-time PQ monitoring and smart metering software.

The parameters are displayed in real time and are presented using an intuitive dashboard, where the data are refreshed dynamically using cutting-edge web technologies such as HTML5, CSS3, and Javascript. Five blocks are plotted for active energy consumption, RMS voltage, RMS current, active power, and grid frequency. Each plot can be maximized for better inspection. All blocks are plotted using a 3 s aggregation interval over the previous 2 h to obtain fine-grained resolution. In addition, the energy block has a more advanced selector in order to choose other resolutions or aggregations. All blocks except for the energy block are synchronized to display information for the same time frame. The rest of the web interface is divided into six sections: voltage, current, power, frequency, voltage events, and energy stats.

Per IEC61000-4-30, the preferred time interval window is 10 cycles of the voltage waveform, i.e., 200 ms for a perfect 50 Hz European grid signal. Using this time interval allows harmonic calculations to be synchronous to all other values such as RMS and Total Harmonic Distortion (THD). In the case of a 60 Hz grid, 200 ms is equivalent to 12 cycles.

Harmonics are calculated using an adapted version of the well-known and stable open-source FFTW3 implementation [83] up to the 50th order for both voltage and current. The data are stored in the local database each 200 ms, and it is possible to retrieve aggregated data using custom methods implemented in the software. Interharmonics components were

minimized thanks to the implemented digital filters, which remove artifacts and allow for precise frequency measurement based on zero-crossing techniques.

External time synchronization was implemented to achieve accurate timestamps by means of network time protocol (NTP) time servers. Accuracy is specified at ±20 ms for 50 Hz and ±16.7 ms for 60 Hz instruments with a 10 min interval sync to clock and a 2 h interval sync to clock. To ensure compliance with standard specifications, an efficient NTP implementation was deployed using the Chrony package for Linux [84].

3.3. APPLICATION AND RESULTS

The oZm was installed and tested at some laboratories of the University of Almeria (UAL) and, additionally, in some houses for domestic use. The acquired data was recorded and stored in the oZm, which is accessible using the campus network at any time. The installation of the device was straightforward. Figure 14 shows the final setup of an oZm installed in one of the laboratories at the University of Almeria.

3.3.1. Voltage analysis

A real-time measurement of the system RMS voltage can be found in the voltage analysis view. Using the selectors, an aggregation level between 3 s and 1 h can be chosen. In this way, the evolution of the voltage for a specific time scale can be displayed in greater or lesser detail. The system can store values of several years depending on the size of the memory chosen on the ARM Nanopi Air board (8-GB standard). The data can be displayed on a daily, weekly, monthly, or annual time scale. The data can be viewed in full screen and can also be downloaded in CSV format for external analysis with specific software. The maximum, minimum, and mean values for the selected time range are shown to the left of the RMS chart.

Below the RMS chart, a detailed chart is available to display the waveform in real time (similar to an oscilloscope) for the last 10 cycles. Harmonics can also be displayed in real time, and the daily evolution of each harmonic from the fundamental to order 50. There is also a visualization that represents a phasor chart for voltage and current. Finally, the events tab can be accessed, where different voltage events occurring in the selected time span can be displayed. These details can be seen in Figure 15, Figure 16 and Figure 17 .

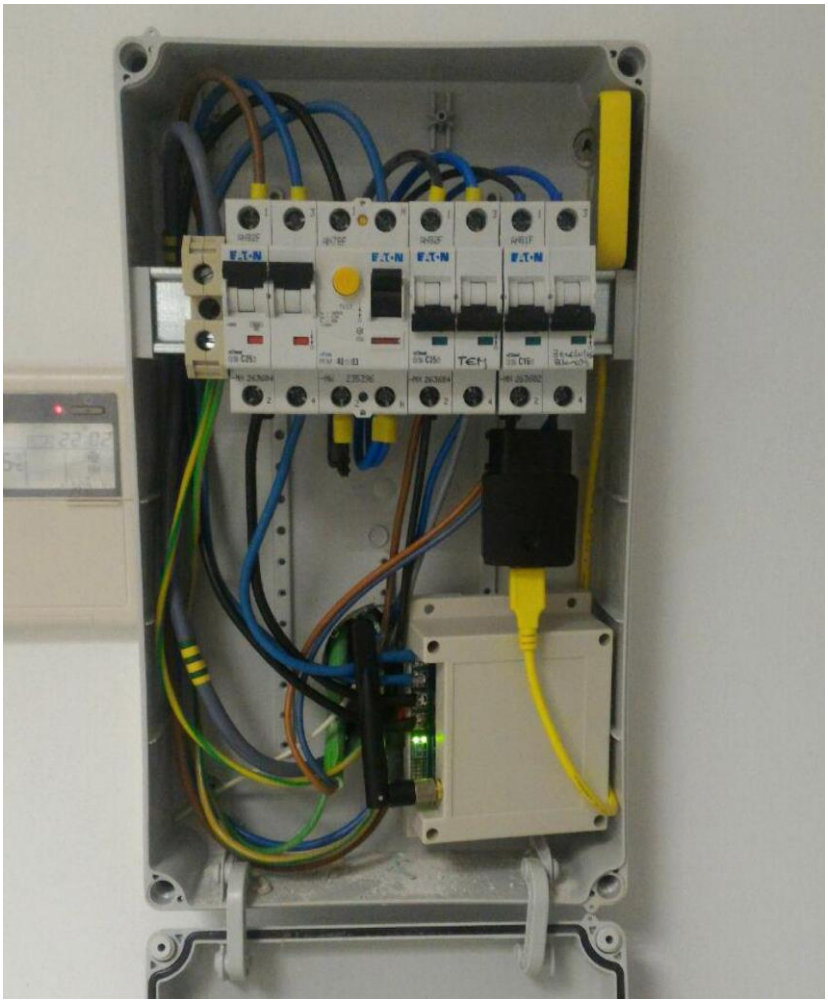

Figure 14 oZm installed in facilities of the University of Almería.

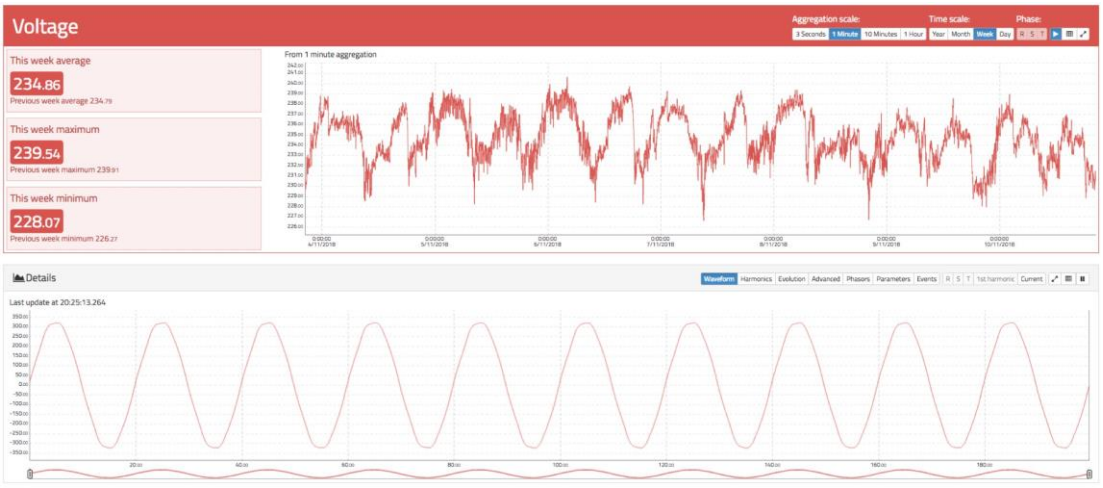

Figure 15 Voltage view of oZm.

Figure 15 shows the RMS voltage variation during a day for a 1 min aggregation scale. It can be observed that the voltage goes up and down during the day, causing an increase as the evening goes by, reaching a minimum around 6:30 p.m. and a maximum around 4:00 a.m.

In the same way, the notches produced by voltage drops in the supply line owing to the connection and disconnection of loads in the installation itself can be clearly seen. If the selected aggregation level is set to a lower value, the RMS signal will contain more noise that captures more details. In the same Figure 15 below, the waveform for the supply voltage can be seen. It has a near sinusoidal shape but has some distortions owing to the presence of harmonics.

Figure 16 shows the harmonic spectral content for the signal in Figure 15. It can be seen that the odd harmonics (typical of commercial supplies) have a higher value than the even harmonics. In particular, the 3rd, 5th, and 7th harmonics have the highest value. In the lower part of Figure 16, the evolution of the values of the power factor, Total Harmonic Distortion for voltage (THDv), and phase angle between the voltage and fundamental current for the last 24 h is shown. Darker colours indicate higher values. For the phase-angle chart, positive (red) and negative (blue) values are shown, so it is possible to visualize the inductive or capacitive nature of the load. Finally, on the right of Figure 16, there is a phasor chart of current and voltage, where the capacitive nature of the load is appreciated since the current overtakes the voltage. The values of this phasor chart are obtained by applying an FFT and plotting the module and phase angle between the fundamental components of the voltage and current.

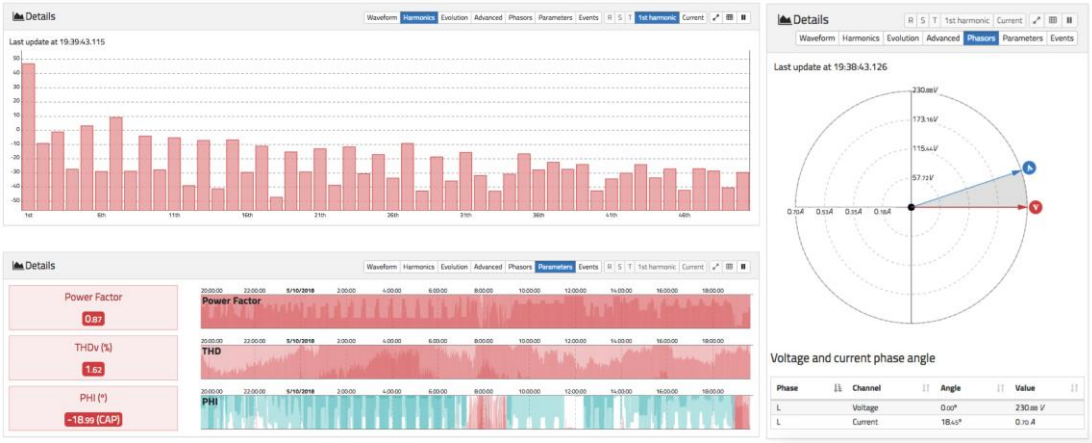

Figure 16 Advanced views of voltage tab (1). (Top left): real-time harmonic content for voltage. (Bottom left): 24 h of power factor, total harmonic distortion voltage (THDv), and phase angle. (Right): phasor representation for voltage and current.

Figure 17 has a similar display as that shown in Figure 16. The evolution of the last 24 h for harmonics up to order 50 can be examined, although owing to space constraints only up to the 7th harmonic is shown. Dark colours in red indicate high values for the magnitude of the value, while dark values in blue indicate low values. Note that even harmonics always exhibit a small value compared to odd harmonics. In addition, it is interesting to observe how

the 3rd harmonic varies between large and small values depending on the time of day. In particular, it has higher values at sunset between 6:00 p.m. and 11:00 p.m. than the rest of the day.

Figure 17 details the view of voltage events. A shows the different events that the system can handle: dip, swell, rapid voltage change (RVC), and interruption. In this case, an interruption of 7.24 s is shown. On the right, it is possible to visualize the precise moment before and after the interruption.

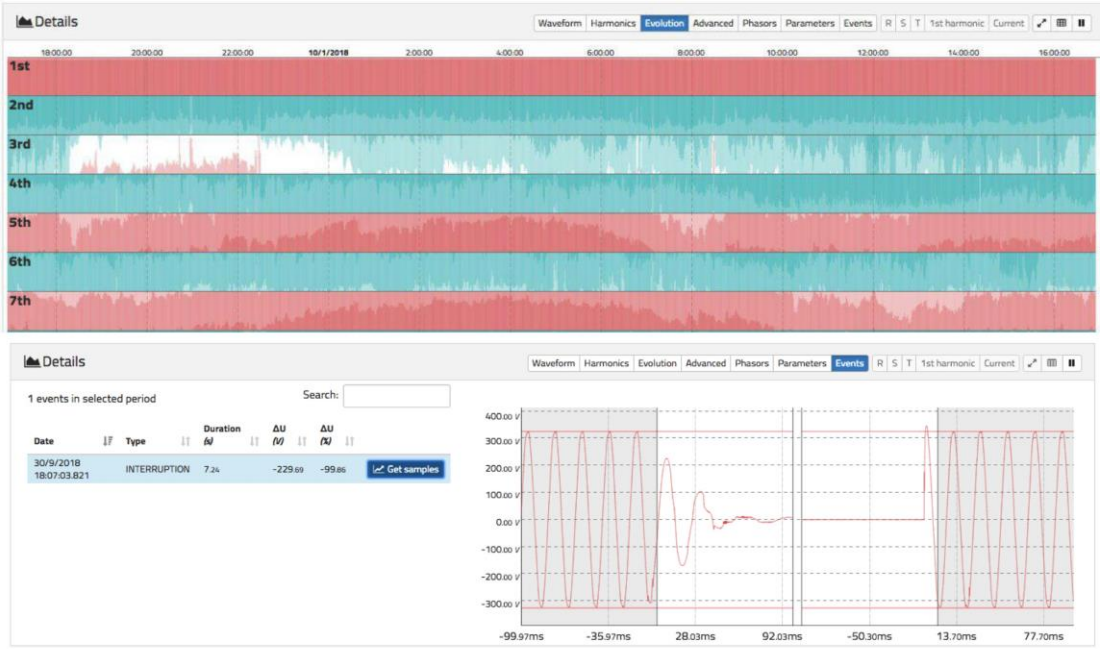

Figure 17 Advanced views of voltage tab (2). (Top): harmonic evolution. Darker red colours indicate higher values than darker blue. (Bottom): events view with pre- and post-event waveforms.

3.3.2. Current analysis

The current analysis view follows the same approach as the voltage view. Here, a main chart showing the evolution of the RMS current for different aggregation levels and time spans in real time is presented. The data can be downloaded in CSV format. It is also possible to visualize the waveform, harmonics evolution, and advanced parameters such as Total Harmonic Distortion for current (THDi) and power factor. Figure 18 and Figure 19 show the relevant information of the current measurement.

Figure 18 shows the evolution of the current RMS value during the connection of different appliances. It is possible to observe the typical footprint of a washing machine (on the right)

and a refrigerator (center) as well as the waveform in real time, where the presence of distortions owing to the effect of nonlinear loads is evident.

Figure 19 above plots the advanced view, where the full frequency spectrum of the current waveform is displayed up to approximately 7700 Hz. The peaks correspond to the odd harmonics. It can be seen that there is a strong presence of the 3rd, 5th, 7th, 9th, 11th, 13th, and 17th harmonics. All of these charts are responsive, allowing for zooming, panning, maximizing, and exporting data. At the bottom, the same visualization as in Figure 17 can be found.

Figure 18 View of root mean square (RMS) and waveform current in oZm.

Figure 19 (top) current spectrum. (bottom) advanced parameters THDi, power factor, and phase angle for current.

3.3.3. Active and reactive power

The power view enables the active and reactive power of the installation to be displayed (see Figure 20). The calculation of the active power is carried out using the well-known expression

$$P = \frac{1}{N}\sum_{n=1}^{N} U_n I_n \qquad \textit{Equation 1}$$

while the reactive power is obtained as the result of the following product

$$Q = U_1 I_1 \sin\varphi \qquad \textit{Equation 2}$$

i.e., the Budeanu approximation is not followed [85], so the power factor is calculated using the angle between the fundamental voltage and current through the FFT (see Section A2 regarding the use of varmeters in the presence of distorted waveforms from IEEE1459). However, the reactive power of the fundamental harmonic is computed. Other implementations are possible based on different proposals such as that defined by Czarnecki [86] and Castro-Nuñez [87] because of the open-source implementation of oZm.

Figure 20 Active and reactive power view of oZm.

Figure 20 shows the active power at the top and the reactive power at the bottom for a time span of 1 week with an aggregation level of 1 min. oZm supports aggregation scales ranging from 3 s to 1 h for web users, but up to 200 miliseconds for API users. On the left side, there is a shaded area corresponding to a weekend. In this case, only positive powers are shown because there is only consumption and no power generation. However, in the reactive power chart, both positive and negative values are observed because there are inductive (positive) and capacitive (negative) reactive power consumptions.

3.3.4. Frequency

The grid frequency is measured with great accuracy following the IEC 61000-4-30 standard. Thanks to the use of techniques based on digital filters and the use of the zero-crossing algorithm, a measurement with an error of less than 10 mHz is obtained in a range of ±15% of the nominal frequency. The zero-crossing algorithm was developed from scratch and takes into account the possible presence of interharmonics and noise. Firstly, five cascade biquad low-pass filters (tuned to the nominal frequency) are used to achieve a significant attenuation above the nominal frequency (50 or 60 Hz). Afterwards, we look for zero-crossing (change in the sign of the signal) at the output of the filter. The duration of each half cycle is stored in order to calculate the frequency, and when there are 20 sign changes the block is released for further processing by other modules of the system. The maximum block size is 10 cycles at

nominal frequency ±15%. If all 20 half-cycles have not been found in that timeframe, the package is released creating a voltage event and labeling it with a flag. Likewise, if a cycle change is detected that is not where it is supposed to be (ahead or delayed ±15% to its position), we keep reading samples (if there is enough space), but the block is marked as a voltage event. Additionally, to detect sign changes, the signal must have a minimum amplitude. If it is below 10% of the nominal value, no cycles are searched, although blocks of the maximum size are read and later marked as interruptions. Using this technique, the system also avoids spectral leakage and picket fence effects because of the integer multiple of cycles computed in every batch of samples.

Figure 21 Frequency view of oZm. Top: general view. Bottom: maximized view.

Figure 21 shows an example of frequency tracking for a full day and an aggregation of 3 s. It can be seen that the average is exactly 50 Hz, oscillating around it with maximums and minimums of a few millihertz. Also noteworthy are the large oscillations at o'clock owing to the entry and exit of generator groups according to the Spanish electrical system's time schedule, where some groups are disconnected/connected to adjust the generation to the demand. This causes accelerations/decelerations in the frequency according to the period of the day.

3.3.5. PQ disturbances

One of the great features of oZm is its ability to measure some well-known PQ events. Several algorithms to monitor swells, dips, interruptions, and RVC following the international standards IEC61000-4-30 and EN-50160 have been implemented. The RMS voltage criterion, updated every half cycle, was used. For a comprehensive overview, three screens were implemented, as shown in Figure 22 The first screen is the ITIC/CBEMA curve, where a permitted zone, prohibited zone, and no-damage zone are defined. For each event detected, a new point is generated according to its magnitude in the voltage and time duration. Next to the curve, there are graphs showing statistics associated with these events.

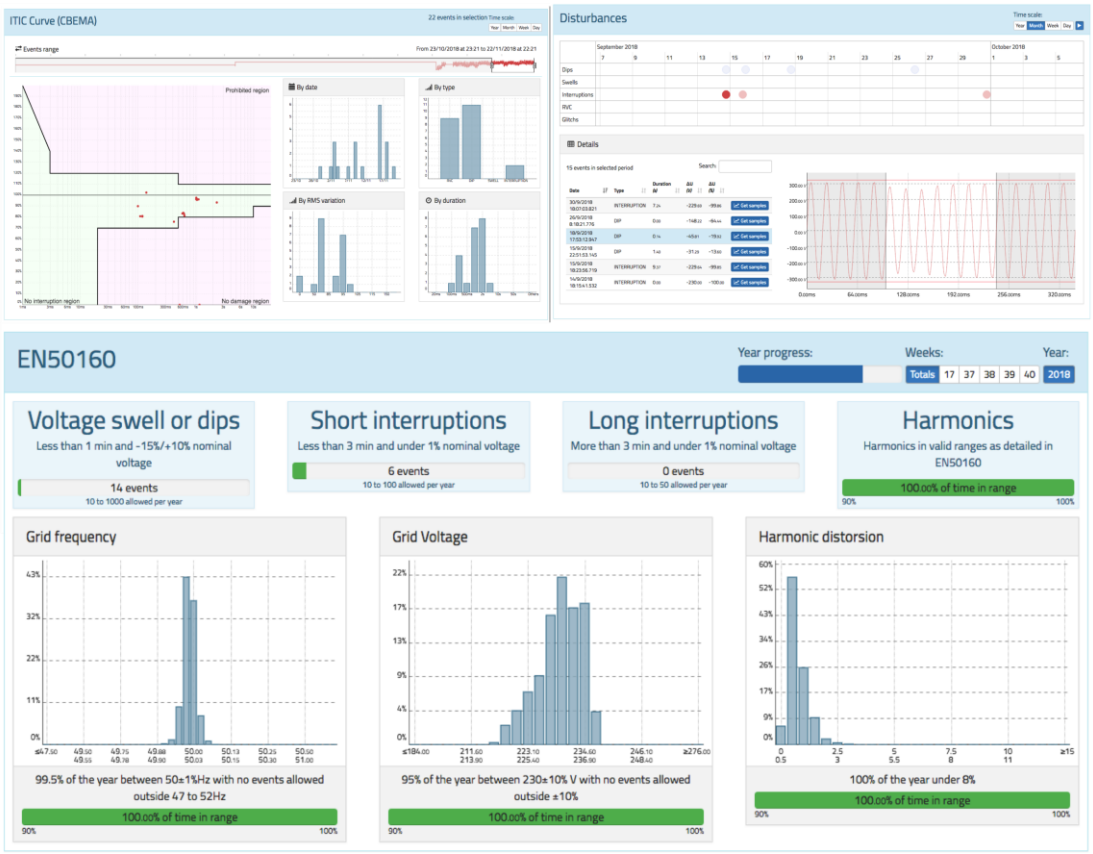

Figure 22 PQ events view of oZm. Top left: information technology industry council (ITIC) curve. Top right: disturbances table and viewer. Bottom: EN-50160 visualization and classification for voltage events.

The second screen is a timetable with points representing each type of event, as well as another table to select and visualize the waveform during the event. In this way, it is easy to observe what happened before and after the normal restoration of the voltage. Finally, following the EN-50160 standard, a visualization and statistics of the different types of events that occurred are presented. The number of events within the margins allowed by the standard are checked.

3.3.6. Active and reactive energy stats

An active and reactive energy measurement is carried out by adding the power measurement over time. Since the power was already analysed in previous sections, it is easy to obtain the accumulated values because this simply requires multiplication of the value of the power by time and determination of the consumption or generation of energy. For a better analysis, two visualizations were implemented, as shown in Figure 23 and Figure 24. Figure 23 shows a visualization more oriented to tables, where it is possible to analyse the energy habits depending on the year, month, week of the year, or day of the week. It is possible to distinguish between day and night periods. This is of great interest because many countries apply different pricing policies depending on whether energy is consumed during the day (where there is much more demand and the system is overloaded) than at night (where demand is much lower and energy prices are also lower).

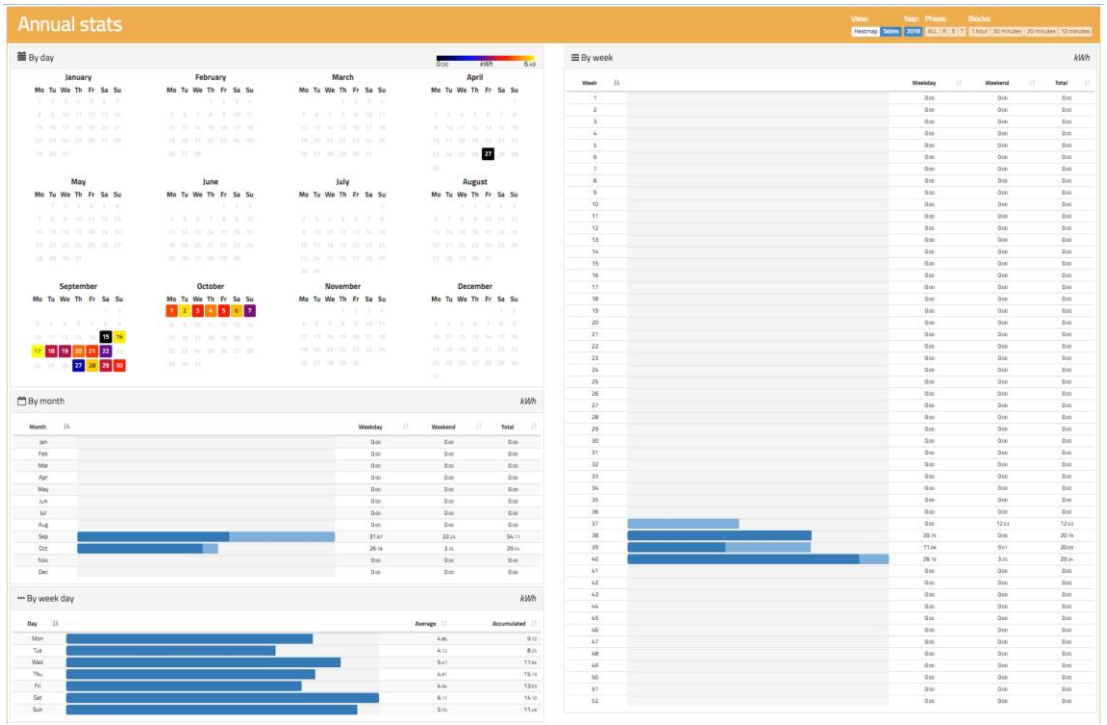

Figure 23 Active and reactive energy view of oZm.

Figure 24 shows a representation based on heat maps. Each coloured "pixel" represents the consumption made in a specific time span that can be adjusted between 10 min and 1 h so that there is more or less resolution according to the user's interests. This visualization allows for a clear vision of the user's consumption habits and provides a clear advantage over other representations when making decisions related to energy savings.

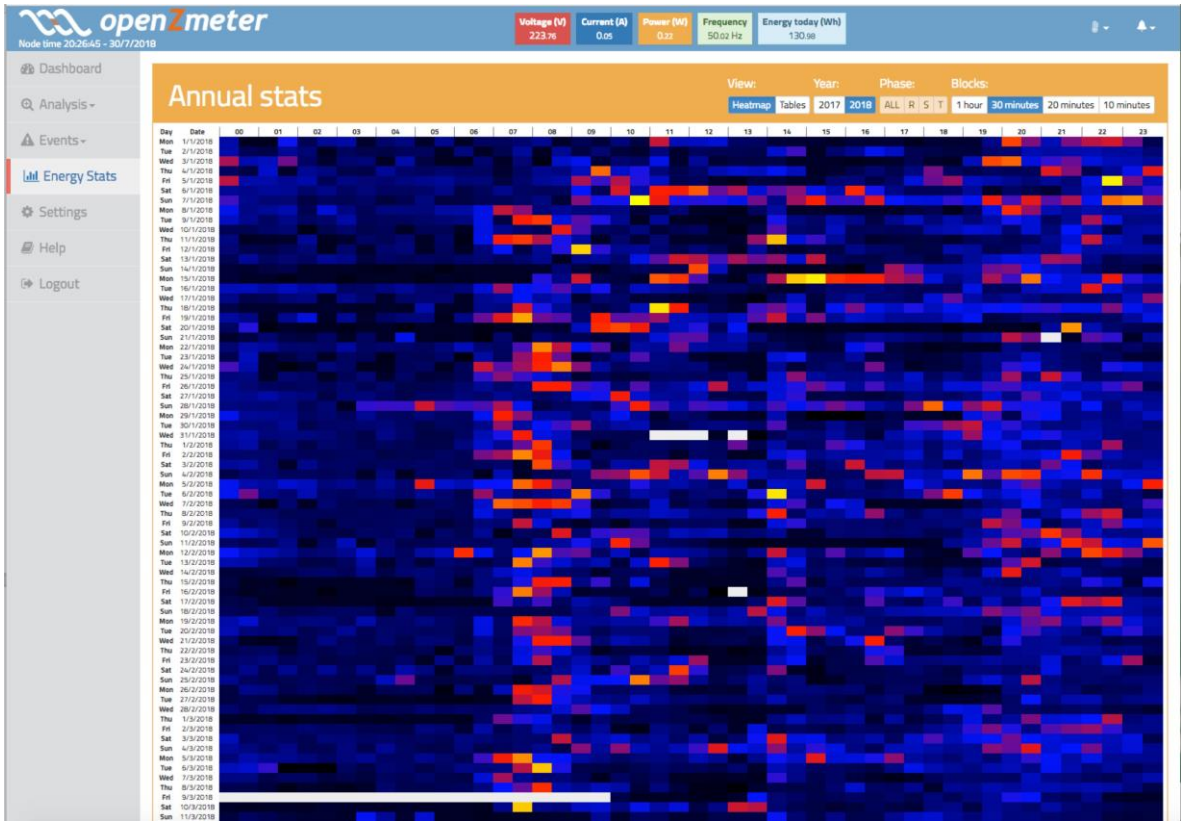

Figure 24 Active energy heat view of oZm.

3.4. COMPARISON WITH COMMERCIAL POWER ANALYZER

In order to validate our proposal against existing commercial and certified devices, the features and operation of oZm have been compared with MyEBOX-1500 (MyEBOX from now on) power and energy analyzer from Circutor manufacturer, a commercial and certified device launched in 2016 which was designed for measurement and recording electrical parameters. According to the manufacturer, it incorporates the latest technology in portable measurement. Table 3shows the main technical features and functions of oZm and Circutor MyEBOX. Moreover, an empirical study has been carried out to show how both devices measure, record, and visualize the electric data recorder in our university laboratory having some linear and non-linear loads.

Three different scenarios have been configured and tested to perform measurements and compare results using oZm and MyEBOX (see Figure 25). First of all, a simple circuit consisting of a variable resistor 1017R from DeLorenzo and a 230VRMS/50 Hz sine wave voltage source from Agilent Technologies has been setup. Afterwards, the Agilent source was replaced by a mains supply from the laboratory grid. Finally, a non-linear load was connected to the

laboratory mains. All scenarios have been monitored using a Picotech 2000 series oscilloscope with a high voltage active differential probe TA041. Figure 26 shows a capture of the measurement process for the non-linear load.

Table 3 List of main features of openZmeter (oZm) and MyEBOX

	oZm	MyEBOX
Active Energy	Yes	Yes
Reactive Energy	Yes	Yes
Active Power	Yes	Yes
Reactive Power	Yes	Yes
Apparent Power	Yes	Yes
Frequency	Yes	Yes
RMS Voltage	Yes	Yes
RMS Current	Yes	Yes
Power Factor	Yes	Yes
Phase	Yes	Yes
4 Quadrants	Yes	Yes
Phasor	Yes	Yes
High Sampling Rate	Yes	Yes
Aggregated Intervals	Yes	Yes
Real-time alert system	Yes	No
Realtime Pricing	Yes	No
IEC61000/IEC61010	Yes	Yes
EN-50160	Yes	Yes
Voltage Events	Yes	Yes
ITIC/CBEMA	Yes	Yes
Zero Crossing	Yes	Yes
FFT	Yes	No
Harmonics	Yes	Yes
THD	Yes	Yes
Flickers	Yes	Yes
4G	Yes	No
Wi-Fi	Yes	Yes
Ethernet	Yes	No
API	Yes	No
HTML5 Interface	Yes	No
Telegram integration	Yes	No
Open Source	Yes	No

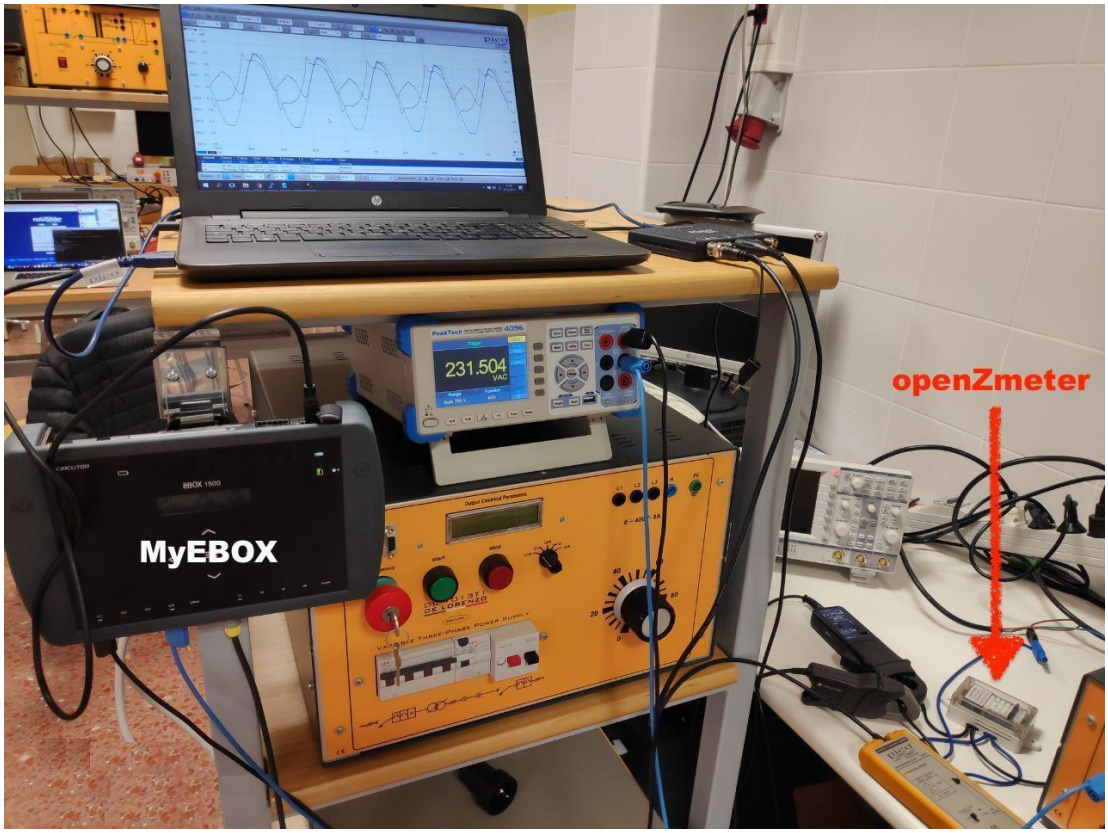

Figure 25 Setup for measurements with oZm and MyEBOX. Precission multimeter Peaktech 4096, Picotech 2000 oscilloscope, and Agilent power source also used.

Table 4 shows a detailed comparison for the above scenarios. Voltage (V), current (I), active power (P), and frequency (F) have been measured during a 1 hour time span. Both oZm and MyEBOX show similar recorded values with minimal deviation. They also coincide with occasional readings using the Picotech oscilloscope and a precission voltimeter Peaktech 4096.

Table 4 Comparative test for oZm and MyEBOX under different scenarios.

		Sinusoidal Source and Resistor				Mains and Resistor				Mains and Non-Linear Load			
		Mean	**Min**	**Max**	**StdDev**	**Mean**	**Min**	**Max**	**StdDev**	**Mean**	**Min**	**Max**	**StdDev**
V	oZm	229.86	229.82	229.90	0.02	237.30	231.98	240.86	1.44	235.96	231.11	238.54	1.41
	MyEbox	229.37	229.33	229.39	0.01	237.46	232.07	241.04	1.45	236.14	230.24	238.87	1.49
I	oZm	2.24	2.23	2.26	0.01	2.30	2.25	2.33	0.01	3.17	3.12	3.20	0.02
	MyEbox	2.24	2.24	2.24	0.00	2.30	2.25	2.34	0.01	3.17	3.10	3.20	0.02
P	oZm	515.09	512.99	518.27	1.52	551.82	527.12	568.18	6.72	638.38	610.44	652.26	7.59
	MyEbox	513.08	513.00	514.00	0.27	546.78	522.00	563.00	6.60	617.81	586.00	633.00	7.94
F	oZm	50.00	50.00	50.00	0.00	49.99	49.92	50.04	0.02	50.00	49.96	50.04	0.02
	MyEbox	50.00	50.00	50.00	0.00	49.99	49.92	50.04	0.02	50.00	49.96	50.04	0.02

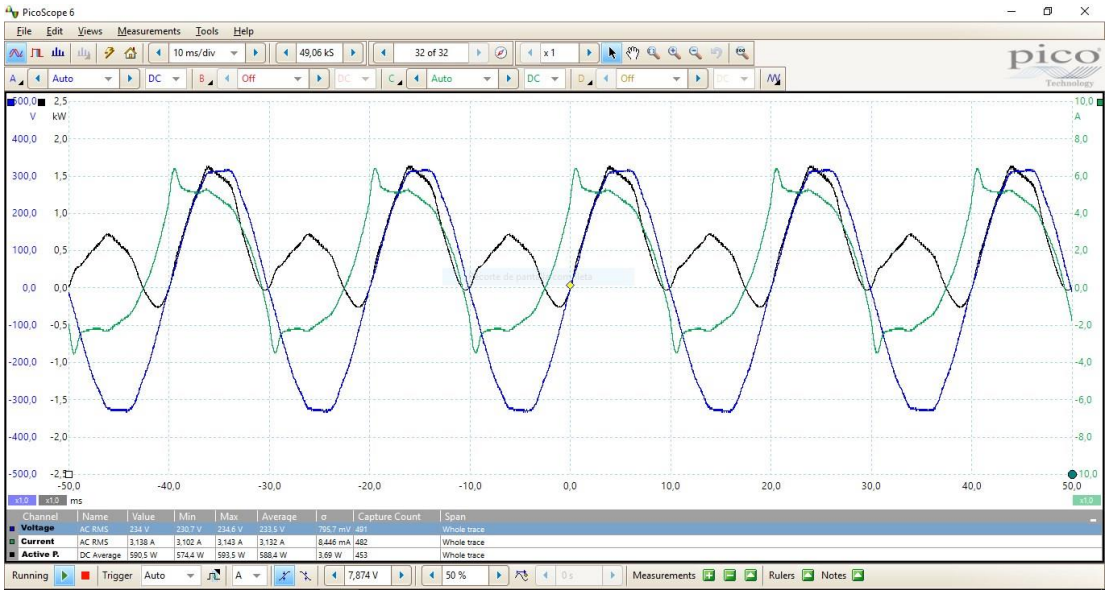

Figure 26 Non-linear load analysis with Picotech oscilloscope

3.5. CONCLUSIONS

Nowadays, most electrical installations are monitored using commercial devices that are often expensive and difficult to handle for non-expert users. The main contribution of this research is the description of the oZm hardware, a low-cost, open-source, Internet-based multipurpose network analyzer and smart meter that has been designed, manufactured, and implemented for power quality and energy metering and submetering of electrical installations. The advanced design of oZm ensures reliable and accurate energy consumption and power quality measurements under a wide range of operating conditions in a single handy device. It can be used by anyone to analyze and visualize power consumption measurements and power quality events that comply with international standards such as IEC 61000-4-30 and EN-50160. Given its small size and large variety of current probes, it can be easily installed at any electrical installation, i.e., it can be used both as bulk metering or as metering/submetering for individual units or appliances. A comparison with commercial devices is also carried out. The characteristics and operation of oZm have been compared with MyEBOX-1500, an advanced commercial and certified power quality and energy meter. The results obtained in the laboratory show similar readings with minimal deviation. This comparison clearly shows that oZm is able to measure and record high precision RMS voltages, currents, frequency, and power quality events in different scenarios. Finally, other important contribution of the paper is to present and display a large number of

measurements with an user-friendly interface that can be customized according the particular needs.

The acquired data is stored in a local PostgreSQL database, which is accessible using the network of the campus and a browser from any connected device. The main dashboard is accessible using the http protocol through an https secure layer. The potential benefits of oZm for domestic or industrial applications were demonstrated by the set of advanced measures it performs. The system proposed can be used for smart-grid studies and for advanced technique development such as non-intrusive load monitoring and machine learning applied to power quality. Moreover, the device is very easy to install and use by nonspecialized staff.

Although not all definitions of international standards IEC 61000-4-30 and EN-50160 were implemented, oZm is a constantly evolving project supported by the community. Research teams from several universities aim to complete and fulfill the requirements imposed by these standards. As a future work, we are now working on the development of a three-phase version of oZm.

CAPÍTULO 4 - ALL-IN-ONE THREE-PHASE SMART METER AND POWER QUALITY ANALYZER WITH EXTENDED IOT CAPABILITIES

The traditional power grid is evolving into a new smart grid which requires the coordination of supply and demand, making it necessary to establish precise monitoring strategies in order to determine grid status in real time. With the aim of providing a low-cost device based on open hardware and open source software to the technicians, engineers, and scientists around the world, this paper presents the three-phase openZmeter (henceforth named 3Ph-oZm), an all-in-one device that allows measuring and computing electrical data related to energy and power quality features in three-phase power networks. It has been designed to perform advanced computations for voltage, current, frequency, power, and energy. 3Ph-oZm is able to process up to 50-order harmonics and log power quality disturbance events defined according to the recommendations of some international standards organizations. The data and its associated features are processed on site using custom software specifically designed and programmed for this purpose that relies on advanced signal analysis techniques. Furthermore, the device has interesting applications for the Internet of Things (IoT) community thanks to its advanced on-board communication capabilities. The system has been calibrated and validated using laboratory testing set-up and real world applications, such as long-term photovoltaic power plant metering. The capabilities of 3Ph-oZm can also support a variety of other electrical applications, such as three-phase induction motor health monitoring, energy savings, or microgrid state estimation.

4.1. INTRODUCTION

For decades, the extension of power grids was not accompanied by the incorporation of advanced and remote metering devices, despite the fact that sensor devices for power metering have been patented for more than forty years [1]. Nonetheless, in recent years, distributed generation has given rise to microgrids and smart grids, as it is now absolutely

imperative to establish procedures that determine grid status to ensure a reliable transmission and distribution network [2].

The global trend in power systems is to be environmentally friendly and eco-resilient, with a clear circular orientation towards the exploitation of resources. Smart grids and microgrid systems allow the delivery of electricity in a controlled environment [44], [45]. Smart grids are built based on complex power models and decentralized electricity generation systems, thereby establishing a synergy between computer processing, control systems, and advanced renewable energy resources [42].

The management of smart grids requires accurately specifying their status in order to track and command them. This, in turn, requires the development of advanced measurement systems (smart sensors/meters). The 2012/27/EU directive [39] defines a *smart meter* as "an electronic system that can measure energy consumption, providing more information than a conventional meter, and can transmit and receive data using a form of electronic communication".

In addition to measuring power and energy, it is important to design high-precision devices to measure power quality (PQ), since the continuous incorporation of distributed generation systems based on renewable energy and non-linear loads in industry and home applications causes harmonics and PQ disturbances [88]. In particular, non-linear loads such as personal computers, fluorescent lamps with electronic ballast, and many other electronic components connected to the network may cause disturbances and deviations from the supplied voltage sinusoidal waveform. These current and voltage disturbances degrade and could damage modern devices [89], [90] and may impose penalties on consumers by adding reactive power, re-dispatch and load curtailment costs [91]. Power quality disturbances include sag/swell, outage, impulses, noise, imbalances, oscillatory transients, flicker and harmonic distortion, among others. The accurate detection and measurement of these disturbances has become a challenge for smart meter designers, who have proposed advanced signal processing techniques such as nonlinear optimization or nonlinear classification methods, including artificial neural networks and support vector machines [63], [64]. Several researchers have proposed techniques for real-time detection and classification of power quality disturbances [47]. Improvement of communication and data processing techniques has allowed the integration of real-time detection events as functional blocks into smart sensors. These techniques include sophisticated and efficient algorithms [48], [49],

[92], such as Neural Network of General Regression for control strategies in microgrids with hybrid power supply sources [51]. The study of power quality often requires the application of signal processing techniques, among which Fourier Transform (FT) is the most widely used to date. Other methods that have become popular in recent years are the Short Time Fourier Transform (STFT) [93], Hilbert-Huang Transform (HHT), Stockwell Transform (ST) and Wavelet Transform (WT) [94], [95].

Given the current context, it is obvious that researchers, scientists, and professionals in the electricity sector demand high-precision devices for monitoring energy consumption and power quality variables in electrical systems complying with international reference standards. The information retrieved and processed by these smart meters can be used to measure the power flow in the grid, energy consumption or other issues related to security, including the verification of special conditions like ground fault current. Information processed by these smart meters will be valuable to implement corrective actions if necessary (e.g., using active or passive harmonic filters) [96], [54].

This study presents 3Ph-oZm, a three-phase smart metering and power quality analyzer with extended IoT capabilities. This innovation, derived from the single-phase openZmeter (oZm) [97], marks a major milestone. Its advanced design ensures a powerful, accurate, and reliable solution for power and electric energy metering in a wide range of operating conditions that satisfies the specifications of IEC 61000-4-30 and EN-50160. Bearing in mind the increasing number of devices that are currently required to monitor the power grid, this open-source device offers a low-cost, compact, and efficient alternative to high-cost commercial meters. The remainder of the paper is organized as follows: Section II describes the hardware design and software features of 3Ph-oZm; Section III presents the empirical validation of the device in different applications; Section IV provides the main conclusions obtained.

4.2. 3PH-OPENZMETER DESCRIPTION: HARDWARE AND SOFTWARE DESIGN AND IMPLEMENTATION

3Ph-oZm has its origins in the single-phase device described in [97], which was designed as a reliable power and electrical energy meter primarily intended for use in urban or rural households. A major upgrade and extension of the original hardware platform has been designed, developed, and manufactured to be used in three-phase power networks, including

advanced industrial applications. More specifically, without significantly increasing the dimensions of the single-phase version, 3Ph-oZm allows independent measurements to be carried out on each phase, that is, it is possible to measure different single-phase circuits at once. Furthermore, 3Ph-oZm admits a wide input current range as well as different types of probes, such as Hall sensors, Rogowski probes, or zero-flux probes to be used in three-phase power networks, mostly found in industrial environments. This feature enables a virtually unlimited current measurement capability (including DC). Another improvement is the fact that 3Ph-oZm incorporates a battery to improve the device's autonomy.

The device has been specifically engineered to be a powerful tool for electrical measurements and to assist in power quality analysis applied to three-phase networks. Voltage and current waveforms are collected and analyzed according to the specifications of international standards IEC 61000-4-30 and EN 50160. 3Ph-oZm is also a multipurpose IoT system since it can act as a power quality monitor, a smart meter, and an electrical event capable of communicating with other devices thanks to its advanced features (WiFi, Bluetooth, 3G/4G/5G, or Ethernet), which allow access to raw and computed data through the Internet. Typical HTTP web server and industrial communication protocols are specially implemented for industrial application, such as the Modbus protocol.

The sampling and conditioning signal stage is performed by a custom-designed Analog Front End (AFE) controlled by a realtime microprocessor-based system. The STM32F042 model, which belongs to the STM32 microcontroller family, was selected based on its strong specifications, functionality, and low price. It is reliable and has high performance, realtime track signal processing capabilities, along with a lowpower consumption combined with energy saving management. The current and voltage signals are sampled by means of a 12-bit Analog Digital Converter (ADC) with oversampling providing 13 effective bits. This ADC can sample signals at 24 kHz per channel, with a total of 7 channels (3 for voltage and 4 for current), encoding the digital data for streaming to the main microprocessor-based component, where the sampled current and voltage signals are preprocessed and conditioned by the STM32's digital signal processing (DSP) module. This preprocessed data is sent to a companion advanced RISC machine (ARM) board (mainboard), which executes the main process tasks. This mainboard ships with a custom compiled Real-Time (RT) Linux core OS (OpenWRT). It performs complex calculations such as Fast Fourier Transform (FFT), zero-crossing frequency estimation, or PQ event detection. The programmed C daemon service

ensures the real-time strategy executing an endless loop with threads and queue management implemented.

4.2.1. Hardware design

In a general sense, electronic device-assisted PQ and/or smart meter systems are based on microprocessors or microcontrollers. Some of them are manufactured based on Field Programmable Gate Array (FPGA), while others use specialized electronic devices with specific modules like the Application-Specific Integrated Circuit (ASIC), which integrate most of the functions as a dedicated piece of hardware. 3Ph-oZm has been designed to maximize its flexibility, versatility, and minimize its cost. The hardware design and software features have been conceived to be both accessible and extensible as much as possible, leaving an open door to the implementation of new functions by adding new custom blocks. Advanced algorithms and specific analysis techniques can be implemented in a straightforward way. Based on the above principles, solutions in which most of the functionality is executed by specific hardware, such as FPGAs or ASICs, are discarded. Therefore, a minimal hardware is selected for acquisition and control, leaving complex and advanced tasks and computations for the RT Linux ARM multicore mainboard. This approach offers a minimal hardware setup for implementing all required basic features. Other complementary tasks like data storage and WEB services are also assumed by the RT Linux kernel. This embedded solution is very simple and efficient. Moreover, this combination of elements and parts also well suited to the concept of open-hardware and open-software.

Figure 27 shows the block diagram of the 3Ph-oZm hardware where four conceptual blocks are clearly identified:

- The first block, in grey, contains the power supply and battery management. The input voltage is rectified from the mains side, converting Alternating Current (AC) to Direct Current (DC) up to 440 V in safety conditions. An analog pi filter is configured as a functional block to prevent noise sources. Rectified mains steps down by means of a buck converter Viper22A from STM Microelectronics, reducing the voltage to 22V and offering up to 4.5W. Finally, a secondary buck converter with the SY8201 chip, allows a stable voltage of 5V. The use of this particular power supply allows the system to operate over a wider range of

voltages than commercial integrated converters can tolerate, typically designed for the 100~240V range.

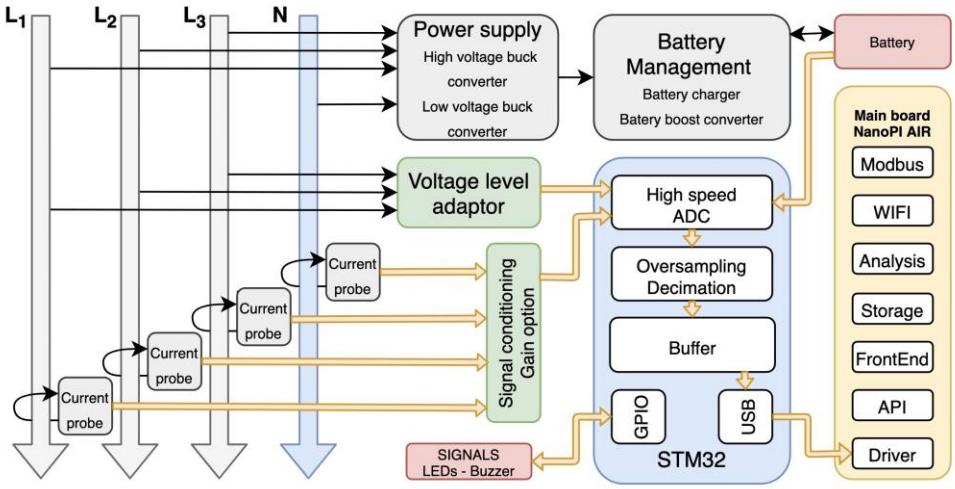

Figure 27 Three-phase openZmeter (3Ph-oZm) hardware block diagram: 1) the signal conditioning and acquisition, highlighted in green; 2) the power supply and battery management elements colored in grey; 3) the STM32 microcontroller (in blue), which controls the overall operation, performs data digitization and communication with the RT Linux kernel; 4) the yellow block representing the Advanced RISC Machine (ARM) RT Linux board controller NanoPi.

3Ph-oZm has a Li-Po built-in battery for normal operation under blackout or abnormal voltage supply. This battery provides a voltage profile between 3.2V and 4.2V. All necessary electronics have been included to boost battery voltage to the board working voltage of 5V (PS7516 module). The boost converter can be disabled by the microcontroller so that the whole system goes into sleep mode without damaging the battery by depletion. The charge process is also controlled while connected to the mains. The load manager chip is the TP4054 module, which limits the maximum charge current to about 100mA. A dedicated metal–oxide–semiconductor field effect transistor (MOSFET) element switches from mains to battery supply when the mains voltage is below 60 V.

- The second block accounts for the signal acquisition part, which is highlighted in green. It contains the elements responsible for capturing the voltage and current waveform signals. For the voltage acquisition stage, a simple voltage divider is placed. It feeds an operational amplifier which also provides a low impedance signal to the ADC of the STM32. After the whole process, the input voltage range is reduced from ±440V to 1.65V±1.65, which is the suitable range tailored to the ADC's technical specification. The conditioning of every current channel is

performed by using an operational amplifier MCP6004 from Microchip Technology, similar to voltage channels. The differential input signal is amplified and then adapted to a suitable input range of the ADC in the STM32 microchip. Moreover, the software-adjustable amplifier can be modified to control the output gain. This gain allows ± 333mV or ± 625mV values from the probes to be converted to the ± 1.65V input range of the ADC. For both voltage and current readings, the signal is filtered to eliminate high frequency noise. A high frequency passive low-pass anti-aliasing RC filter is configured to attenuate frequencies above 12 kHz, half the sampling frequency.

- The blue block is the STM32 microcontroller, which controls the overall operation, performs data digitization and communication with the Linux kernel using the USB channel. The system has been designed to operate at a high sampling rate. The voltage and current input values are sampled at high speed, along with the battery level and the internal voltage reference. The frequency sample is 96kHz per channel, with 12-bit precision. Afterwards, a decimation process executed in the STM microcontroller allows resolution to increase, reducing the rate by 4. This yield a 24kHz sampling frequency per channel with a 13 effective bit rate.
- The yellow block is the NanoPi Advanced RISC Machine (ARM) Linux board controller, which mainly analyzes, computes, stores and provides visualization services for the data obtained. It also provides a communication layer for WiFi and Bluetooth. Other technologies can be added by plugging USB peripherals, like an 3G/4G/5G USB modem, for example.

All these blocks are integrated in a compact electronic device, with a typical width and height ratio for a DIN electrical device. The connectors for voltage terminals are located on the top side, whereas the terminals for the current probes can be found on the bottom side. The aforementioned terminals are mounted on the AFE board located immediately below the ARM mainboard (NanoPI). The Li-Po battery, WiFi antenna, and others auxiliary components are properly placed around the printed circuit board (PCB). Figure 28 shows the basic components of 3Ph-oZm. Note that the Li-Po battery, the heat dissipator, and other components are already included inside the enclosureIt can be seen that the main board design comprises the signal conditioning and acquisition stage, the power supply and

management, the STM32 microcontroller and the interface to communicate with the ARM Linux board controller.

Figure 28 Electronic components layout including the Li-Po battery and heat sink. The enclosure covers the device becoming a very compact one.

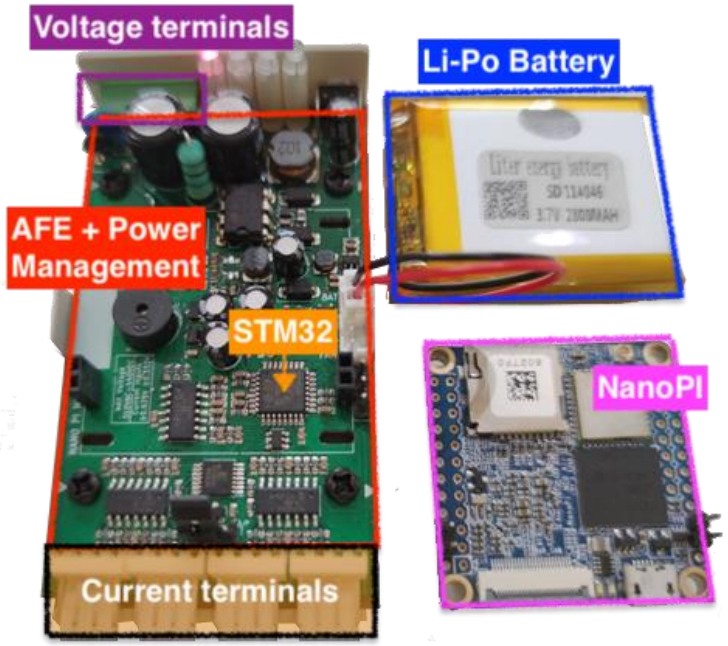

Figure 29 Main parts of 3Ph-oZm: Main board (left side), the Li-Po battery (top right) and the ARM Linux board controller (bottom right).

Figure 30 Split core current transformers probes (top left); Hall effect sensors (bottom left); Rogowski probes (right).

Voltage terminals are used for a dual purpose: to perform the measurements and to power the electronics of the board. The power supply is not isolated from mains, which greatly simplifies the design due to the fact that all voltages are referenced to the neutral point. 3Ph-oZm is completely functional even if only one phase is active (used for the power supply), so it can also be used in single-phase and two-phase systems. Every line current can be measured separately, including the neutral. It allows different configurations to adapt to different measurement probes. The probes can be configured for two voltage supply levels (3.3V and 5V). The operating mode is performed by changing the position of a jumper, which must be provided with the appropriate connection. The input voltage range of the current probe can be adjusted to ±333mV or ±625mV by software control, which is a typical differential input. The current channels can be configured for different types of probes. Among the probes that can be connected to the device are:

- Current *transformers*, a type of passive probe that requires no power supply. They are very low cost and widely used in many measuring devices. Their accuracy is acceptable with a significant phase variation.
- *Hall effect sensors* are active probes requiring external power supply. They have good accuracy and phase response. These sensors typically operate at 5V and have an output of 2.5V ±625mV.
- *Rogowski probes*, admit high currents for specific applications in large electrical installations. The set-up is accomplished by clamping to the busbars. Most of them have an output of ±333mV at 1000 A. They are typically supplied at 5V and have high accuracy and very good phase response.

Figure 32 shows the designed scheme of the manufactured electronic device. The scheme and silkscreen of the PCB has been created using the cross-platform Kicad [82], an open source electronics design automation suite.

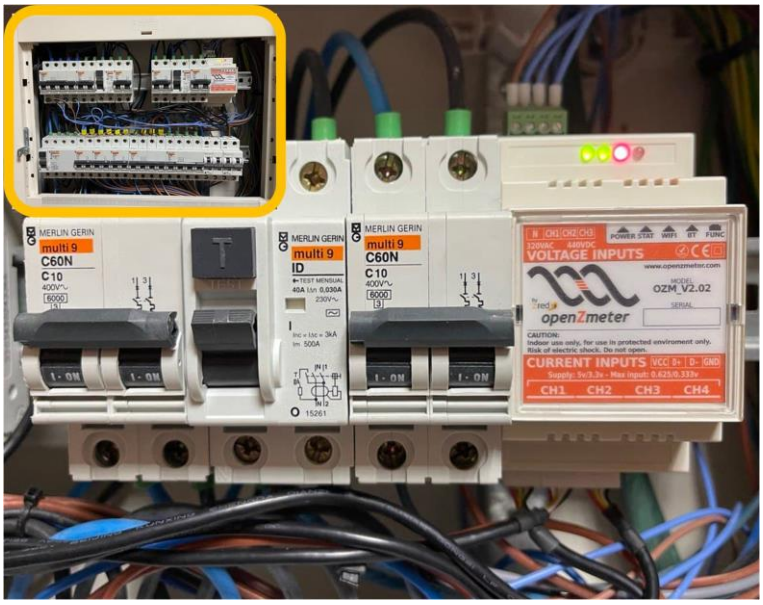

Figure 31 Electrical panel with a 3Ph-oZm installed along with circuit breakers and residual current breaker.

As it can be seen in Figure 31, the installation of 3Ph-oZm in a real electric cabinet is very straightforward since it has been designed to be attached directly to the DIN rail. Voltage wires need to be connected to the terminal block. The current probes can be installed on each phase wire without altering the installation.

4.2.2. Software design

The description of the software design of 3Ph-oZm is divided into two parts: daemon services and web frontend.

1) Daemon services: The software runs in an endless loop programmed through daemon services, which are executed automatically at startup. The embedded ARM unit is in charge of executing the code by means of a real-time kernel (Linux RT). It ships a wireless module (AMPAK AP6212) with WiFi 802.11b/g/n and Bluetooth 4.0 dual mode, ready for Internet applications. The daemon software is coded using C++ to achieve a robust and reliable service. To make the service as extensible as possible, two distinct blocks have been defined within the service: The first one is the capture driver, that is responsible for reading the raw samples as well as making the necessary adjustments and passing them to the second block (the analyzer). This analyzer is responsible for processing the samples, storing them, and serving

the results to the clients. The driver feeds one or several analyzer blocks, each one working independently on the input sample stream and generating results on the injected channels.

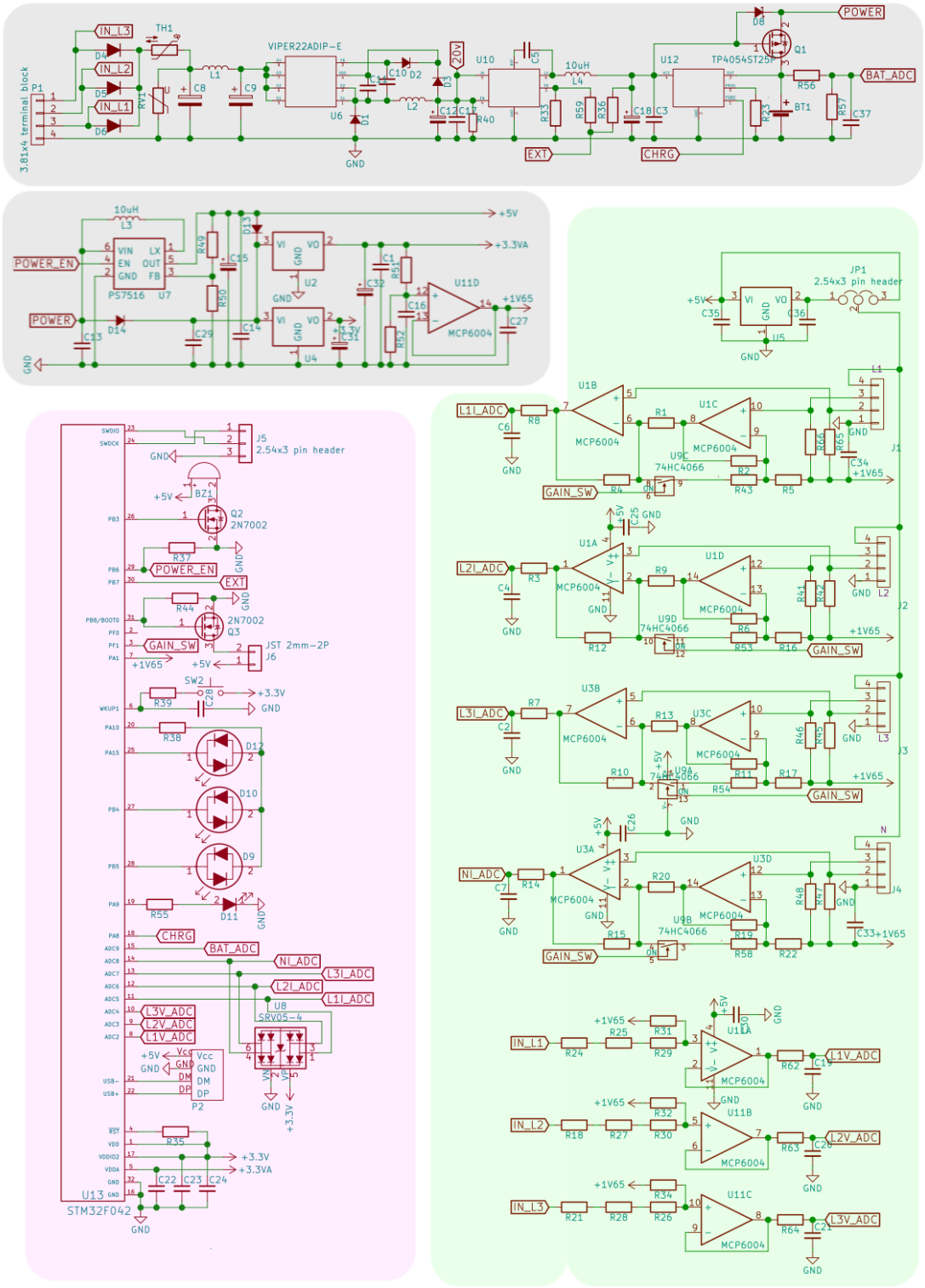

Figure 32 Electric scheme of the 3Ph-oZm. It is composed by the conditioning signal (green area), power management and power supply (grey areas) and the STM32 microcontroller (pink area). Note the connection to the ARM Linux board by pins USB+ and USB- in the STM area.

Figure 33 summarizes the analysis process consisting of data input through the USB port of STM32 microcontroller until results are obtained and stored. The first block, in blue, corresponds to the reading of the data generated by the STM32 microcontroller. Since it has a very small amount of internal memory, the reading from the USB port must be continuous and without interruptions for more than a few milliseconds. After receiving the data, the configured calibration settings are applied to translate the value obtained by the ADCs to the corresponding voltage and current, labeling the samples with the timestamp corresponding to the instant of reading. This time stamp is accurately preserved by using a network time synchronization service. The channel rearrangement is the final stage. Here, the channels used, their polarity and the order of the different available analysis modes can be selected, which allows the device to be used in facilities with 3 phases and neutral, 3 phases without neutral or even for the measurement of several independent single-phase systems. It also allows repair of connection errors regarding the order of the phases without the need to modify the physical connections.

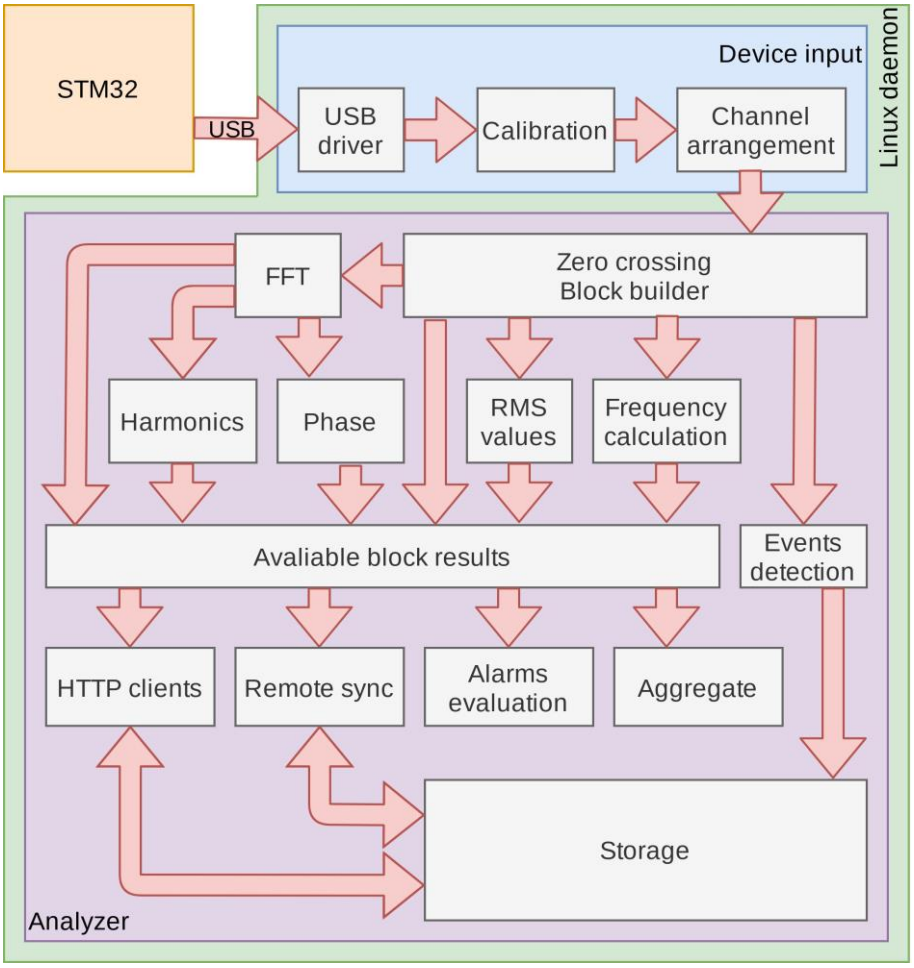

Figure 33 3Ph-oZm Linux daemon blocks, driver capture in blue, analysis stages in purple

As the data input flow is continuous and the time required for the analysis process and data storage may vary depending on the system load or connected clients, the first step of the analysis is the storage and segmentation of the samples into blocks. The zero crossing block takes the input voltage waveform and passes it through a bandpass filter. A five stage biquadratic (2-poles and 2-zeros) digital filter is used. The required filter coefficients are calculated at the start of the capture process so that the nominal frequency can be conveniently detected (defined in settings), and the zero crossing detector can count the number of cycles properly. The phase shift introduced by the filter needs to be compensated, adding the same delay to the rest of the channels. Using the recommendations of IEC61000-4-30, the preferred time interval for the voltage waveform is 200ms, which means 10 cycles for 50 Hz systems and 12 cycles for 60 Hz systems. Therefore, a 200ms data package is used to compute all subsequent parameters and features.

Figure 34 Application screen display of 3Ph-oZm. Top right shows the main hardware parameters summary. In the top left, the main status parameters are displayed, such as battery charge, WiFi connectivity and data storage level. On the left, 3Ph-oZm offers different options. The main screen area displays the detailed measurements, namely voltage, current, active power and frequency.

The ARM board has a 4-core CPU so it has a high concurrent processing capacity. Thus, for each basic block of 200ms and channel, the Root Mean Square (RMS) values of voltage and current are calculated. Moreover, an FFT is initiated using a stable well-known open-source implementation (FFTW3) [83] so that harmonic voltage and current are also computed. For the real grid frequency, the length of each half-cycle during the last 10 seconds

is taken into account. Once the FFT is completed, further calculated parameters can be obtained: active, reactive, and apparent power, power factor, harmonics up to 50th for current and voltage, phase shift between current and voltage, active and reactive energy, symmetrical components and unbalance factor. The event detection process runs in a separate thread since an event can span several 200ms blocks. If an event starts or is running in the current block, the start and end samples are stored (both waveform and RMS voltage values) and the block and subsequent aggregations are marked as affected.

The results produced after the analysis of each block can be consulted in real time, including the waveforms of each channel and the spectrum obtained by the FFT in the frequency domain. However, following IEC61000-4-30, the data obtained are aggregated in larger time blocks of 3 seconds, 1 minute, 10 minutes, 15 minutes and 1 hour. The data are stored into a local database and it is possible to retrieve aggregated data using custom methods implemented in the software. Furthermore, all captured data can be retrieved through an API Rest, with the possibility of synchronization with cloud services through the MQTT protocol. This enables real-time data provided by multiple devices to be available at a central location.

2) Web frontend: All the information generated by 3PhoZm is stored locally in a PostgreSQL database and can be queried through a series of functions defined in a Rest API. However, one of the main tools provided is the visualization and monitoring application, accessible through the web portal embedded in the device itself. All measured data are served in real time, refreshed dynamically using leading-edge web technologies such as HTML5, CSS3, and Javascript. Different graphs are synchronized to display information for the same time span. The web application is mainly organized into three sections: Analysis, Events and Energy stats. It also includes a general dashboard view with the main variables and other menus for the configuration of the device. The main dashboard of the application is shown in Figure 34 which display the most relevant features and parameters of the electrical system. The application layout is distributed as follows: top right, brief overview for RMS voltage, RMS current, active power, frequency, and energy; middle, last 2 hours evolution for RMS voltage, RMS current, active power and frequency; bottom, last 24 hours evolution for several important features; left, sidebar to access all menus.

Regarding the PQ disturbances, 3Ph-oZm features three tools for management, visualization and analysis. The first tool is based on the international standards IEC 61000-4-

30 and EN-50160, and includes the event counting and statistical distribution of frequency, mains voltage, total harmonic distortion (THD), and unbalance. The second tool is the event manager, which is based on the recommendations provided by the Information Technology Industry Council (ITIC) and Computer Business Equipment Manufacturers Association (CBEMA) and allows visualizing the distribution of recorded grid events, such as rapid voltage changes, voltage gaps, among others.

4.3. EXPERIMENTAL RESULTS

Testing and calibration setup were executed at the electrical engineering laboratories of the University of Almería (Spain). All data were recorded and stored locally in the 3Ph-oZm, but they were also publicly available using the WiFi network of the university (it is also possible to send the data to a server or cloud using a 4G USB modem). The setup requires installing the 3Ph-oZm in the DIN rail of an electrical panel, as Figure 5 shows. The calibration set-up is shown in Figure 35, which includes a three-phase variable voltage supply (model DL1013, manufactured by DeLorenzo Group), two highaccuracy 8.5 digit reference multimeters (Fluke 8558A) and a programmable single-phase power source (model Agilent 6812). The calibration procedure consists of a series of specific steps. First, a nominal grid voltage is generated and applied to a linear load for about 5 minutes. During this period, raw readings of the generated waveform for each of the channels (voltage and current) are recorded with the 3Ph-oZm and the precision multimeters. The instantaneous synchronization function of the multimeters is used to ensure that these readings are taken at the same instant. Subsequently, the RMS voltage and current values are calculated in the multimeters as well as in 3Ph-oZm, applying the necessary gain and offset corrections (both adjustments are made by software). After this step, the consumed active power is computed, and the phase correction values are applied. Phase correction, which is applied in all the available channels, is necessary for accurate active and reactive power readings, especially since each type of current sensor may require different values to compensate for the phase shifts introduced by construction.

In order to verify the calibration process, the voltage and current harmonic values obtained by 3Ph-oZm where compared with the equivalent measurements provided by a Fluke 8558A analyzer as a reference standard, under sinusoidal conditions at a frequency range of about 50 Hz, where the Fluke 8558A analyzer presents its best performance with an very high accuracy. The methodology to be used to determine the quality of the

measurements will follow the pattern of other recent studies on new smart meters in which different operating scenarios are analysed [98].

Case	Description
1	Voltage applied: 143V T-phase has a parallel RC load (R is moved from position 0 to 7 for 1 second; L in position 7 all time).
2	Voltage applied: 143V T-phase has a parallel RL load (R is moved from position 0 to 7 for 1 second; L in position 7 all time).
3	Voltage applied: 220V T-phase has a parallel RL load (R is moved from position 6 to 7 for 1 second; L in position 7 all time).
4	Voltage applied: 220V S-phase and T-phase are connected to the inverter. T-phase has a parallel RL load (R is moved from position 0 to 7 for 1 second; L position 2 all time).
5	Voltage applied: 220V T-phase has a parallel RL load (R is moved from position 3 to 4 for 1 second; L in position 4 all time).

Table 5 Operating scenarios considered in empirical study

	Device	Min	Max	Mean	SD	Skewness	Kurtosis
Experiment #1							
V	3Ph-oZm	139.511	143.070	141.599	0.961	-0.388	-0.323
	Fluke	140.177	144.433	142.603	1.236	-0.208	-0.958
I	3Ph-oZm	0.774	1.373	0.860	0.175	2.786	6.605
	Fluke	0.776	1.375	0.866	0.174	2.790	6.628
Experiment #2							
V	3Ph-oZm	139.256	142.541	140.876	1.005	-0.118	-1.009
	Fluke	139.710	143.559	141.489	1.163	-0.059	-0.791
I	3Ph-oZm	0.742	1.374	0.875	0.234	1.585	0.915
	Fluke	0.748	1.375	0.881	0.231	1.591	0.937
Experiment #3							
V	3Ph-oZm	217.810	220.510	219.698	0.745	-1.301	0.857
	Fluke	218.090	220.981	220.063	0.814	-1.161	0.449
I	3Ph-oZm	0.391	1.442	0.497	0.108	2.887	7.038
	Fluke	0.397	1.422	0.492	0.315	2.888	7.038
Experiment #4							
V	3Ph-oZm	217.610	220.310	219.498	0.715	-1.276	0.812
	Fluke	218.095	220.983	220.062	0.814	-1.159	0.445
I	3Ph-oZm	0.383	1.340	0.422	0.102	2.485	6.991
	Fluke	0.388	1.325	0.452	0.215	2.666	7.247
Experiment #5							
V	3Ph-oZm	219.510	220.050	219.764	0.140	-0.079	-0.329
	Fluke	220.077	220.571	220.272	0.140	0.317	-0.214
I	3Ph-oZm	0.710	0.911	0.744	0.063	2.059	2.645
	Fluke	0.697	0.915	0.765	0.064	1.877	2.261

Table 6 Comparison between the measurements of 3PH-OZM and FLUKE 8558A considering the five first voltage and current harmonics

The operating scenarios here analyzed are described in Table 5. They and are based on the use of inductive (DL 1017L), capacitive (DL 1017C), and resistive (DL 1017R) loads

controlled by switches with seven steps (positions) each. R, S and T phases are connected to the three-phase variable source in all the scenarios, but the channels are configured in different ways, as it is described in Table 5.

Figure 35 Equipment used to calibrate 3Ph-oZm: On top, some 3Ph-oZm's prepared to be calibrated. A variable three-phase power supply in the middle (Yellow box). Finally, two 8.5 digit high accuracy multimeters Fluke 8558A and an Agilent 6812 digital power supply at the bottom.

Table 6 presents the average statistical measurements of the five scenarios presented in Table 5 for the 3Ph-oZm and the high-accuracy 8.5-digit reference multimeter (Fluke 8558A) when measuring voltage and current fundamental harmonic. where it is possible to observe that the measurements obtained by 3Ph-oZm are similar to those obtained by Fluke 8558A when measuring voltage and current harmonics. The standard deviation (SD) is less than 1V. The experiments are carried out using two different voltages, 143V and 220V respectively. The statistical asymmetry for voltage is very low giving centered values for this measurement.

On the other side, the one for current is slightly positively positioned, as expected, due to the sequential increase of the resistance in the successive experiments. All values for Shapiro–Wilk normality test were far above for the chosen significance level (0.05). Therefore, we do not reject the null hypothesis. Parametric tests were performed because all variables followed a normal distribution.

Table 7 Analysis of variance for 3ph-ozm and fluke 8558A. This Analysis yield that the significance is higher than 0.05. The differences in the current and voltage for the 50 harmonics Measured and both instruments prove the non-independence of the two variables compared, 3ph-ozm and fluke 8558A.

		Σx^2	df	$\bar{x}^2$	F	Sig
V_1	Between Groups	5.015	1	5.015	0.004	0.952
	Within Groups	188,910.361	138	1368.916		
	Total	188,915.376	139			
I_1	Between Groups	0.000	1	0.000	0.001	0.979
	Within Groups	32.728	138	0.237		
	Total	32.728	139			
V_2	Between Groups	0.016	1	0.016	0.045	0.832
	Within Groups	47.978	138	0.348		
	Total	47.993	139			
I_2	Between Groups	0.000	1	0.000	0.087	0.769
	Within Groups	0.025	138	0.000		
	Total	0.025	139			
V_3	Between Groups	37.140	1	37.140	42.646	0.977
	Within Groups	120.185	138	0.871		
	Total	157.325	139			
I_3	Between Groups	0.000	1	0.000	0.005	0.942
	Within Groups	1.399	138	0.010		
	Total	1.399	139			
Angle	Between Groups	0.381	1	0.381	0.000	0.994
	Within Groups	1,048,872.624	138	7600.526		
	Total	1,048,873.006	139			

An analysis of variance (ANOVA) with a 200 × 50 (50 harmonics calculated using FFT) was carry out between 3PhoZm and high-accuracy 8.5-digit reference multimeter (Fluke 8558A) to determine differences in the current and voltage for the 50 harmonics measurements. See Table 7. The Mauchly´s sphericity test applied to the ANOVA results was performed to assess the assumptions of variance. Th type I error of measurement was reduced using the Greenhouse–Geisser method for the correction of the freedom degrees in order to obtain sphericity assumptions. Statistical calculations were performed using the IBM SPSS software v.26. The significance level was set at alpha of 0.05 (p ¡ 0.05). Obviously, values of significance levels much higher than 0.05 were observed, proving the nonindependence of the two variables compared.

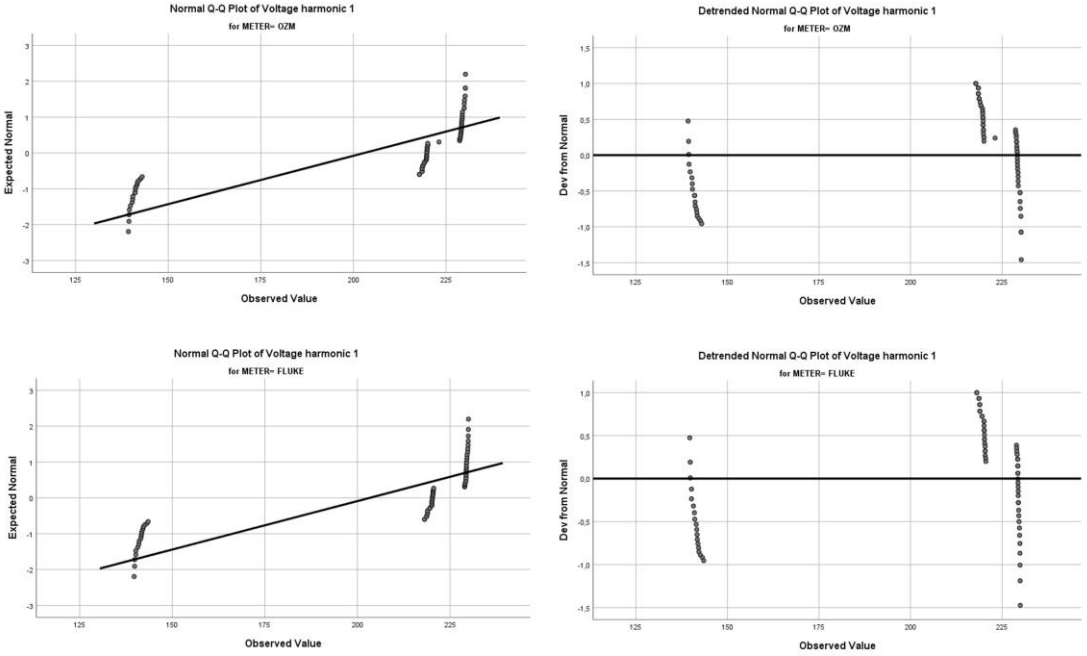

Figure 36 Normal Q-Q plot (left) and Detrended Normal Q-Q plot (rigth) of 3Ph-oZm (top) and Fluke 8558A (bottom) considering the first voltage harmonic.

4.4. OPERATION OF 3PH-OZM IN REAL ENVIRONMENTS: THE CASE OF A PV POWER PLANT

This section describes the use of 3Ph-oZm in real-world applications. More specifically, the information here presented corresponds to the measurements taken in a 100 kW photovoltaic (PV) power plant located in Almeria (Spain) and an industrial facility. Figure 37 shows the main dashboard for the PV power plant. The daily energy cycle for a period of one week can be observed. As expected, the energy cycle exactly matches the sun's cycle from sunrise to sunset.

The device performed satisfactorily and it was possible to perform the monitoring and PQ analysis remotely on a central location using a modern browser:

- *Voltage Analysis*: The voltage and its RMS value are measured in real time. The measurement are presented for both instantaneous value and the wave form. The visualization of the waveform is conducted every 10 cycles. Moreover, this voltage view (see Figure 38) has advanced options, such as harmonic visualization, FFT visualization, complex phasors representation, among others.

Figure 37 Main dashboard for a real 100kW PV power plant located in Almeria (Spain). This view displays the energy generated and the main RMS values.

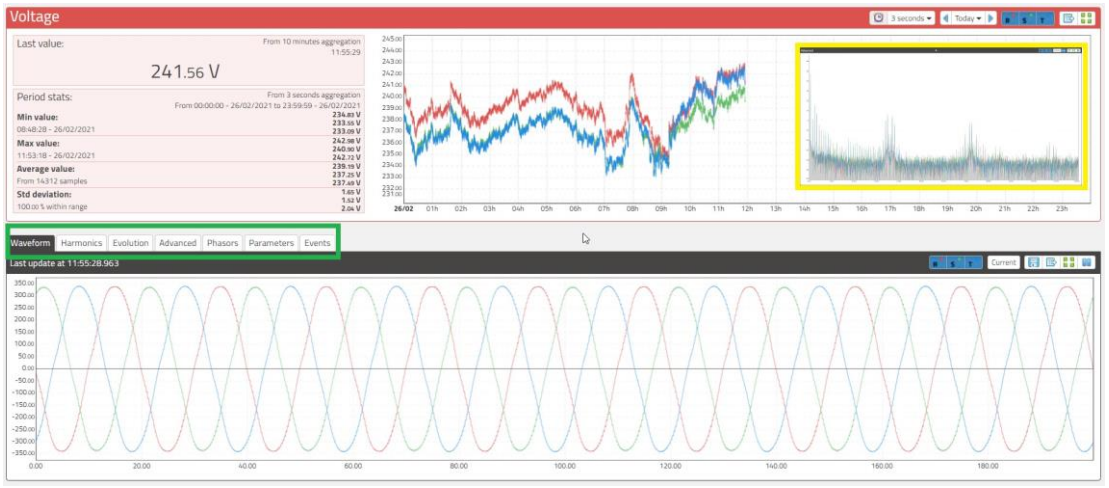

Figure 38 Voltage view for the 3 phases measured. The view shows the RMS for each phase and the voltage waveform. The green rectangle shows the different options available in the this view. The yellow rectangle shows the advanced option where it is possible to observe the three-phase FFT.

- *Current Analysis*: The current waveform is measured in real time for all three phases. The raw samples and RMS value are presented in several web views. The waveform visualization is retrieved every 10 cycles. In addition, the Current web view (see Figure 39) has advanced options, such as harmonic visualization, FFT visualization, phasors, among others. These options can be selected using the tab control green rectangle as shown in Figure 39.
- PQ Analysis: This device is able to log PQ events. The standards IEC61000-4-30 and EN-50160 establish and define which PQ disturbances have to be registered. Custom algorithms have been developed to monitor swells, dips, interruptions, and rapid voltage changes (RVC). The layout for PQ disturbance visualization was

organized using three views (see Figure 40). The first view is the ITIC/CBEMA curve, where a permitted zone, prohibited zone, and no-damage zone are defined. Every disturbance is presented by registering the magnitude of voltage RMS value and time duration. There are some charts that show the statistics computed from these events. The second view is a timetable where each recorded event is presented, while another table is used to select and visualize the waveform during the event (several cycles before and after). In this way, it is easy to observe what happened before and after the normal restoration of the voltage. The last view, following the EN-50160 standard, displays a visualization and statistics of the different types of events that occurred. The number of events within the margins allowed by the standard are checked.

- Active and reactive energy stats: These measurements are carried out using a time interval. It is easy to calculate the accumulated energy values. A better analysis can be performed because two ways of energy presentation can be shown. The first visualization (Figure 41) shows the energy grid data, which makes it possible to analyze the energy consumption habits. The second visualization (Figure 41) shows an energy heat map. Each colored “pixel” shows the consumption made in a specific interval time.

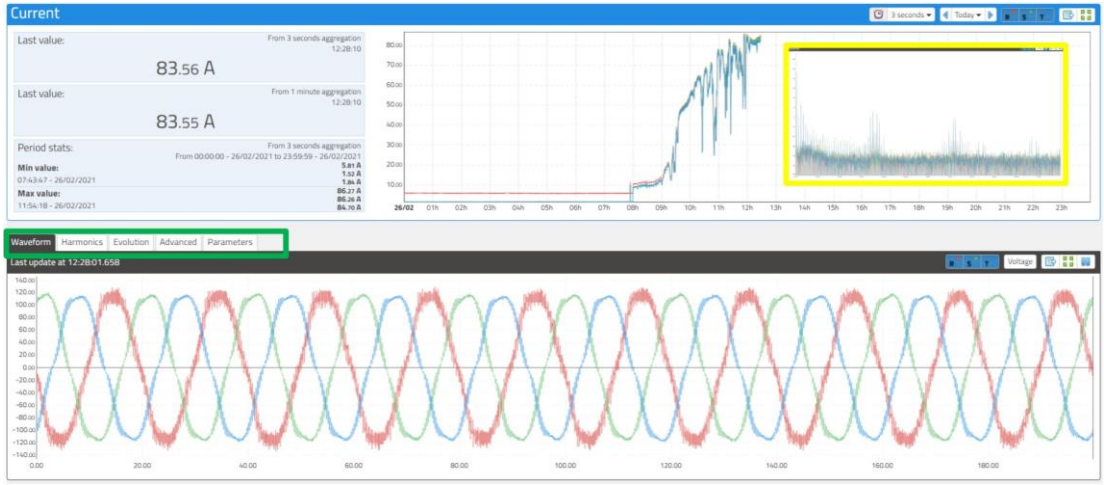

Figure 39 Current view for the three phases measured. The view shows the RMS for each phase and the current waveform. The green rectangle shows the different options available in the this view. The yellow rectangle shows the advanced option where it is possible to observe the 3 phase FFT

Figure 40 Statistics based on standard EN-50160.

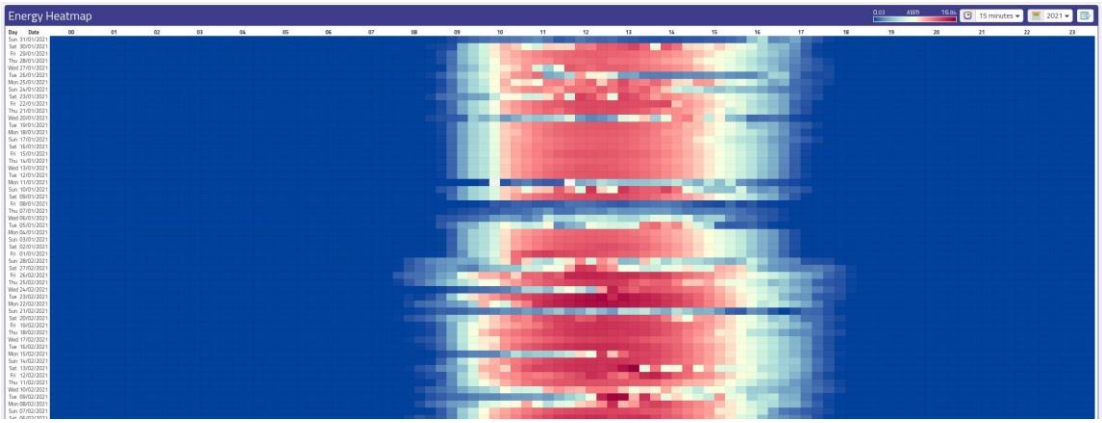

Figure 41 Active energy heatmap processed by 3Ph-oZm in a 100kW PV power plant located in Almería.

4.5. CONCLUSIONS

This paper presents 3Ph-oZm, an all-in-one three-phase smart meter and power quality analyzer with advanced IoT capabilities intended for industrial applications in large electric facilities. This device has been developed by the authors in the last few years following an open-hardware and open-source policy. 3Ph-oZm satisfies several international standards suchas IEC 61000-4-30 and EN 50160. The accuracy marks are for RMS voltages with an accuracy up to 0.1%, frequency up to 10 mHz (between 42.5 and 57.5 Hz), and RMS currents according to different sensor probes (the basic version can handle up to 400 V and 50 A RMS using an onboard Hall effect sensor with a precision of 1%). The chosen STM32 microcontroller is able to process the signal supplied by the Analog Front End (AFE), in real-time and processing it with low-power consumption. The advanced features like real-time oscillography and FFT analysis are performed by a Linux kernel ARM unit. The data are stored and refreshed dynamically using a modern user interface web. The device has been calibrated using ultra-high precision reference multimeters. The laboratory tests and the use of 3Ph-oZm

in a real PV power plant have shown that it is a precise and high-quality multipurpose smart meter. The PQ analysis and measurements done in the different applications yield the expected outcomes. The accessibility of the device via the Internet ease in checking the PQ analysis and the measurements performed. The three-phase electronic device assisted PQ analysis is an open hardware and open source software, easy to use with advanced features for electrical applications.

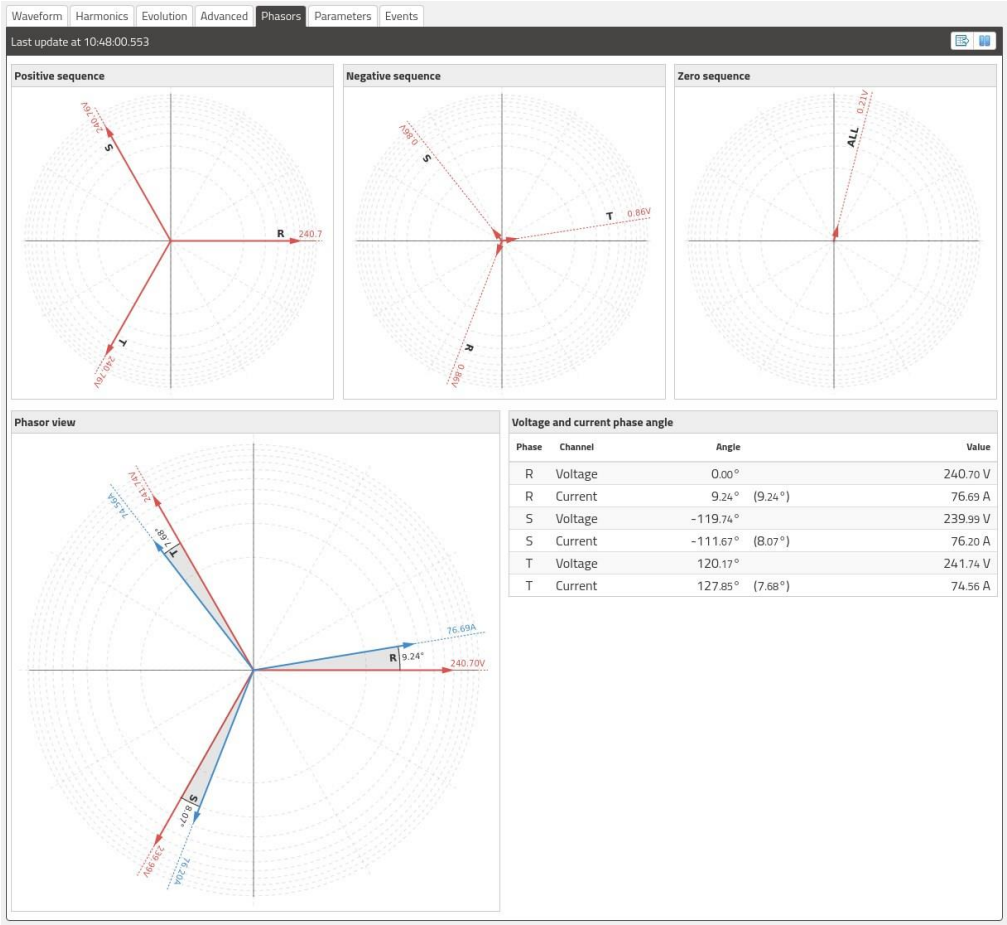

Figure 42 Phasor view for the three phase system. Symmetrical components are shown at the top and the complex phasor representation at the bottom.

The main innovation of the project is the creation of an autonomous, small-size and low-cost device that is able to process electrical and energy data along with power quality events in three-phase electrical grids. It is designed not only as a stand-alone device that can process the collected information on-site, but also as an IoT endpoint that syncs the information with the cloud. Finally, it is essential to remark that this device is a proven alternative to commercial meters that, due to their high unit cost, cannot be deployed to multiple locations in electricity grids. Future work includes the design and implementation a multi-phase version to be used by electrical machines of up to six phases.

CAPÍTULO 5 - ANALYSIS OF NON-ACTIVE POWER IN NON-SINUSOIDAL CIRCUITS USING GEOMETRIC ALGEBRA

A new approach for the definition of non-active power in electrical systems is presented in this paper. Through the use of geometric algebra, it is possible to define a new term called geometric non-active power, which is applicable to both sinusoidal and non-sinusoidal systems, and to both linear and nonlinear loads. The classic definitions of distortion and reactive power are compared and discussed in our proposal. We verify how geometric non-active power can appear in both purely resistive and purely reactive systems. The superiority of geometric algebra is revealed through several examples of electrical circuits previously analysed in specialised literature. Furthermore, a new geometrical current decomposition is proposed, for the first time, to provide a greater physical sense to existing geometric power. The results obtained confirm that classic concepts based on apparent power S are based on a lack of physical meaning, which is why geometric algebra theory should be adopted instead.

5.1. INTRODUCTION

Multiple studies have demonstrated that new electrical networks must function under numerous adverse conditions [99] [41] [100]. From the integration of new sources of distributed and renewable energy to the massive proliferation of nonlinear loads, this issue represents a remarkable challenge that must be approached properly to avoid degradation and abnormal operation of the power grid [101].

To achieve this, the use of valuable mathematical tools, and theories that allow a superior understanding of the physics behind the problem, are essential for engineers in the administration of daily power-grid management tasks. In this sense, the existing theories that describe the power flow in electrical systems have been the subject of debate and controversy for more than a hundred years [3] [4] [5]. Traditionally, two major proposals have dominated studies during this time: those based on the time domain [6], and those based on the frequency domain [4]. Selected proposals have ventured even further and have proposed mixing the concepts of the two approaches, generating a theory halfway between the time

and frequency domains. Undoubtedly, Steinmetz's theory based on complex numbers [3] has achieved the greatest influence among the scientific community, and is the basis for the definition of the apparent power concept $\boldsymbol{S}$.

$$\boldsymbol{S} = P + jQ \qquad \textit{Equation 3}$$

This concept is so ingrained in the world of electrical engineering that it is quite difficult to argue against it without being criticised by the community. Despite this, numerous examples have confirmed that S is no longer valid under non-sinusoidal conditions; hence, it should yield to other alternatives with a clearer physical meaning [102] [103] [104]. This implies that associated concepts such as reactive power and distortion must be re-evaluated as

$$S^2 = P^2 + N^2 = P^2 + Q^2 + D^2 = \| V \|^2 \| I \|^2 \qquad \textit{Equation 4}$$

where V and I are the RMS values of the voltage and current, respectively. P is the active power defined as

$$P = \frac{1}{T}\int_0^T p(t)dt = \sum_{n=0}^{\infty} P_n = \sum_{n=0}^{\infty} V_n I_n \cos\,\varphi_n, \qquad \textit{Equation 5}$$

where V_n and I_n are the RMS voltage and current of harmonic n, respectively, and $\cos\,\varphi_n$ is the phase angle between V_n and I_n. In Equation 4, N is the non-active power according to the Fryze definition, Q is the reactive power, and D is the distortion power according to the Budeanu definition.

From the definition of $\boldsymbol{S}$, it can be derived that it is possible to determine N, Q, or D only if P and S are known. If it has been demonstrated that $\boldsymbol{S}$ is not a concept that represents a magnitude with physical meaning, we must conclude that the remaining terms do not have this either. Therefore, it is not worthwhile to continue directing efforts to justify the fitting of merely mathematical concepts, as other authors have proposed [105].

Conversely, the development of an electric power theory based on geometric algebra (GA) has provided a new and fresh approach for solving the problem of power flow in electrical systems of any nature, owing to its flexibility and ability to represent the multi-component concept of power flow in non-sinusoidal systems. References [106] [107] demonstrate the success of GA in disciplines such as relativistic physics, electromagnetism, and computer vision. Specifically, the studies of Castro-Nuñez [108] [109], Montoya [110],

and Castilla and Bravo [111] reveal the capabilities that GA can provide in the analysis of electrical systems. In this sense, the concept of non-active power, with the definition of quadrature power and degraded power, acquire a certain relevance as they allow an unambiguous physical association with certain components in the time domain. Using this approach, it is possible to understand energy balances more effectively, and even more relevant, to confirm the compliance of the principle of conservation of energy (PoCOE) and, similarly, to ensure that Tellegen's theorem is verified.

Nomenclature	
A	Clifford multivector
B	Susceptance
CN	Non-active geometric power
$CN_{r(hi)}$	Reactive geometric power due to voltage and current cross products
$CN_{r(ps)}$	Reactive geometric power due to voltage and current phase shift of same components
CN_d	Degraded power
CN_r	Quadrature geometric power or reactive geometric power
D	Distortion power
G	Conductance
i_a	Active geometric current
i_b	Quadrature geometric current
i_d	Degraded geometric current
i_g	Parallel geometric current
M	Geometric apparent power
M_a	Active geometric power
M_b	Quadrature geometric apparent power
M_d	Degraded geometric power
M_g	Parallel geometric apparent power
N	Non-active power
P	Active power
Q	Reactive power
R	Resistance
S	Apparent power
σ_{12}	Bivector
σ_i	Base vector
X	Reactance
Z	Impedance

Table 8 Nomenclature

In this work, non-active net geometric power is analysed in sinusoidal and non-sinusoidal systems, and then compared with the traditional theories using different loads proposed in the literature. Moreover, one of the major contributions related to the previous publications is a new decomposition of currents beyond that proposed by Castro-Nuñez that links with the

proposal of Fryze and Czarnecki. Hence, it is possible to obtain an active geometrical current that minimises the current to be supplied for the required active power of both linear and nonlinear loads.

5.2. TRADITIONAL DEFINITIONS FOR DISTORTED AND REACTIVE POWER

In general, the different proposals throughout history have attempted to justify the apparent power definition by adding quadrature terms [10,19] to the active power P such that it satisfies

$$S^2 = P^2 + R^2, \qquad \textit{Equation 6}$$

where R is a term that justifies the observable physical evidence in numerous electrical systems, given by

$$S \geq P \qquad \textit{Equation 7}$$

Several authors have found it impossible to identify a physical justification to Equation 7. Apparent power is an artificial mathematical concept that does not comply with the PoCOE; therefore, it is not conservative. One of the main quadrature terms is the so-called reactive power Q, introduced by Budeanu [4] for sinusoidal systems and linear loads

$$Q = VI\sin\ \varphi, \qquad \textit{Equation 8}$$

and later extended to nonlinear systems with harmonic generation

$$Q = \sum_n V_n I_n \sin\ \varphi_n \qquad \textit{Equation 9}$$

For non-sinusoidal systems, it was necessary to add a new term D such that Equation 4 remains valid, although it has no direct definition and depends on the main definition of $\boldsymbol{S}$, which a priori could seem contradictory.

$$D^2 = S^2 - P^2 - Q^2 \qquad \textit{Equation 10}$$

Other authors have made proposals in the same fashion [112], i.e., adding quadratic terms to justify the Equation 4. Among these authors are Fryze, Kusters and Moore, and Shepard and ZakiKhani; however, a breakthrough that manages to create a totally coherent theory of power has not yet been presented. More sophisticated theories, such as the currents' physical components (CPC) theory of Czarnecki [113] continue investigating the concept of apparent

power through a decomposition that arises from three current components: active, scattered, and reactive. These investigations have proceeded despite the deep criticism that the author himself has made of apparent power $\boldsymbol{S}$ over the years [102] [114] [115].

5.3. POWER CONCEPTS IN GEOMETRIC ALGEBRA

The use of GA has recently been proven a powerful tool for the analysis of electrical circuits specifically, and engineering problems in general. Its innate ability to work naturally with multi-component systems has been used to provide the resolution of circuits with harmonic components [87] [116] [111].

GA has its origins in the study of Clifford and Grassman in the nineteenth century. Despite its advantages over Gibbs' proposals and its vector analysis, Clifford's premature death prevented its development. The research of Hestenes and others [106] [117] has rescued and promoted the use of GA again in many engineering disciplines. The lack of space does not allow an extensive introduction to GA, however the reader can refer to the classic references of Jancewicz [118], Dorst [119], and Hestenes [107].

From any orthonormal basis $\mathcal{A} = \{\sigma_i\}$, where $i = 1, \dots, n$, for an n-dimensional vector space $\mathcal{V}_n$, a set of basis elements can be generated that determine a larger space called the GA of subspaces denoted by $\mathcal{G}_n$. A basis for the linear subspace of k-vectors can be generated by forming all possible independent outer products of the vectors from the set $\mathcal{A} = \{\sigma_i\}$. For example, in $\mathcal{V}_3$, there exist three independent basis vectors $\{\sigma_1, \sigma_2, \sigma_3\}$. The corresponding algebra is $\mathcal{G}_3$, which is spanned by $\{1, \sigma_1, \sigma_2, \sigma_3, \sigma_{12}, \sigma_{23}, \sigma_{13}, \sigma_{123}\}$, i.e., one scalar, three vectors, three bivectors and one trivector. These elements define a linear space of dimension $2^3 = 8$.

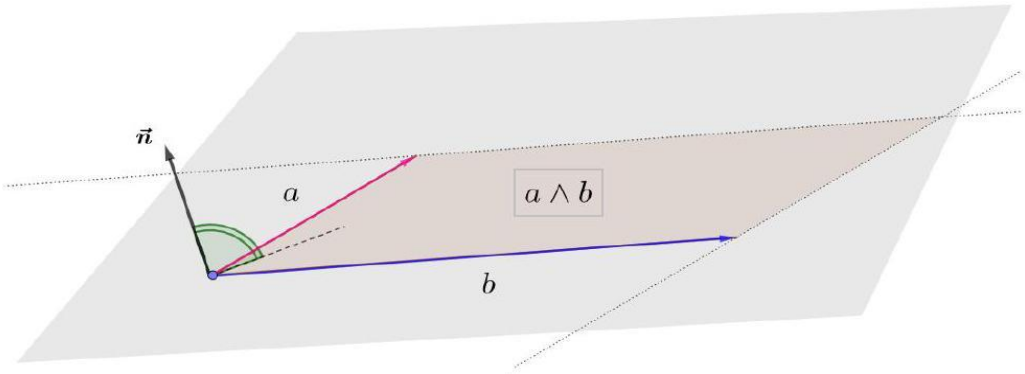

Figure 43 Bivector $a \wedge b$. Note that classical vector product $a \times b$ is also represented as perpendicular vector to plane formed by a and b.

The feature that makes GA an exceptional tool is its ability to accommodate vectors, complex numbers, quaternions, and spinors as subspaces mathematically. Moreover, GA can easily be extended to any number of dimensions. One of the keys is the use of geometric multidimensional objects such as bivectors, which arise from the exterior product or Grassman product defined by

$$a \wedge b = -b \wedge a \qquad \textit{Equation 11}$$

and result in an area delimited by vectors a and b, which have a magnitude and direction (see Figure 43). The bivector is a key concept that does not exist in vector analysis and has its own entity. As with vectors, a bivector can also be expressed as a linear combination of a bivector base.

The other major pillar of GA is the geometric product. Defined mainly for vectors, it can be easily extended to multi-vectors. Consider a and b as any two vectors in the geometric space $\mathcal{G}_2$ covered by the base σ_1, σ_2

$$\begin{aligned} a &= a_1\sigma_1 + a_2\sigma_2 \\ b &= b_1\sigma_1 + b_2\sigma_2 \end{aligned} \qquad \textit{Equation 12}$$

We can then define the geometric product as the linear combination of the scalar or internal product and the external or Grassman product. The result is a multi-vector $\boldsymbol{A}$,

$$\begin{aligned} \boldsymbol{A} = ab = a \cdot b + a \wedge b = \langle \boldsymbol{A} \rangle_0 + \langle \boldsymbol{A} \rangle_2 = \\ (a_1a_2 + b_1b_2) + (a_1b_2 - b_1a_2)\boldsymbol{\sigma}_{12}, \end{aligned} \qquad \textit{Equation 13}$$

where $\langle \boldsymbol{A} \rangle_0$ is the scalar part and $\langle \boldsymbol{A} \rangle_2$ is the bivector.

Castro-Nuñez presents the fundamental theory [109] that allows the transformation from the time domain to geometric space:

$$\begin{aligned}
\varphi_{c1}(t) &= \sqrt{2}\cos\omega t \;\leftrightarrow\; \sigma_1,\\
\varphi_{s1}(t) &= \sqrt{2}\sin\omega t \;\leftrightarrow\; -\sigma_2,\\
\varphi_{c2}(t) &= \sqrt{2}\cos 2\omega t \leftrightarrow\; \sigma_2\sigma_3,\\
\varphi_{s2}(t) &= \sqrt{2}\sin 2\omega t \leftrightarrow\; \sigma_1\sigma_3,\\
&\vdots\\
\varphi_{cn}(t) &= \sqrt{2}\cos n\omega t \leftrightarrow \bigwedge_{i=2}^{n+1}\sigma_{\mathrm{i}}\\
\varphi_{sn}(t) &= \sqrt{2}\sin n\omega t \leftrightarrow \bigwedge_{\substack{i=1\\ i\neq 2}}^{n+1}\sigma_{\mathrm{i}}
\end{aligned}$$

Equation 14

where $\bigwedge_n \sigma_i$ is the product of n vectors σ_i. Recently, a detailed explanation of why this transformation was chosen from others is presented in [120]. The main reasons follow.

- Its ability to codify the amplitude, phase, and frequency of the sinusoidal signal.
- It makes it possible to apply the Principle of Superposition.
- It guarantees the fulfilment of KCLs.
- It provides the ability to perform energy analyses through Tellegen theorem.

As an example, consider the voltage $v(t)$,

$$v(t) = \sqrt{2}[(230\cos(\omega t - 30) + 20\sin(4\omega t + 45)], \qquad \textit{Equation 15}$$

that can be expressed as

$$\begin{aligned}
v(t) &= \sqrt{2}[230(\cos\omega t\cos 30 + \sin\omega t\sin 30) + 20(\sin 4\omega t\cos 45 + \cos 4\omega t\sin 45)]\\
&= \sqrt{2}\left[230\left(\frac{\sqrt{3}}{2}\cos\omega t + \frac{1}{2}\sin\omega t\right) + 20\left(\frac{\sqrt{2}}{2}\sin 4\omega t + \frac{\sqrt{2}}{2}\cos 4\omega t\right)\right]
\end{aligned}$$

Following the transformation proposed in Equation 14, the transformed voltage is obtained by

$$\boldsymbol{u} = \underbrace{199.18\sigma_1 - 115\sigma_2}_{\langle \boldsymbol{u}\rangle_1} + \underbrace{14.14\sigma_{1345} + 14.14\sigma_{2345}}_{\langle \boldsymbol{u}\rangle_4}. \qquad \textit{Equation 16}$$

Similarly, it is possible to apply transformation Equation 14 to determine the value of the impedance and admittance of any load. In general terms, as Castro-Nuñez demonstrates in [87], impedance is defined as

$$\boldsymbol{Z} = \boldsymbol{Y}^{-1} = R + X\boldsymbol{\sigma}_{12} \qquad \textit{Equation 17}$$

It should be noted that the reactance $X = 1/\omega C$ is positive if the load is capacitive, and $X = -L\omega$ is negative if it is inductive.

In this manner, any non-sinusoidal voltage can be expressed as

$$v(t) = \sum_{i=1}^{n} v_i(t) = \\ D_1 \cos(\omega t) + E_1 \sin(\omega t) + \sum_{h=2}^{d} D_h \cos(h\omega t) + \sum_{h=2}^{k} E_h \sin(h\omega t) \qquad \textit{Equation 18}$$

where d and k are the number of cosine and sine components, respectively.

It should be noted that Equation 18 can be generalised to include interharmonics and subharmonics [121]. The DC component can also be included as a scalar element. The geometric voltage is

$$\boldsymbol{v} = D_1\sigma_1 - E_1\sigma_2 + \sum_{h=2}^{d}\left[D_h \bigwedge_{i=2}^{h+1} \sigma_i\right] + \sum_{h=2}^{k}\left[E_h \bigwedge_{i=1,i\neq 2}^{h+1} \sigma_i\right] \qquad \textit{Equation 19}$$

Similarly, the current can be calculated by applying Ohm's law for each of the harmonic components

$$i = \sum_{h=1}^{n} i_h \qquad \textit{Equation 20}$$

such that the result is

$$i = i_{\parallel} + i_{\perp} = i_g + i_b \qquad \textit{Equation 21}$$

with

$$\begin{aligned} i_g &= G_1 D_1 \sigma_1 - G_1 E_1 \sigma_2 + \sum_{h=2}^{d}\left[G_h D_h \bigwedge_{i=2}^{h+1} \sigma_i\right] + \\ &+ \sum_{h=2}^{k}\left[G_h E_h \bigwedge_{i=1,i\neq 2}^{h+1} \sigma_i\right] \\ i_b &= -B_1 E_1 \sigma_1 - B_1 D_1 \sigma_2 + \sum_{h=2}^{d}\left[B_h D_h \bigwedge_{i=1,i\neq 2}^{h+1} \sigma_i\right] - \\ &- \sum_{h=2}^{k}\left[B_h E_h \bigwedge_{i=2}^{h+1} \sigma_i\right] \end{aligned} \qquad \textit{Equation 22}$$

where G_h and B_h are the conductance and susceptance of harmonic h, respectively. Both i_g and i_b can be transformed back to the time domain by simply performing the inverse

transformation according to Equation 14. Finally, the geometric apparent power or net power $\boldsymbol{M}$ is defined as the product of $\boldsymbol{u}$ and $\boldsymbol{i}$:

$$M = ui = \underbrace{\overbrace{\langle M_g \rangle_0}^{P} + \sum_{i=1}^{n+1} \langle M_g \rangle_i}_{M_g} \underbrace{CN_{r(ps)} + CN_{r(hi)}}_{M_b = CN_r} \overset{+}{\overset{CN_d}{}} \qquad \textit{Equation 23}$$

where

$\boldsymbol{M_g}$ is the parallel geometric apparent power,

$\boldsymbol{M_b}$ is the quadrature geometric apparent power,

$\boldsymbol{P}$ is the active power,

$\boldsymbol{CN_d}$ is the degraded power,

$\boldsymbol{CN_r}$ is the quadrature geometric power or reactive geometric power,

$\boldsymbol{CN_{r(ps)}}$ is the reactive geometric power due to voltage and current phase shift of same components,

$\boldsymbol{CN_{r(hi)}}$ is the reactive geometric power due to voltage and current cross products.

It should be noted that Castro-Nuñez [87] establishes a correction factor $f = (-1)^{k(k-1)/2}$ for the product of the voltage and current to consider that the product of k-vectors of the same degree do not always square to $+1$. Thus, for scalars resulting from the product of bivectors as in σ_{13}^2, the sign changes as $k = 2$.

Based on the above definitions, the net or geometric power factor can be defined as

$$pf = \frac{P}{\| \boldsymbol{M} \|} = \frac{\langle \boldsymbol{M} \rangle_0}{\sqrt{\langle \boldsymbol{M}^\dagger \boldsymbol{M} \rangle_0}} \qquad \textit{Equation 24}$$

From Equation 23, it can be observed that power $\boldsymbol{M}$ is composed of two terms: $\boldsymbol{M_g}$, which is the parallel geometric power, and M_b, which is the quadrature power. Each power is obtained by multiplying the voltage $\boldsymbol{u}$ by the current i_g and i_b, respectively. From the parallel geometric power M_g, the active power P and the degraded power $\boldsymbol{CN_d}$ are obtained, whereas from the quadrature geometric power $\boldsymbol{M_b}$, the reactive geometric power of the harmonic components of the same order $\boldsymbol{CN_{r(ps)}}$ and the reactive geometric power due to cross-products of different frequency components $\boldsymbol{CN_{r(hi)}}$ are obtained. Of course, power M can also be decomposed according to an even more basic criterion

$$\boldsymbol{M} = P + \boldsymbol{CN} \qquad \textit{Equation 25}$$

where $\boldsymbol{CN}$ includes all terms that do not contribute to the active power, called the non-active geometric power.

The physical meaning of each of these terms is revealed through its definition based on the current component from which it is derived. M_b results from the current i_b, i.e., the current term in quadrature with the voltage due to the susceptance B of the load. All current i_b, and therefore all the power M_b, can be eliminated with a passive LC compensator, as demonstrated in [17]. Similarly, the remaining power M_g, which results from the product of the voltage $\boldsymbol{u}$ and the current parallel to the voltage $\boldsymbol{i_g}$, can be decomposed into active power P and degraded power $\boldsymbol{CN_d}$. Unlike the quadrature power, the purpose for compensation is not to eliminate the term $\boldsymbol{CN_d}$ (due to $\boldsymbol{i_g}$), rather only a certain portion according to a new decomposition of i_g, not previously published. Indeed, if we consider the proposal of Fryze, it is possible to define the active current i_a as that which contributes only to the active power P

$$\boldsymbol{i_a} = \frac{P}{V^2}\boldsymbol{u} = \frac{\langle \boldsymbol{M} \rangle_0}{\| \boldsymbol{u} \|^2}\boldsymbol{u} \qquad \textit{Equation 26}$$

where V is the RMS value of the voltage. In this manner, the remaining current is

$$i_d = i_g - i_a. \qquad \textit{Equation 27}$$

This current i_d is called the degraded current and coincides with the scattered current defined by the CPC theory of Czarnecki. This result is further evidence of the superiority of GA with respect to complex number algebra and to the power theories established to date. The energy flow phenomena that occur in a circuit can be explained clearly and with physical significance using the theory defined by Castro-Nuñez [120] [122] while complying with PoCOE and Tellegen's theorem.

Equation 20 is now

$$i = i_a + i_d + i_b \qquad \textit{Equation 28}$$

It is demonstrated that the three currents in Equation 28 are orthogonal to each other and satisfy

$$\| \boldsymbol{i} \|^2 = \|\boldsymbol{i_a}\|^2 + \|\boldsymbol{i_d}\|^2 + \|\boldsymbol{i_b}\|^2. \qquad \textit{Equation 29}$$

It should be noted that unlike the quadrature current, the current i_d can be compensated only by active elements, typically power active filters.

If we multiply the expression Equation 28 by the voltage $\boldsymbol{u}$, we obtain

$$M = ui = ui_a + ui_d + ui_b = M_a + M_d + M_b \qquad \textit{Equation 30}$$

Comparing Equation 30 with Equation 23, it can be inferred that the power $\boldsymbol{M}_g$ is the sum of $\boldsymbol{M}_a$ and $\boldsymbol{M}_d$, although it is not always true that $M_a = P$ or that $M_d = CN_d$. The above expression leads to an interesting approach: the active geometric power includes not only the active power P but also terms derived from the cross-product of the voltage and parallel current of different frequencies, which on average do not contribute to the net power flow.

5.4. NON-ACTIVE POWER IN LINEAR AND NONLINEAR LOADS

This section discusses practical examples of linear and nonlinear loads under non-sinusoidal voltages. Simple examples with resistive loads are studied and then expanded to more complex loads.

5.4.1. Linear loads - Pure resistor

Figure 44 Resistor load and non-sinusoidal source

The first case study represents one of the simplest, yet no less interesting, examples: a simple resistor powered by a non-sinusoidal source (Figure 44) of value

$$u(t) = 100\sqrt{2}\sin\ \omega t + 100\sqrt{2}\sin\ 2\omega t. \qquad \textit{Equation 31}$$

The voltage $u(t)$ is transferred to the geometric domain by Equation 13

$$u = -100\sigma_2 + 100\sigma_{13} \qquad \textit{Equation 32}$$

and, considering Ohm's law, the current is

$$i = \frac{u}{R} = -100\sigma_2 + 100\sigma_{13}. \qquad \textit{Equation 33}$$

The geometric apparent power M becomes the geometric product of the voltage and current:

$$M = ui = (-100\sigma_2 + 100\sigma_{13})(-100\sigma_2 + 100\sigma_{13}) = \underbrace{\underbrace{20{,}000}_{P} + \underbrace{20{,}000\sigma_{123}}_{CN_d}}_{M_a = M_g}. \qquad \textit{Equation 34}$$

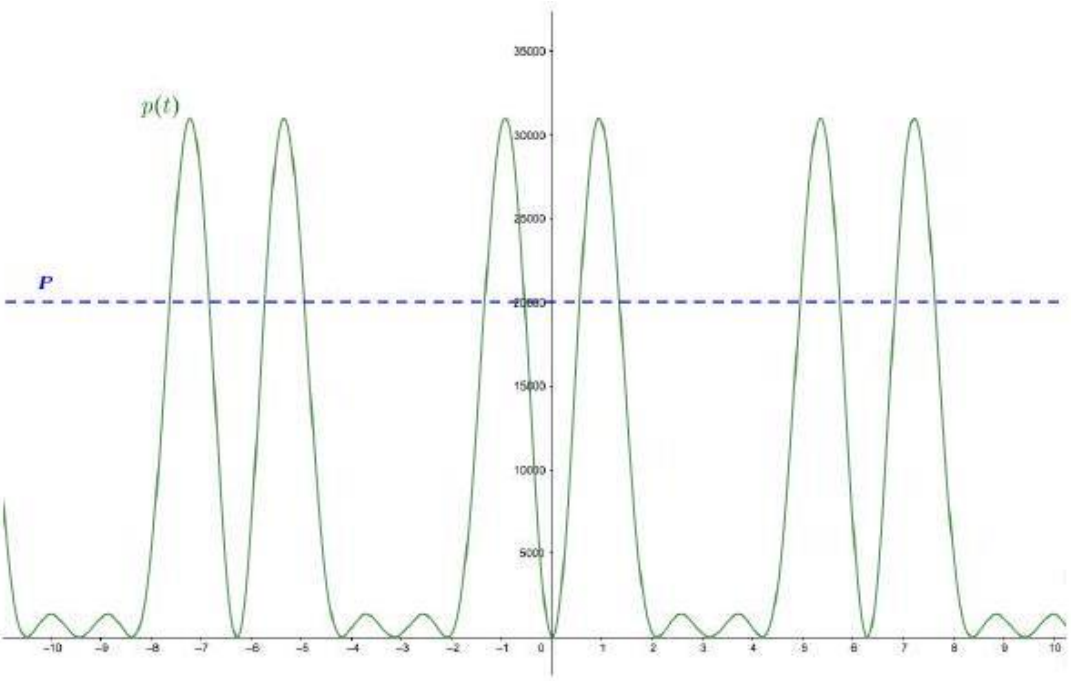

Figure 45 Instantaneous power

As expected, there is no quadrature power $\boldsymbol{M_b}$; there is only parallel power $\boldsymbol{M_g}$. Moreover, all the parallel power is active geometric power $\boldsymbol{M_a}$; that is, there is no degraded power $\boldsymbol{M_d}$ because there is no degraded current $\boldsymbol{i_d}$ as

$$i = i_g = i_a. \qquad \textit{Equation 35}$$

The instantaneous power in the time domain can be determined easily by multiplying $u(t)$ and $i(t)$, obtaining

$$p(t) = 2[10{,}000\sin^2\ \omega t + 10{,}000\sin^2\ 2\omega t + 20{,}000\sin\ \omega t \sin\ 2\omega t]. \qquad \textit{Equation 36}$$

Figure 45 displays the waveform of the power $p(t)$. This wave is fluctuating, yet always of positive value; that is, the energy flows from the source to the load and never backwards. The average value is the active power P consumed by the resistor. It can be observed that there is a clear equivalence between expression Equation 34 and Equation 36.

If we analyse the circuit of Figure 44 Resistor load and non-sinusoidal source using the classic technique of complex numbers and apply the CPC theory, the result is as follows:

$$\begin{aligned} S = P &= 20{,}000, \\ I &= 100\sqrt{2}, \\ V &= 100\sqrt{2}, \end{aligned} \qquad \textit{Equation 37}$$

which is in accordance with the expected result. Note that the CPC theory cannot capture the nuance of the undulatory term $20{,}000\sigma_{123}$ present in the active geometric power M_a. This means it is impossible to capture the terms caused by the cross-interaction of harmonics of the different frequencies using classical power theories, because it is not defined. Therefore, it is impossible to achieve the vector product of a different frequency in the complex plane. This is among the major deficiencies of the use of complex numbers in contemporary power theories.

5.4.2. Linear loads - Pure reactive load

The second case presents a purely reactive load composed of an inductor and capacitor, as displayed in Figure 46.

Figure 46 Pure reactive load

Following the steps described in the previous example, and considering that according to Equation 16, the admittances are $\boldsymbol{Y}_1 = \sigma_{12}$ and $\boldsymbol{Y}_2 = 0.285\sigma_{12}$, the transferred values for voltage, current, and geometric power can be obtained as

$$\begin{aligned} \boldsymbol{u} &= -100\sigma_2 + 100\sigma_{13} \\ \boldsymbol{i} &= \boldsymbol{i_b} = \boldsymbol{Y_1}\langle \boldsymbol{u} \rangle_1 + \boldsymbol{Y_2}\langle \boldsymbol{u} \rangle_2 = -100\sigma_1 - 28.57\sigma_{\boldsymbol{23}}, \\ \boldsymbol{M} &= \boldsymbol{ui} = \underbrace{-7142.8\boldsymbol{\sigma}_{12}}_{CN_{r(ps)}} + \underbrace{12{,}857.14\sigma_3}_{CN_{r(hi)}} \end{aligned} \qquad \textit{Equation 38}$$

In this case, all current is in quadrature and $i = i_b$. Therefore, the power in quadrature due to the interaction between the harmonics of the voltage and current of the same

frequency is determined by $CN_{r(ps)}$ and the cross-products are determined by $CN_{r(hi)}$. This decomposition or detail cannot be captured by the apparent power S in any manner.

The values obtained by the CPC theory are

$$\begin{aligned} S &= Q = 14{,}708, \\ V &= 141.42, \\ I &= 104.00. \end{aligned} \qquad \textit{Equation 39}$$

5.4.3. Arbitrary linear load

If we apply the previous non-sinusoidal voltage to an arbitrary linear load, as indicated in Figure 47, we can again obtain the voltage, current, and geometric power.

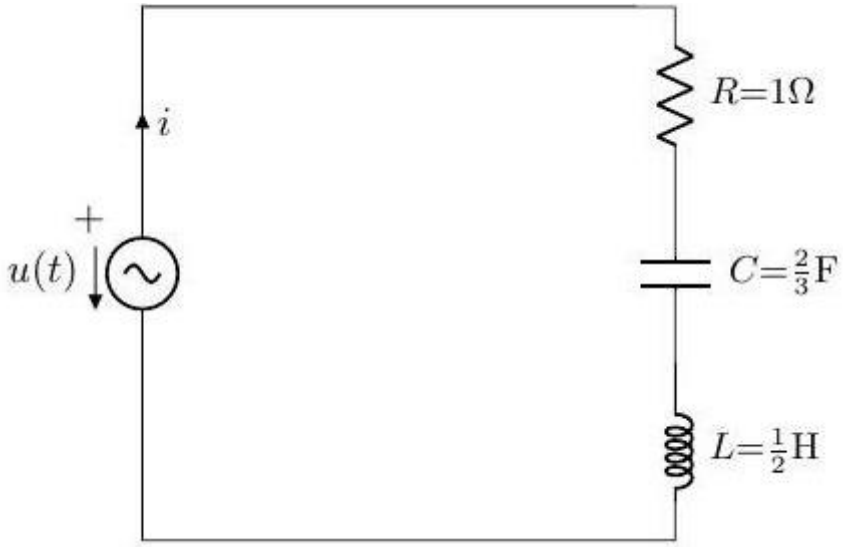

Figure 47 Arbitrary linear load

The impedances and admittances are as follows:

$$\begin{aligned} \boldsymbol{Z_1} &= 1 + \left(-\frac{1}{2} + \frac{1}{\frac{2}{3}}\right)\boldsymbol{\sigma}_{12} = 1 - \sigma_{12} \rightarrow \boldsymbol{Y}_1 = \boldsymbol{Z}_1^{-1} = 0.5 + 0.5\boldsymbol{\sigma}_{12} \\ Z_2 &= 1 + \left(-2\frac{1}{2} + \frac{1}{2\frac{2}{3}}\right)\sigma_{12} = 1 + 0.25\sigma_{12} \rightarrow Y_2 = Z_2^{-1} = 0.941 - 0.235\sigma_{12} \end{aligned} \qquad \textit{Equation 40}$$

The current in this case is

$$i = \boldsymbol{Y_1}\langle \boldsymbol{u} \rangle_1 + \boldsymbol{Y_2}\langle \boldsymbol{u} \rangle_2 = \underbrace{-50\sigma_2 + 94.11\sigma_{13}}_{i_g}\ \underbrace{-50\sigma_1 + 23.53\sigma_{23}}_{i_b} \qquad \textit{Equation 41}$$

and the geometric power is

$$M = \underbrace{14{,}411.76 + 14{,}411.76\sigma_{123}}_{M_g}\underbrace{-7352{,}94\sigma_{12} + 2647.05\sigma_3}_{M_b} \quad \text{Equation 42}$$

Once the power M is determined, we can determine the active current i_a,

$$i_a = \frac{\langle \boldsymbol{M} \rangle_0}{\| \boldsymbol{u} \|^2}\boldsymbol{u} = \frac{14{,}411.76}{20{,}000}(-100\sigma_2 + 100\sigma_{13}) = -72.05\sigma_2 + 72.05\sigma_{13}, \quad \text{Equation 43}$$

and the degraded current as

$$i_d = i_g - i_a = 22.05\sigma_2 + 22.05\sigma_{13}. \quad \text{Equation 44}$$

It can be verified that the currents i_a, i_d, and i_b are mutually orthogonal:

$$\begin{aligned} i_a \cdot i_d &= (-72.05\sigma_2 + 72.05\sigma_{13}) \cdot (22.05\sigma_2 + 22.05\sigma_{13}) = 0, \\ i_a \cdot i_b &= (-72.05\sigma_2 + 72.05\sigma_{13}) \cdot (-50\sigma_1 + 23.53\sigma_{23}) = 0, \\ i_d \cdot i_b &= (22.05\sigma_2 + 22.05\sigma_{13}) \cdot (-50\sigma_1 + 23.53\sigma_{23}) = 0 \end{aligned} \quad \text{Equation 45}$$

which satisfies

$$\begin{aligned} \| \boldsymbol{i} \|^2 = \|\boldsymbol{i_a}\|^2 + \|\boldsymbol{i_d}\|^2 + \|\boldsymbol{i_b}\|^2 \;\longrightarrow\; & 14411.76 \\ = 10384.94 + 973.18 + 3053.62. & \end{aligned} \quad \text{Equation 46}$$

Table 9 displays a summary of the current decomposition for the different physical components. Unlike the CPC theory of Czarnecki, where it is possible to obtain only the magnitude of the currents through GA, it is possible to obtain a complete decomposition according to Ohm's and Kirchhoff's laws.

	Vector		Bivector		
Current	σ_1	σ_2	σ_{13}	σ_{23}	Norm
i	−50.00	−50.00	94.11	23.52	120.00
i_b	−50.00	–	23.52	55.26	
i_g	–	−50.00	94.11	–	106.50
i_a	–	−72.05	72.05	–	101.90
i_d	–	22.05	22.05	–	31.19

Table 9 Current decomposition

Figure 48 displays the waveform of each power calculated in the geometric domain, transferred to the time domain. It can be observed how the instantaneous power $p(t)$ (Figure 48.e) presents both positive and negative values, which indicates the bidirectional flow of energy. The dashed line indicates the average value or active power P. However, in Figure 6.b), it can be observed that the power is always positive and never negative. This power $\boldsymbol{M_a}$ is calculated from the active current i_a.

The values obtained by the CPC theory are

$$S = 16{,}970,\ P = 14{,}411.76,\ Q = 7814.94,\ D_s = 4410.93,$$
$$V = 141.42$$
$$I = 120.00.$$

Equation 47

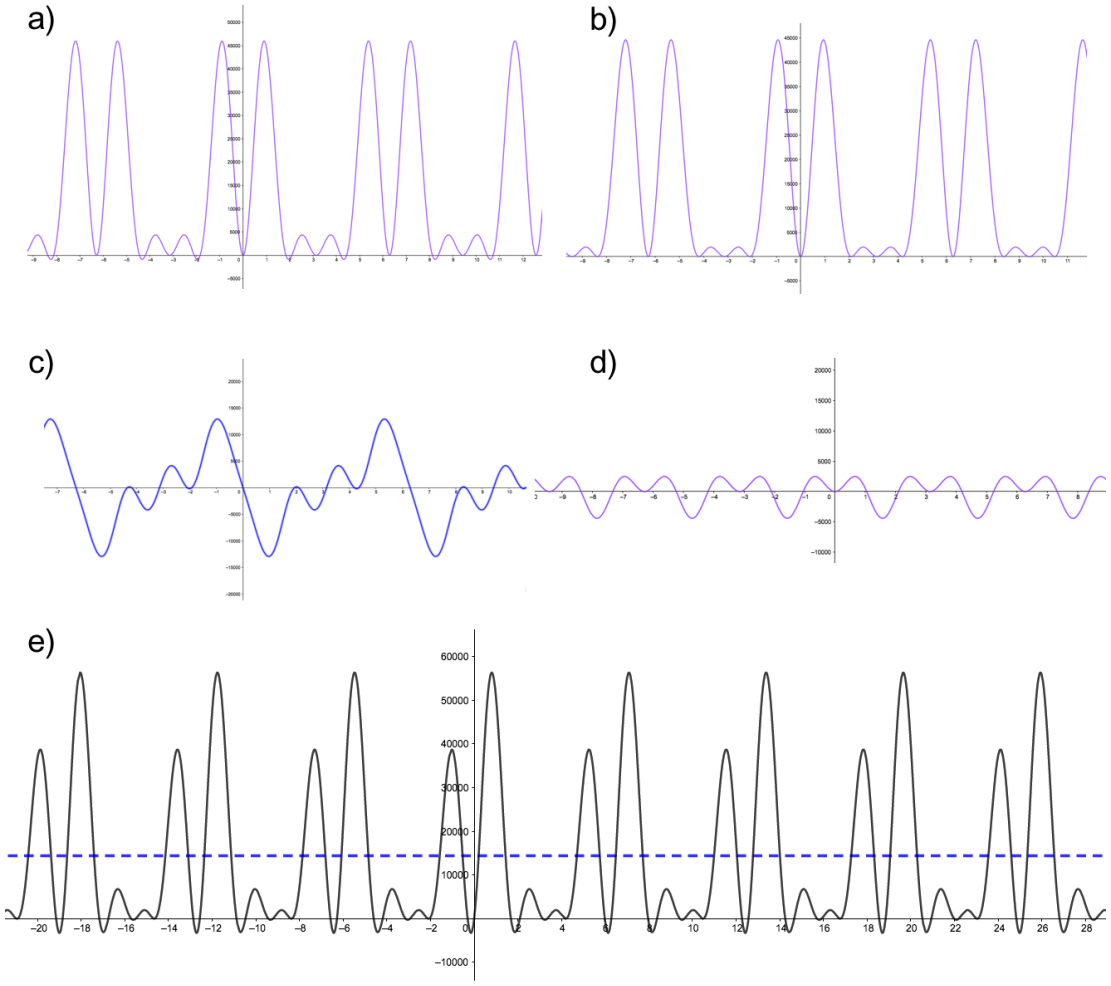

Figure 48 Instantaneous power waves. a) Parallel instantaneous power $p_g(t), b)$ active instantaneous power $p_a(t), c)$ quadrature instantaneous power $p_b(t), d)$ degraded instantaneous power $p_d(t)$, and e) total instantaneous power $p(t)$

5.4.4. Nonlinear load

The last problem was previously examined by Czarnecki in [33], establishing an unnecessary current decomposition between the source and nonlinear loads owing to the lack of powerful mathematical tools such as those provided by GA. Figure 7 presents the circuit to be analysed with the following characteristics:

$$u(t) = 100\sqrt{2}\cos\ \omega t + 50\sqrt{2}\cos\ 3\omega t + 10\sqrt{2}\sin\ 4\omega t,$$
$$j(t) = 50\sqrt{2}\cos\ 2\omega t + 10\sqrt{2}\sin\ 3\omega t + 30\sqrt{2}\cos\ 4\omega t.$$

Equation 48

Following the steps of the previous examples, we proceed to perform the transformation from the time domain to the geometric domain, such that

$$\boldsymbol{u} = 100\sigma_1 + 50\sigma_{\mathbf{234}} + 10c \qquad \textit{Equation 49}$$

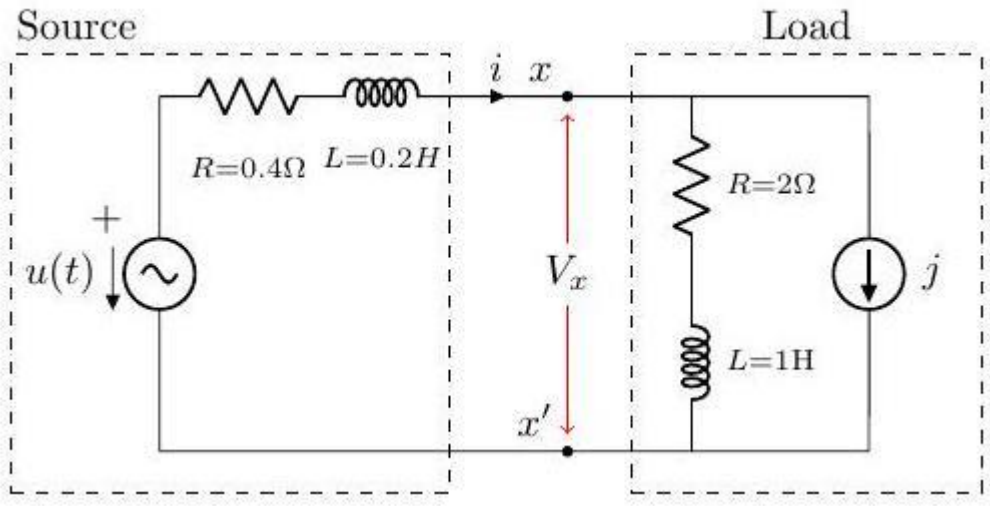

Figure 49 Nonlinear load and non-sinusoidal voltage source

The impedance and admittance for every harmonic of the source and the load is

$$\begin{aligned}
Z_{s1} &= 0.4 - 0.2\sigma_{12} & Y_{s1} &= 2.00 + 1.00\sigma_{12}\\
Z_{s2} &= 0.4 - 0.4\sigma_{12} & Y_{s2} &= 1.25 + 1.25\sigma_{12}\\
Z_{s3} &= 0.4 - 0.6\sigma_{12} & Y_{s3} &= 0.77 + 1.15\sigma_{12}\\
Z_{s4} &= 0.4 - 0.8\sigma_{12} & Y_{s4} &= 0.50 + 1.00\sigma_{12}\\
Z_{l1} &= 2.0 - 1.0\sigma_{12} & Y_{l1} &= 0.40 + 0.20\sigma_{12}\\
Z_{l2} &= 2.0 - 2.0\sigma_{12} & Y_{l2} &= 0.25 + 0.25\sigma_{12}\\
Z_{l3} &= 2.0 - 3.0\sigma_{12} & Y_{l3} &= 0.15 + 0.23\sigma_{12}\\
Z_{l4} &= 2.0 - 4.0\sigma_{12} & Y_{l4} &= 0.20 + 0.10\sigma_{12}
\end{aligned} \qquad \textit{Equation 50}$$

The current now can be calculated by applying Ohm's law and Kirchhoff's laws:

$$\boldsymbol{i} = \langle \boldsymbol{i} \rangle_1 + \langle \boldsymbol{i} \rangle_2 + \langle \boldsymbol{i} \rangle_3 + \langle \boldsymbol{i} \rangle_4 \qquad \textit{Equation 51}$$

$$\langle i \rangle_1 = \frac{1}{Z_{s1} + Z_{l1}} \langle u \rangle_1 = 33.3\sigma_1 - 16.6\sigma_2 \qquad \textit{Equation 52}$$

$$\langle i \rangle_2 = \frac{Y_{s2}}{Y_{s2} + Y_{l2}} \langle j \rangle_2 = 41.7\sigma_{23}$$

$$\langle i \rangle_3 = \frac{1}{Z_{s3} + Z_{l3}} \langle u \rangle_3 + \frac{Y_{s3}}{Y_{s3} + Y_{l3}} \langle j \rangle_3 = 17.9\sigma_{134} + 6.4\sigma_{234}$$

$$\langle i \rangle_4 = \frac{1}{Z_{s4} + Z_{l4}} \langle u \rangle_4 + \frac{Y_{s4}}{Y_{s4} + Y_{l4}} \langle j \rangle_4 = 0.8\sigma_{1345} + 23.3\sigma_{2345}$$

… … … … …

$$i = 33.3\sigma_1 - 16.6\sigma_2 + 41.7\sigma_{23} + 17.9\sigma_{134} + 6.4\sigma_{234} + 0.8\sigma_{1345} + 23.3\sigma_{2345}$$

$$\| i \| = 63.5 \text{ A.}$$

Once the current is determined, the voltage drop in the impedance of the source can be obtained as

$$\begin{aligned} \boldsymbol{V}_1 &= \boldsymbol{Z}_{s1}\langle i\rangle_1 + Z_{s2}\langle i\rangle_2 + Z_{s3}\langle i\rangle_3 + Z_{s4}\langle i\rangle_4 \\ &= 16.7\sigma_1 - 16.7\sigma_{13} + 16.7\sigma_{23} + 3.3\sigma_{134} + 13.3\sigma_{234} - 18.3\sigma_{1345} + 10\sigma_{2345} \end{aligned}$$

Therefore, the voltage in the load V_x is

$$\begin{aligned} \boldsymbol{V_x} &= \boldsymbol{V} - \boldsymbol{V}_1 = 83.3\sigma_1 + 16.7\sigma_{13} - 16.7\sigma_{23} - 3.3\sigma_{134} + 36.6\sigma_{234} + 28.3\sigma_{1345} - 10\sigma_{2345} \\ \|\boldsymbol{V_x}\| &= 98.78\ \mathrm{V} \end{aligned}$$

Once the voltage and current are determined, the power M can be calculated:

			k-vector												
	$\|\cdot\|$	Scalar	σ_3	σ_4	σ_5	σ_{12}	σ_{34}	σ_{45}	σ_{123}	σ_{124}	σ_{125}	σ_{345}	σ_{1234}	σ_{1245}	σ_{12345}
M	6696.9	3662.2		−2083.3	−987.2	−535.9	961.5		4166.7		105.8	−250.0	−1025.6	−416.7	2500.0
M_J	5932.5	1166.7		2000.0	816.7	−383.3	−833.3	−1000.0	−4166.7	0.0	−200.0			1916.7	−2500.0
Gen	5346.8	4828.8		−83.3	−170.5	−919.2	128.2	−1000.0	0.0	0.0	−94.2	−250.0	−1025.6	1500.0	0.0
M_1	2816.2	1613.4	833.3	−363.2	−578.8	198.5	188.0	−791.7	972.2	267.1	−363.7	791.7	−393.2	1166.7	416.7
M_I	3928.6	3215.5	−833.3	279.9	408.3	−1117.7	−59.8	−208.3	−972.2	−267.1	269.4	−1041.7	−632.5	333.3	−416.7
Demd	5346.8	4828.8	−83.3	−170.5	−919.2	128.2	−1000.0	0.0	0.0	−94.2	−250.0	−1025.6	1500.0	0.0	
M_x	5348.9	2048.8	−833.3	−1720.1	−408.3	−734.4	773.5	791.7	3194.4	−267.1	469.4	−1041.7	−632.5	−1583.3	2083.3

Table 10 Power decomposition for circuit displayed in Figure 49

From the above expression, the following values are highlighted:

$$\begin{aligned} P &= 2048.8 \\ CN_{r(ps)} &= 734.4 \\ CN_{r(hi)} &= 4064.2 \\ CN_d &= 3431.8 \\ \hline \|\ \boldsymbol{M}\ \| &= 5348.9 \end{aligned}$$

Once the current and power are obtained, their decomposition can be performed to verify that Kirchhoff's laws and PoCOE are satisfied, respectively. Tables 3 and 4 detail this decomposition. It can be observed that the power demanded by the resistors, of both the source and load, is equal to that generated by the sources. Similarly, it is possible to perform a detailed decomposition of each specific term of the active, reactive, and degraded power. Moreover, the current decomposition complies with Kirchhoff's first law for all k-vectors of which it is composed. The current I_a is the minimum current (according to Fryze) that generates the active power P necessary for the operation of the load. There are several strategies of compensation, depending on the objectives established; however, owing to the geometric power theory, these can be accomplished without any major inconvenience.

k-vector									
Current	$\|\cdot\|$	σ_1	σ_2	σ_{13}	σ_{23}	σ_{134}	σ_{234}	σ_{1345}	σ_{2345}
$\boldsymbol{I}$	63.51	33.33	−16.67		41.67	17.95	6.41	0.83	23.33
$\boldsymbol{I}_b$	44.53		−16.67	20.83	20.83	18.38	1.67	7.42	21.01
$\boldsymbol{I}_g$	45.28	33.33		−20.83	20.83	−0.43	4.74	−6.58	2.32
$\boldsymbol{I}_a$	20.74	17.50		3.50	−3.50	−0.70	7.70	5.95	−2.10
$\boldsymbol{I}_d$	40.25	15.84		−24.33	24.33	0.27	−2.96	−12.53	4.42

Table 11 Current decomposition for circuit in Figure 49

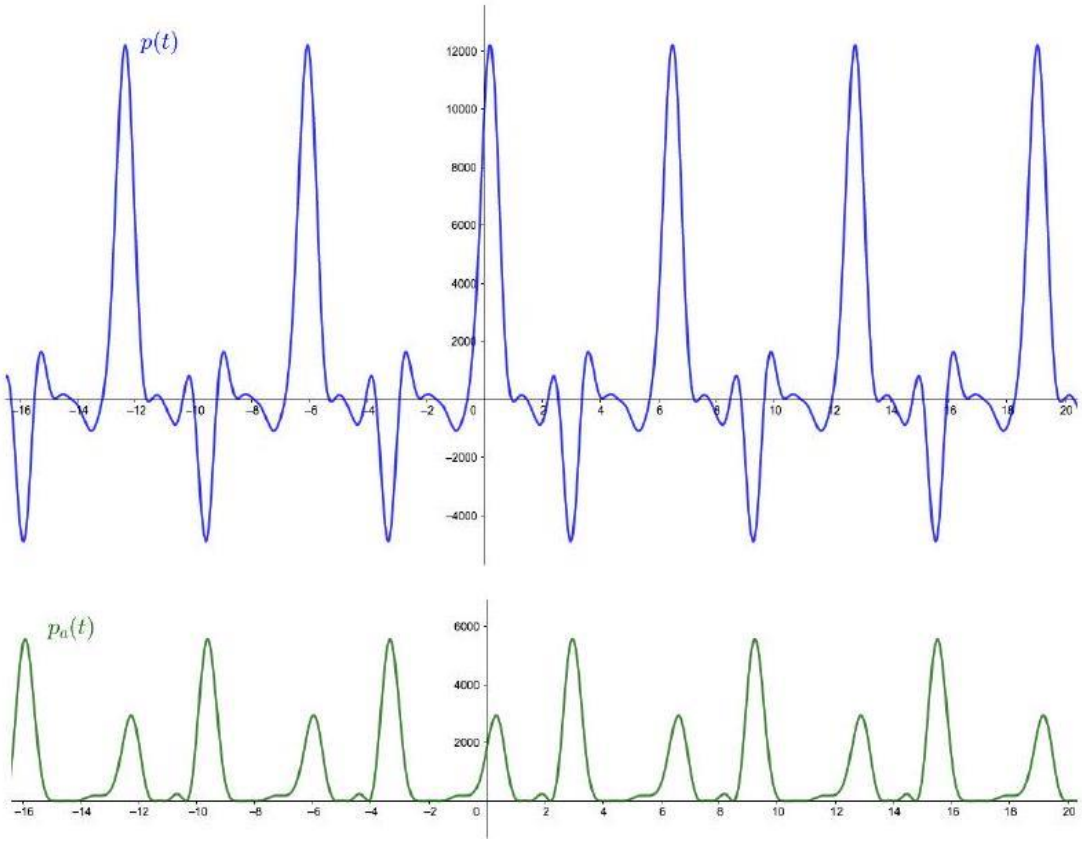

Figure 50 Instantaneous power for nonlinear load: top) total instantaneous power $p(t)$ and bottom) active instantaneous power $p_a(t)$

Figure 50 displays the values obtained for the total instantaneous power and active instantaneous power by applying the inverse transformation of the geometric domain to the time domain. This indicates that the power $p_a(t)$ presents only positive values.

Applying any of the existing power theories to this circuit to obtain the apparent power S is completely unfeasible, because there is no method to collect the contributions of the harmonics' cross-terms. Moreover, there is no approach where the PoCOE can be achieved, nor is there any expectation that Kirchoff's first law can be realised for currents in the different branches of the circuit based on the proposed decomposition.

5.5. CONCLUSIONS

In this paper, a detailed analysis of the use of GA applied to electric power systems was conducted. Owing to its flexibility, it is possible to correctly define new terms that comply with the PoCOE that are not satisfied by the traditional definition of apparent power S. This superiority has been proven repeatedly in the scientific literature. The non-active term net geometric power was analysed in non-sinusoidal systems and compared with traditional theories, revealing the ability of GA to verify net power flows in addition to their sense and magnitude. This proposed work, for the first time, allows a new decomposition of currents beyond those proposed by Castro-Nuñez, which link with the proposal of Fryze and Czarnecki; hence, it is possible to obtain an active geometrical current that minimises the current to be supplied for the required active power of both linear and nonlinear loads. Finally, it was demonstrated how traditional concepts based on apparent power S should be abandoned owing to their lack of physical meaning and the deficiency of their definition.

CAPÍTULO 6 - CONCLUSIONES

Como resultado del trabajo realizado durante el desarrollo de la tesis doctoral se han obtenido diferentes publicaciones en revistas especializadas de impacto internacional, destacando principalmente las tres publicaciones (capítulos 2, 3 y 5) aceptadas en revistas incluidas en el listado Journal Citation Reports (JCR) de la Web of Science (WOS), y una cuarta publicación en proceso de revisión (capítulo 4). Esto supone el desarrollo de una herramienta completa de suma utilidad para el estudio de redes eléctricas, enfocada principalmente en la investigación y el desarrollo de una teoría de análisis de potencia que rompe con las limitaciones de las teorías clásicas limitadas a sistemas con señales senoidales.

A continuación, se presentan más detalladamente las principales aportaciones del trabajo de investigación.

6.1. RESULTADOS Y DISCUSIÓN

Los desarrollos monofásicos y trifásicos presentados bajo plataforma “openZmeter”, y descritos en tres de los artículos, denotan como la posibilidad de establecer sinergias entre diferentes tecnologías, tales como la programación WEB, las comunicaciones, la electrónica o el uso de dispositivos embebidos. Se ha demostrado que el uso de herramientas y recursos libres pueden dar lugar a dispositivos que solventen las limitaciones encontradas en productos comerciales de alta gama y con coste mucho más elevado que, a pesar de su funcionalidad y precisión, adolecen de ciertas características que se han mostrado necesarias en laboratorios e instalaciones reales.

El uso de una herramienta matemática como es el algebra geométrica ha demostrado ser válida para proponer una teoría alternativa a la teoría tradicional de cálculo de potencia, discutida por ser un método impreciso para este tipo de cálculo en las redes eléctricas actuales, en las que la presencia de fuentes y cargas no lineales introducen una serie de variables que no son tenidas en cuenta por estas teorías.

A continuación, se muestran los resultados y conclusiones extraídas de cada uno de los artículos presentados.

6.1.1. Publicación científica 1: "OpenZmeter An Efficient Low-Cost Energy Smart Meter and Power Quality Analyzer"

Esta publicación, presentada en el Capítulo 2, parte del problema existente con los contadores de energía y medidores de calidad eléctrica comerciales, usados y enfocados para su uso por profesionales del sector. Estos dispositivos profesionales suelen tener un alto coste y su compleja utilización no los hace aptos para su uso por personal no experto. En esta primera publicación se presenta openZmeter (oZm) como un medidor inteligente de energía y calidad eléctrica enfocado al uso doméstico, esto es, redes monofásicas y baja potencia.

Con este dispositivo se han conseguido los objetivos propuestos, en concreto se ha conseguido un sistema de bajo coste, no solo capaz de actuar como medidor energético y monitor de calidad de red, si no también capaz de recuperar gran cantidad de parámetros de utilidad sobre la red. Un punto clave alcanzado es el cumplimiento de los estándares internacionales en referencia a medidas del suministro y calidad eléctrica, lo que convierten a "openZmeter" en un dispositivo de medida de referencia en su campo.

Este trabajo demuestra que el uso de sistemas de código abierto puede ayudar a la sostenibilidad y, más específicamente, al uso sostenible de la energía al proporcionar información valiosa a los usuarios para que puedan tomar decisiones de ahorro energético apoyados en datos fiables y abiertos obtenidos en entornos reales. Al tratarse de un dispositivo de fácil instalación y utilización, orientado a su incorporación en hogares de zonas rurales o urbanas, el acceso a la información por parte de cualquier tipo de usuario queda garantizado. El uso de dispositivos abiertos que proporcionan información relevante en tiempo real en el marco de las redes inteligentes se muestra, por tanto, de suma importancia para favorecer un desarrollo sostenible y proporcionar a los usuarios los medios y la información necesarios para implantar las políticas de ahorro energético que estime oportunas, teniendo en cuenta sus consumos y características reales de la red.

Cabe señalar que, además de los datos mostrados en este artículo, este dispositivo se instaló en el cuadro eléctrico de varias viviendas durante la elaboración de esta tesis doctoral. Los resultados obtenidos fueron satisfactorios, ya que se pudo comprobar cómo oZm es capaz de recuperar una importante cantidad de datos que se procesan y visualizan mediante una interfaz gráfica avanzada. Los gráficos incluidos en el correspondiente articulo (consumo de energía, formas de onda de voltaje y corriente, frecuencia y eventos de calidad de la energía)

pueden ser interpretados fácilmente por usuarios no expertos, y son de gran utilidad para llevar a cabo otros estudios o bajo la mirada de un usuario más experto.

Al ser los resultados obtenidos favorables y alcanzarse los objetivos propuestos tras la finalización del diseño se extendió el dispositivo creado para su uso en grandes edificios y otras instalaciones donde se requiere el análisis de una red trifásica (publicación científica 3).

6.1.2. Publicación científica 2: "An Open Hardware Design for Internet of Things Power Quality and Energy Saving Solutions"

En la publicación expuesta en el Capítulo 3, se aborda una situación en la que la mayoría de las instalaciones eléctricas se controlan mediante dispositivos comerciales que a menudo son costosos y difíciles de manejar para usuarios no expertos. Como extensión al primer artículo, que se incluye en el Capítulo 2, en esta publicación se describe la construcción del hardware usado por "openZmeter" y diversas mejoras realizadas sobre el software de análisis.

Como se ha visto "openZmeter" integra un software inteligente que le permite funcionar como analizador de red multipropósito y medidor de calidad eléctrica. Utilizando código abierto implementa los estándares internacionales como IEC 61000-4-30 y EN-50160 y facilita al usuario de todos los niveles una interface simple e intuitiva, accesible desde Internet. Una parte de los objetivos que se buscaban dependen del software que se ha implementado, pero también ha sido necesaria la elaboración de un hardware de captura y control que mantenga el concepto inicial de construir un sistema accesible a cualquier entorno y usuario. En este sentido, la construcción de oZm es también un diseño abierto, pensado para tener un bajo coste y así poder realizar un despliegue eficiente de dispositivos de medida en cualquier red.

El diseño avanzado del hardware de captura de oZm garantiza mediciones fiables y precisas del consumo de energía y de la calidad de la energía en una amplia gama de condiciones de funcionamiento en un solo dispositivo práctico y compacto. Dado sus dimensiones reducidas y las sondas de corriente que puede incorporar, se puede instalar fácilmente en cualquier instalación eléctrica, es decir, se puede utilizar tanto como medición del cuadro general o como medición en unidades o aparatos individuales.

Una de las pruebas realizadas sobre oZm ha sido la comparación con dispositivos comerciales. Las características y el funcionamiento de oZm se han comparado con el modelo MyEBOX-1500 de CIRCUTOR, un medidor de energía y calidad eléctrica comercial avanzado y certificado. Los resultados obtenidos en el laboratorio muestran lecturas similares con

mínima desviación. Esta comparación muestra claramente que oZm puede medir y registrar voltajes, corrientes, frecuencia y eventos de calidad de energía RMS de alta precisión en diferentes escenarios. La calidad del equipo de captura complementa al software presentado anteriormente y permite que la gran cantidad de parámetros analizados y mostrados en la interface de usuario mediante cálculo matemático sean fiables.

También se ha conseguido que los datos obtenidos por el equipo sean fácilmente accesibles, un objetivo de gran importancia para poder realizar futuros estudios. Toda la información obtenida es almacenada de forma local en una base de datos en el propio dispositivo y puede accederse a la misma a través de la propia base de datos, por medio de la interface de usuario desde donde puede exportarse o bien mediante el uso de una potente API de consulta, que permite automatizar diversas tareas y es accesible desde prácticamente cualquier lenguaje de programación.

Los beneficios potenciales de oZm para aplicaciones domésticas o industriales quedan demostrados por el conjunto de medidas avanzadas que realiza y por la precisión del hardware de captura usado para la obtención de dichas medidas, como se ha comprobado mediante la comparativa con equipos certificados, tal y como se ha comentado previamente. Todo esto convierten al sistema propuesto en un elemento de utilidad para estudios de redes inteligentes y para el desarrollo de técnicas avanzadas, como el monitoreo de carga no intrusivo y el aprendizaje automático aplicado a la calidad de la energía. Sin duda la facilidad de acceso a los datos y el carácter abierto del proyecto propicia todo tipo de investigaciones futuras y ampliaciones en las funciones incorporadas actualmente.

No obstante, los estándares internacionales IEC 61000-4-30 y EN-50160 que se han implementados son amplios y todas las definiciones incluidas en los mismos no ha sido incluida aún. Al tratarse oZm es un proyecto en constante evolución apoyado por la comunidad las funciones restantes y muchas otras serán incorporadas próximamente ya que los equipos de investigación de varias universidades tienen como objetivo completar y cumplir los requisitos impuestos por estos estándares. A partir del diseño hardware presentado en esta publicación ha sido posible desarrollar una versión trifásica, de forma que sea posible analizar este tipo de redes e instalaciones.

6.1.3. Publicación científica 3: "All-in-one three-phase smart meter and power quality analyzer with extended IoT capabilities"

El dispositivo "openZmeter", presentado en el Capítulo 2 a nivel de software principalmente y en el Capítulo 3 en su diseño hardware, ha sido diseñado pensando en una fácil ampliación de las funciones disponibles, para que cualquier miembro de la comunidad pueda aportar mejoras. Una muestra de la posibilidad de añadir nuevas funciones se expone en el Capítulo 4, donde se extienden los conceptos vistos en los capítulos anteriores a un nuevo equipo de medida valido para redes trifásicas, que conservando todas las funciones de su versión monofásica más distintas mejoras lo convierten en un medidor inteligente de energía y analizador de calidad eléctrica para aplicaciones industriales y grandes instalaciones.

Como en el diseño anterior el concepto de diseño abierto, tanto en hardware como software se mantiene. También se mantiene el cumplimiento de los estándares internacionales como IEC 61000-4-30 y EN 50160, de los que se han extendido todos los apartados desarrollados para incorporar la medida trifásica. Otras funciones han sido añadidas específicamente para este tipo de redes como la medida fasorial y de componentes homopolares.

Para dotar al equipo de la máxima flexibilidad posible el proceso de análisis se ha optimizado para acomodar un numero arbitrario de canales, con el hardware diseñado actualmente son posibles hasta tres de tensión y cuatro de corriente, aunque distintos modos son posibles para hacer el sistema de utilidad en redes bifásicas o varias medidas monofásicas simultaneas.

El uso de características avanzadas del núcleo de Linux, como el modo de tiempo real ha permitido que con una potencia de cómputo reducida y una planificación de las tareas meticulosa sea posible realizar todos los cálculos necesarios, incluyendo aquellos que requieren de gran cantidad de operaciones, como transformadas de Fourier para todos los canales, o la detección de eventos, manteniendo la necesidad de obtener información en tiempo real. Todo el proceso de análisis se ejecuta simultáneamente con las funciones básicas de almacenamiento y presentación al usuario de la información obtenida por medio de la interface WEB mejorada.

En este diseño, la exactitud en los datos obtenidos se ha evaluado en laboratorio, utilizando multímetros de precisión y arrojando unas lecturas correctas para el rango de

operación establecido. Aun no siendo un equipo de precisión, los datos calculados son fiables y hacen apto al equipo para las tareas de medición de consumo energético y análisis de calidad eléctrica para el que ha sido diseñado. La precisión en valor RMS de la tensión se sitúa en el 1%, pudiendo llegar al 0.1% con una correcta calibración previa a su instalación. Respecto a la frecuencia se cumple el valor de 10 mHz (entre 42.5 y 57.5 Hz) que establece la norma. Al utilizarse sondas externas para las medidas de corriente, la precisión de la medida se ve afectada por la calidad de las sondas. No obstante, descartando esta desviación, las lecturas RMS de corriente se sitúan en el mismo rango de precisión que las de tensión. El resto de valores obtenidos son consecuencia directa de las lecturas de tensión y corriente, ya que se obtienen por cálculo matemático.

Para la evaluación en un entorno real se ha realizado la instalación del mismo en una planta solar fotovoltaica, donde se ha monitorizado de forma continuada durante más de un año, con el objetivo de poder obtener los datos de producción, siendo los datos obtenidos válidos y de utilidad para monitorizar y evaluar el correcto funcionamiento de la planta y la detección de eventos que se produzcan en la misma.

Una de las principales aportaciones de este artículo es la posibilidad de acceder a los datos obtenidos desde cualquier lugar, convirtiendo a los equipos en un punto de medición autónomo para una red de sensores IoT (*Internet of Things*). Las posibilidades de acceso del usuario, en este sentido, se han visto mejoradas ya que se hace posible el uso de un servidor central en el que los distintos dispositivos oZm pueden enviar la información obtenida, bien en tiempo real si disponen de acceso permanente a Internet o bien de forma intermitente, almacenando localmente y enviando cuando la conexión esté disponible.

Esta función de sincronización ha demostrado ser de gran utilidad para instalaciones reales, como la propuesta para la evaluación de oZm, al permitir que la comunicación con equipos situados en lugares remotos, donde el acceso a Internet es limitado o intermitente pueda realizarse de forma fluida, consultando datos del histórico aun no disponiendo los dispositivos de captura de conexión en dicho momento. También se cumple otro de los objetivos principales, al poder disponer de un servidor único donde se almacenan y coordinan distintos puntos de medida.

Se puede concluir, por tanto, que el equipo propuesto es una alternativa real a dispositivos comerciales, ofreciendo unas buenas prestaciones y permitiendo reducir de forma considerable los costes de una instalación con múltiples puntos de medida.

6.1.4. Publicación científica 4: "Analysis of non-active power in non-sinusoidal circuits using geometric algebra"

En el artículo presentado en el Capítulo 5, se ha realizado un análisis detallado del uso del algebra geométrica aplicado a sistemas de energía eléctrica, elaborando una nueva teoría que permita un cálculo preciso de la potencia aplicando esta herramienta matemática.

Debido a su flexibilidad, es posible definir correctamente nuevos términos que cumplen con principio de conservación de la energía, que no son satisfechos por la definición tradicional de potencia aparente S. Esta superioridad ha sido probada repetidamente en la literatura científica. El término potencia geométrica neta no activa se analizó en sistemas no sinusoidales y se comparó con las teorías tradicionales, revelando la capacidad del algebra geométrica para verificar los flujos de potencia neta además de su sentido y magnitud.

El trabajo propuesto, por primera vez, permite una nueva descomposición de corrientes más allá de las propuestas por Castro-Nuñez, que enlazan con la propuesta de Fryze y Czarnecki, siendo posible obtener una corriente geométrica activa que minimiza la corriente a suministrar para la potencia activa requerida de cargas lineales y no lineales.

Finalmente, se demuestra que las deficiencias de los conceptos tradicionales basados en la potencia aparente S (falta de significado físico y deficiencia de su definición) pueden ser compensados mediante el uso de álgebra geométrica. La teoría propuesta ha sido implementada entre las funciones de "openZmeter", demostrando la flexibilidad de la plataforma para incorporar nuevos algoritmos y técnicas. De esta forma los datos generados durante el análisis pueden ser comparados con las teorías clásicas en tiempo real y ante distintas cargas, lineales y no lineales.

6.2. CONCLUSIONES GENERALES

Los objetivos marcados al inicio de esta tesis doctoral han quedado cubiertos al haberse cumplido el propósito general de crear herramientas de análisis de redes eléctricas con un bajo coste, un fácil uso, abierta y adecuada para su aplicación en distintos ámbitos, y con posibilidad de incluir nuevas técnicas que se puedan desarrollar. Cada uno de los objetivos

particulares ha sido incorporado a lo largo de las distintas versiones de “openZmeter” tal como se expone.

El cumplimento de los objetivos ha sido validado por distintas pruebas en laboratorio y la aplicación de los dispositivos desarrollados en entornos reales. Adicionalmente se ha demostrado la capacidad de integración en “openZmeter” de nuevas técnicas y mejoras, al tratarse de una plataforma enfocada a la investigación, incorporando una teoría alternativa para el cálculo de potencia.

6.3. TRABAJO FUTURO

Actualmente están en curso diversas ampliaciones relacionadas con la línea de investigación de esta tesis, enfocadas a ampliar las funcionalidades del hardware y software descrito *“openZmeter”*, para convertirlo en un elemento de referencia en lo que a últimas técnicas de análisis de redes eléctricas se refiere. La incorporación de sincronización a nivel de muestra por medio de GPS y una mayor flexibilidad en la captura abren un nuevo campo al permitir incorporar nuevas funciones como el uso de PMU *(Phasor Measurement Unit)* y la medida en redes multifásicas usando distintos dispositivos sincronizados capturando en paralelo. Tras la incorporación de estas funciones se espera que oZm inicie diversos controles necesarios para convertirse en un dispositivo homologado para medición de redes eléctricas.

Existen proyectos en curso relacionados con NILM *(Non Intrusive Load Monitoring)* que haciendo uso de las capacidades de captura de openZmeter pretenden identificar las cargas bajo observación. Una vez finalizados los estudios se espera poder incorporar esta función directamente en el dispositivo.

En lo referente a la teoría descrita en el Capítulo 5, se está trabajando intensivamente en modelos matemáticos que puedan extender las funciones de análisis de potencia utilizando algebra geometría a redes multifásicas. Este modelo de análisis estará disponible en *“openZmeter”* lo que permitirá la visualización en tiempo real de nuevos parámetros de la red.

REFERENCIAS BIBLIOGRÁFICAS

[1] P. Theodore, "Sensor monitoring device". Patent US3842208A, January 1970.

[2] N. Uribe-Pérez, L. Hernández, D. de la Vega and I. Angulo, "State of the Art and Trends Review of Smart Metering in Electricity Grids," vol. 6, p. 68, 2016.

[3] C. P. Steinmetz, Theory and Calculation of Alternating Current Phenomena, McGraw-Hill Book Company, Incorporated, 1916.

[4] C. Budeanu, Puissances réactives et fictives, Impr. Cultura națională, 1927.

[5] A. E. Emanuel, "Powers in nonsinusoidal situations-a review of definitions and physical meaning," vol. 5, pp. 1377-1389, 1990.

[6] V. Staudt, *Fryze - Buchholz - Depenbrock: A time-domain power theory,* 2008.

[7] M. Pritoni, K. Salmon, A. Sanguinetti, J. Morejohn and M. Modera, "Occupant thermal feedback for improved efficiency in university buildings," vol. 144, pp. 241-250, 2017.

[8] F. Torrent-Fontbona and B. López, "Power re-allocation for reducing contracted electric power costs," vol. 89, pp. 112-122, 2015.

[9] L. Pérez-Lombard, J. Ortiz and C. Pout, "A review on buildings energy consumption information," vol. 40, pp. 394-398, 2008.

[10] M. Aiad and P. H. Lee, "Unsupervised approach for load disaggregation with devices interactions," vol. 116, pp. 96-103, 2016.

[11] L. Morales-Velazquez, R. de Jesus Romero-Troncoso, G. Herrera-Ruiz, D. Morinigo-Sotelo and R. A. Osornio-Rios, "Smart sensor network for power quality monitoring in electrical installations," vol. 103, pp. 133-142, 2017.

[12] D. R. Muñoz, D. M. Pérez, J. S. Moreno, S. C. Berga and E. C. Montero, "Design and experimental verification of a smart sensor to measure the energy and power consumption in a one-phase AC line," vol. 42, pp. 412-419, 2009.

[13] Y. Kabalci, "A survey on smart metering and smart grid communication," vol. 57, pp. 302-318, 2016.

[14] I. S. Bayram and T. S. Ustun, "A survey on behind the meter energy management systems in smart grid," vol. 72, pp. 1208-1232, 2017.

[15] B. Stephen, A. J. Mutanen, S. Galloway, G. Burt and P. Jarventausta, "Enhanced Load Profiling for Residential Network Customers," vol. 29, pp. 88-96, 2014.

[16] E. O'Driscoll and G. E. O'Donnell, "Industrial power and energy metering – a state-of-the-art review," vol. 41, pp. 53-64, 2013.

[17] S. Lanzisera, S. Dawson-Haggerty, H. Y. I. Cheung, J. Taneja, D. Culler and R. Brown, "Methods for detailed energy data collection of miscellaneous and electronic loads in a commercial office building," vol. 65, pp. 170-177, 2013.

[18] Y.-K. Seo and W.-H. Hong, "Constructing electricity load profile and formulating load pattern for urban apartment in Korea," vol. 78, pp. 222-230, 2014.

[19] S. Ahmadi-Karvigh, A. Ghahramani, B. Becerik-Gerber and L. Soibelman, "Real-time activity recognition for energy efficiency in buildings," vol. 211, pp. 146-160, 2018.

[20] F. G. Montoya, A. García-Cruz, M. G. Montoya and F. Manzano-Agugliaro, "Power quality techniques research worldwide: A review," *Renewable and Sustainable Energy Reviews,* vol. 54, pp. 846-856, 2016.

[21] C. Miller and F. Meggers, "Mining electrical meter data to predict principal building use, performance class, and operations strategy for hundreds of non-residential buildings," vol. 156, pp. 360-373, 2017.

[22] A. Kluczek and P. Olszewski, "Energy audits in industrial processes," vol. 142, pp. 3437-3453, 2017.

[23] G. Pellegrinelli, M. Baù, F. Cerini, S. Dalola, M. Ferrari and V. Ferrari, "Portable Energy-logger Circuit for the Experimental Evaluation of Energy Harvesting

Solutions from Motion for Wearable Autonomous Sensors," vol. 87, pp. 1230-1233, 2014.

[24] T. Atalik, I. Cadirci, T. Demirci, M. Ermis, T. Inan, A. S. Kalaycioglu and O. Salor, "Multipurpose Platform for Power System Monitoring and Analysis With Sample Grid Applications," vol. 63, pp. 566-582, 2014.

[25] E. M. G. Rodrigues, R. Godina, M. Shafie-khah and J. P. S. Catalão, "Experimental Results on a Wireless Wattmeter Device for the Integration in Home Energy Management Systems," vol. 10, p. 398.

[26] L. Tomesc, P. Dobra and M. Abrudean, "LOW-COST POWER QUALITY ANALIZER," *IFAC Proceedings Volumes,* vol. 40, pp. 157-162, 2007.

[27] "OpenEnergyMonitor".

[28] R. Pereira, J. Figueiredo, R. Melicio, V. M. F. Mendes, J. Martins and J. C. Quadrado, "Consumer energy management system with integration of smart meters," vol. 1, pp. 22-29, 2015.

[29] Z. Mumtaz, S. Ullah, Z. Ilyas, N. Aslam, S. Iqbal, S. Liu, J. Meo and H. Madni, "An Automation System for Controlling Streetlights and Monitoring Objects Using Arduino," vol. 18, p. 3178.

[30] B. Martinez, X. Vilajosana, I. Kim, J. Zhou, P. Tuset-Peiró, A. Xhafa, D. Poissonnier and X. Lu, "I3Mote: An Open Development Platform for the Intelligent Industrial Internet," vol. 17, p. 986.

[31] M. Syafrudin, N. L. Fitriyani, D. Li, G. Alfian, J. Rhee and Y.-S. Kang, "An Open Source-Based Real-Time Data Processing Architecture Framework for Manufacturing Sustainability," *Sustainability,* vol. 9, 2017.

[32] L. Pocero, D. Amaxilatis, G. Mylonas and I. Chatzigiannakis, "Open source IoT meter devices for smart and energy-efficient school buildings," vol. 1, pp. 54-67, 2017.

[33] R. Masnicki, "Validation of the Measurement Characteristics in an Instrument for Power Quality Estimation—A Case Study," vol. 10, p. 536.

[34] N. C. Woolley, J. M. Avendaño-Mora and J. V. Milanović, "Methodology for robust monitoring of voltage sags based on equipment trip probabilities," vol. 90, pp. 107-116, 2012.

[35] W. Hernandez, C. Calderón-Córdova, E. Brito, E. Campoverde, V. González-Posada and J. G. Zato, "A method of verifying the statistical performance of electronic circuits designed to analyze the power quality," vol. 93, pp. 21-28, 2016.

[36] M. A. S. Masoum and E. F. Fuchs, *Impact of Poor Power Quality on Reliability, Relaying and Security,* 2015, pp. 681-778.

[37] S. Few, "Time on the Horizon," 2008.

[38] T. Paraskevakos, "Sensor Monitoring Device". Patent 3,842,208, 15 October 1974.

[39] E. Union, "Directive 2012/27/EU of the European Parliament and of the Council of 25 October 2012 on EnergyEfficiency, Amending Directives 2009/125/EC and 2010/30/EU and Repealing Directives 2004/8/EC and 2006/32/EC".

[40] E. Union, *Communication from the Commission to the European Parliament, the Council, the European Economic and Social Committee and the Committee of the Regions,* Brussels, Belgium, 2014.

[41] X. Fang, S. Misra, G. Xue and D. Yang, "Smart Grid — The New and Improved Power Grid: A Survey," vol. 14, pp. 944-980, 2012.

[42] C.-C. Chu and H. H.-C. Iu, "Complex Networks Theory For Modern Smart Grid Applications: A Survey," vol. 7, pp. 177-191, 2017.

[43] I. Zunnurain, M. Maruf, M. Rahman and G. M. Shafiullah, "Implementation of Advanced Demand Side Management for Microgrid Incorporating Demand Response and Home Energy Management System," vol. 3, p. 50.

[44] S. Kakran and S. Chanana, "Smart operations of smart grids integrated with distributed generation: A review," vol. 81, pp. 524-535, 2018.

[45] A. Hirsch, Y. Parag and J. Guerrero, "Microgrids: A review of technologies, key drivers, and outstanding issues," vol. 90, pp. 402-411, 2018.

[46] G. Zhang, G. G. Wang, H. Farhangi and A. Palizban, "Data mining of smart meters for load category based disaggregation of residential power consumption," vol. 10, pp. 92-103, 2017.

[47] E. G. Ribeiro, T. M. Mendes, G. L. Dias, E. R. S. Faria, F. M. Viana, B. H. G. Barbosa and D. D. Ferreira, "Real-time system for automatic detection and classification of single and multiple power quality disturbances," vol. 128, pp. 276-283, 2018.

[48] K. Sharma and L. M. Saini, "Performance analysis of smart metering for smart grid: An overview," vol. 49, pp. 720-735, 2015.

[49] L. Yu, T. Jiang and Y. Zou, "Distributed Real-Time Energy Management in Data Center Microgrids," *IEEE Transactions on Smart Grid,* vol. 9, pp. 3748-3762, June 2018.

[50] J.-M. Wang, M.-T. Yang and P.-L. Chen, "Design and Implementation of an Intelligent Windowsill System Using Smart Handheld Device and Fuzzy Microcontroller," vol. 17, p. 830.

[51] T.-C. Ou and C.-M. Hong, "Dynamic operation and control of microgrid hybrid power systems," vol. 66, pp. 314-323, 2014.

[52] T.-C. Ou, "Ground fault current analysis with a direct building algorithm for microgrid distribution," vol. 53, pp. 867-875, 2013.

[53] T.-C. Ou, "A novel unsymmetrical faults analysis for microgrid distribution systems," vol. 43, pp. 1017-1024, 2012.

[54] M. M. Esfahani, A. Sheikh and O. Mohammed, "Adaptive real-time congestion management in smart power systems using a real-time hybrid optimization algorithm," vol. 150, pp. 118-128, 2017.

[55] *International Electrotechnical Commission. Electromagnetic Compability (EMC)—Part 4: Testing and Measurement Techniques—Power Quality Measurement Methods,* Switzerland, 2003.

[56] Y. Shen, F. Hussain, L. Hui and D. Addis, *Power Quality Disturbances Classification Based on Curvelet Transform,* 2019.

[57] J. Niitsoo, M. Jarkovoi, P. Taklaja, J. Klüss and I. Palu, "Power Quality Issues Concerning Photovoltaic Generation in Distribution Grids," vol. 06, pp. 148-163, 2015.

[58] C. B. Khadse, M. A. Chaudhari and V. B. Borghate, "Conjugate gradient back-propagation based artificial neural network for real time power quality assessment," vol. 82, pp. 197-206, 2016.

[59] R. Kumar, B. Singh, D. T. Shahani and C. Jain, "Dual-Tree Complex Wavelet Transform-Based Control Algorithm for Power Quality Improvement in a Distribution System," vol. 64, pp. 764-772, 2017.

[60] D. Li, K. Yang, Z. Q. Zhu and Y. Qin, "A Novel Series Power Quality Controller With Reduced Passive Power Filter," vol. 64, pp. 773-784, 2017.

[61] A. S. Bubshait, A. Mortezaei, M. G. Simoes and T. D. C. Busarello, "Power Quality Enhancement for a Grid Connected Wind Turbine Energy System," vol. 53, pp. 2495-2505, 2017.

[62] *IEEE Recommended Practice for Monitoring Electric Power Quality,* NY, USA, 2009.

[63] Y. Wan, J. Cao, H. Zhang, Z. Zhu and S. Yao, *Optimization of the power quality monitor number in Smart Grid,* 2014.

[64] Mohibullah and S. H. Laskar, *Power quality issues and need of intelligent PQ monitoring in the smart grid environment,* 2012.

[65] Q. Tang, Y. N. Wang, S. Guo and F. Jiang, "Power quality disturbance classification based on S transform and Fourier transform," *J. Hunan Univ. (Nat. Sci.), 4, 009,* 2009.

[66] Z. Moravej, A. A. Abdoos and M. Pazoki, "Detection and Classification of Power Quality Disturbances Using Wavelet Transform and Support Vector Machines," vol. 38, pp. 182-196, 2009.

[67] F. Wang, Z. Jin, Z. Zhu and X. Wang, *Application of Extended Kalman Filter to the Modeling of Electric Arc Furnace for Power Quality Issues.*

[68] G. Hu, "Power Quality Disturbance Based on Gabor-Wigner Transform," vol. 12, pp. 329-337, 2015.

[69] T. Yalcin, O. Ozgonenel and U. Kurt, "Multi-class power quality disturbances classification by using ensembleempirical mode decomposition based SVM," *In Proceedings of the 2011 7th International Conference on IEEEElectrical and Electronics Engineering (ELECO), Bursa, Turkey,* pp. 1-122, December 2011.

[70] Y. Shen, H. Wu, G. Liu, H. Liu, H. Zhang and W. Xia, *Study on identification of power quality disturbances based on compressive sensing,* 2014.

[71] S. Shaik, U. R. Babu and S. Subhani, *Detection and classification of power quality disturbances: Using curvelet transform and support vector machines,* 2016.

[72] W. W. Liu, X. Y. Jiang, H. Cai and C. B. Yuan, "Power quality disturbance classification based on Hilbert transform and classification trees," *Electr. Meas. Instrum 11, 006,* 2010.

[73] Z. Cai, F. Ning, W. Li and T. A. Gulliver, *Power quality signal analysis for the smart grid using the Hilbert-Huang transform,* 2013.

[74] A. F. López-Lopera, M. A. Álvarez and Á. Á. Orozco, *Sparse Linear Models Applied to Power Quality Disturbance Classification,* 2017, pp. 521-529.

[75] A. A. Abdoos, P. K. Mianaei and M. R. Ghadikolaei, "Combined VMD-SVM based feature selection method for classification of power quality events," vol. 38, pp. 637-646, 2016.

[76] S. Adhikari, N. Sinha and T. Dorendrajit, "Fuzzy logic based on-line fault detection and classification in transmission line," vol. 5, 2016.

[77] J. Ma, J. Zhang, L. Xiao, K. Chen and J. Wu, "Classification of Power Quality Disturbances via Deep Learning," *IETE Technical Review,* vol. 34, pp. 408-415, 2017.

[78] H. Liu, F. Hussain and Y. Shen, "Power Quality Disturbances Classification Using Compressive Sensing and Maximum Likelihood," vol. 35, pp. 359-368, 2018.

[79] F. G. Montoya, A. Alcayde, P. Sanchez, J. Gomez and F. Martin, *zEnergy: An open source project for power quality assessment and monitoring,* 2011.

[80] M. Vallés, J. Reneses, R. Cossent and P. Frías, "Regulatory and market barriers to the realization of demand response in electricity distribution networks: A European perspective," vol. 140, pp. 689-698, 2016.

[81] E. Viciana, A. Alcayde, F. Montoya, R. Baños, F. Arrabal-Campos, A. Zapata-Sierra and F. Manzano-Agugliaro, "OpenZmeter: An Efficient Low-Cost Energy Smart Meter and Power Quality Analyzer," vol. 10, p. 4038.

[82] J. P. Charras, "Kicad: GPL PCB Suite".

[83] M. Frigo and S. G. Johnson, "The Design and Implementation of FFTW3," vol. 93, pp. 216-231, 2005.

[84] P. Volgyesi, A. Dubey, T. Krentz, I. Madari, M. Metelko and G. Karsai, *Time synchronization services for low-cost fog computing applications,* 2017.

[85] *IEEE Standard Definitions for the Measurement of Electric Power Quantities under Sinusoidal, Nonsinusoidal, Balanced, or Unbalanced Conditions,* NY, USA, 2010.

[86] L. S. Czarnecki, *Currents’ Physical Components (CPC) concept: A fundamental of power theory,* 2008.

[87] M. Castro-Nunez, R. Castro-Puche and E. Nowicki, *The use of geometric algebra in circuit analysis and its impact on the definition of power,* 2010.

[88] L. Asnin and V. Backmutsky, *A new numeric technique of accurate frequency and harmonics estimation for power system protection and power quality applications.*

[89] J. Arrillaga, M. H. J. Bollen and N. R. Watson, "Power quality following deregulation," vol. 88, pp. 246-261, 2000.

[90] J. F. Fuller, E. F. Fuchs and D. J. Roesler, "Influence of harmonics on power distribution system protection," vol. 3, pp. 549-557, 1988.

[91] D. Sharon, J.-C. Montano, A. Lopez, M. Castilla, D. Borras and J. Gutierrez, "Power Quality Factor for Networks Supplying Unbalanced Nonlinear Loads," vol. 57, pp. 1268-1274, 2008.

[92] W.-Y. Chiu, H. Sun and H. V. Poor, *Demand-side energy storage system management in smart grid,* 2012.

[93] Y. H. Gu and M. H. J. Bollen, "Time-frequency and time-scale domain analysis of voltage disturbances," vol. 15, pp. 1279-1284, 2000.

[94] M. Uyar, S. Yildirim and M. T. Gencoglu, "An expert system based on S-transform and neural network for automatic classification of power quality disturbances," vol. 36, pp. 5962-5975, 2009.

[95] R. G. Stockwell, L. Mansinha and R. P. Lowe, "Localization of the complex spectrum: the S transform," vol. 44, pp. 998-1001, 1996.

[96] IEC, *Electromagnetic compatibility (EMC) - Part 4-36: Testing and measurement techniques - IEMI immunity test methods for equipment and systems,* 2020.

[97] E. Viciana, A. Alcayde, F. Montoya, R. Baños, F. Arrabal-Campos and F. Manzano-Agugliaro, "An Open Hardware Design for Internet of Things Power Quality and Energy Saving Solutions," vol. 19, p. 627.

[98] L. D. O. Arenas, G. de Azevedo e Melo and C. A. Canesin, "A Methodology for Power Quantities Calculation Applied to an FPGA-Based Smart-Energy Meter," vol. 70, pp. 1-11, 2021.

[99] I. Colak, S. Sagiroglu, G. Fulli, M. Yesilbudak and C.-F. Covrig, "A survey on the critical issues in smart grid technologies," vol. 54, pp. 396-405, 2016.

[100] M. H. J. Bollen, R. Das, S. Djokic, P. Ciufo, J. Meyer, S. K. Ronnberg and F. Zavodam, "Power Quality Concerns in Implementing Smart Distribution-Grid Applications," vol. 8, pp. 391-399, 2017.

[101] L. U. O. An, X. U. Qianming, M. A. Fujun and C. H. E. N. Yandong, "Overview of power quality analysis and control technology for the smart grid," vol. 4, pp. 1-9, 2016.

[102] L. S. Czarnecki, "What is wrong with the Budeanu concept of reactive and distortion power and why it should be abandoned," Vols. IM-36, pp. 834-837, 1987.

[103] P. S. Filipski, "Apparent power - a misleading quantity in the non-sinusoidal power theory: Are all non-sinusoidal power theories doomed to fail?," vol. 3, pp. 21-26.

[104] L. S. Czarnecki, "Energy flow and power phenomena in electrical circuits: illusions and reality," vol. 82, pp. 119-126, 2000.

[105] M. Balci and M. Hocaoglu, "New Power Decomposition for Sinusoidal and Nonsinusoidal Conditions," 2006.

[106] G. S. D. Hestenes, Clifford algebra to geometric calculus: a unified language for mathematics and physics, Vol. 5, Springer Science & Business Media, 2012.

[107] D. Hestenes, New Foundations for Classical Mechanics, Springer Netherlands, 2012.

[108] M. Castro-Nunez and R. Castro-Puche, "The IEEE Standard 1459, the CPC Power Theory, and Geometric Algebra in Circuits With Nonsinusoidal Sources and Linear Loads," vol. 59, pp. 2980-2990, 2012.

[109] M. Castro-Nunez and R. Castro-Puche, "Advantages of Geometric Algebra Over Complex Numbers in the Analysis of Networks With Nonsinusoidal Sources and Linear Loads," vol. 59, pp. 2056-2064, 2012.

[110] F. Montoya, A. Alcayde, F. Arrabal-Campos and R. Baños, "Quadrature Current Compensation in Non-Sinusoidal Circuits Using Geometric Algebra and Evolutionary Algorithms," vol. 12, p. 692.

[111] M. Castilla, J. C. Bravo, M. Ordonez and J. C. Montano, "Clifford Theory: A Geometrical Interpretation of Multivectorial Apparent Power," vol. 55, pp. 3358-3367, 2008.

[112] S. Q. Sun and Q. R. Xiang, "Waveform distortion and distortion power," vol. 139, p. 303, 1992.

[113] L. S. Czarnecki, "Currents' physical components (CPC) in circuits with nonsinusoidal voltages and currents. Part 1, Single-phase linear circuits," *Electrical Power Quality and Utilisation. Journal,* Vols. Vol. 11, nr 2, pp. 3-14, 2005.

[114] L. S. Czarnecki, "Considerations on the Reactive Power in Nonsinusoidal Situations," Vols. IM-34, pp. 399-404, 1985.

[115] L. S. Czarnecki, "On some misinterpretations of the instantaneous reactive power p-q theory," *IEEE Transactions on Power Electronics,* vol. 19, pp. 828-836, 2004.

[116] F. Montoya, R. Baños, A. Alcayde, M. Montoya and F. Manzano-Agugliaro, "Power Quality: Scientific Collaboration Networks and Research Trends," vol. 11, p. 2067.

[117] J. M. Chappell, S. P. Drake, C. L. Seidel, L. J. Gunn, A. Iqbal, A. Allison and D. Abbott, "Geometric Algebra for Electrical and Electronic Engineers," *Proceedings of the IEEE,* vol. 102, pp. 1340-1363, 2014.

[118] J. Bernard, Multivectors and Clifford algebra in electrodynamics, World Scientific, 1989.

[119] L. Dorst, D. Fontijne and S. Mann, "Geometric algebra for computer science - an object-oriented approach to geometry," in *The Morgan Kaufmann series in computer graphics*, 2007.

[120] M. Castro-Núñez, D. Londoño-Monsalve and R. Castro-Puche, "Theorems of compensation and Tellegen in non-sinusoidal circuits via geometric algebra," vol. 2019, pp. 3409-3417, 2019.

[121] F. G. Montoya, R. Baños, A. Alcayde and F. M. Arrabal-Campos, "Analysis of power flow under non-sinusoidal conditions in the presence of harmonics and interharmonics using geometric algebra," vol. 111, pp. 486-492, 2019.

[122] M. Castro-Núñez, D. Londoño-Monsalve and R. Castro-Puche, "M , the conservative power quantity based on the flow of energy," vol. 2016, pp. 269-276, 2016.

[123] M. A. Slonim and J. D. van der Wyk, "Power components in a system with sinusoidal and nonsinusoidal voltages and/or currents," vol. 135, p. 76, 1988.

[124] H. Liu, Y. Tang, Y. Feng and X. Ma, *A Power Quality Disturbance Classification Method Based on Park Transform and Clarke Transform Analysis,* 2008.

[125] T. Yalcin, O. Ozgonenel and U. Kurt, "Multi-class power quality disturbances classification by using ensemble empirical mode decomposition based SVM," *ELECO 2011 - 7th International Conference on Electrical and Electronics Engineering,* January 2011.

[126] L. S. Czarnecki and T. Swietlicki, "Powers in nonsinusoidal networks: their interpretation, analysis, and measurement," vol. 39, pp. 340-345, 1990.

[127] M. Castro-Núñez, *The Use of Geometric Algebra in the Analysis of Non-sinusoidal Networks and the Construction of a Unified Power Theory for Single Phase Systems - A Paradigm Shift,* PRISM, 2013.